

TEXTE

18/2020

Development of a method to determine the bioaccumulation of manufactured nanomaterials in filtering organisms (Bivalvia)

Final Report

TEXTE 18/2020

Environmental Research of the
Federal Ministry for the
Environment, Nature Conservation
and Nuclear Safety

Project No. (FKZ) 3716 66 410 0
Report No. FB000061/ENG

Development of a method to determine the bioaccumulation of manufactured nanomaterials in filtering organisms (Bivalvia)

by

Prof. Dr. Christian Schlechtriem, Dr. Burkhard Knopf, Sebastian Kühr,
Boris Meisterjahn, Nicola Schröder
Fraunhofer Institute for Molecular Biology and Applied Ecology (Fraunhofer
IME), Division Applied Ecology, Schmallenberg

On behalf of the German Environment Agency

Imprint

Publisher:

Umweltbundesamt
Wörlitzer Platz 1
06844 Dessau-Roßlau
Tel: +49 340-2103-0
Fax: +49 340-2103-2285
buergerservice@uba.de
Internet: www.umweltbundesamt.de

 /umweltbundesamt.de
 /umweltbundesamt

Study performed by:

Fraunhofer Institute for Molecular Biology and
Applied Ecology (Fraunhofer IME),
Division Applied Ecology
57392 Schmallenberg

Study completed in:

March 2019

Edited by:

Section IV 2.2 Arzneimittel, Wasch- und Reinigungsmittel
Dr. Doris Völker

Publication as pdf:

<http://www.umweltbundesamt.de/publikationen>

ISSN 1862-4804

Dessau-Roßlau, January 2020

The responsibility for the content of this publication lies with the author(s).

Abstract: Development of a method to determine the bioaccumulation of manufactured nanomaterials in filtering organisms (Bivalvia)

Increasing amounts of MNMs are produced for industrial purpose and released to the environment by their usage or disposal of the products. Due to the high production volume MNMs are subject to PBT-assessment to estimate their potential environmental impact. The classical method to elucidate the bioaccumulation potential of chemicals is the flow-through approach with fish according to OECD TG 305 providing a BCF estimate. However, most MNMs tend to sediment in the aquatic environment and are thus difficult to be tested following the established test concept where constant and continuous exposure conditions need to be achieved. The freshwater filter feeding bivalve *Corbicula fluminea* has previously shown to ingest and accumulate MNMs present in the water phase. To investigate the suitability of *C. fluminea* as test organism for bioaccumulation studies we developed a new flow-through system to expose the mussels under constant exposure conditions. Different MNMs, each having different characteristics, were applied to determine their bioaccumulation potential. The silver nanoparticle NM 300K (Ag NP) was tested as a well dispersable and ion releasing MNM. In addition, *C. fluminea* was exposed to AgNO₃ as a source of dissolved Ag⁺ to compare the bioaccumulation of Ag from dissolved and nanoparticulate sources. The titanium dioxide NP NM 105 was used for testing a non ion releasing MNM and the polystyrene nanoparticle (nPS) Fluoro-Max™, containing a fluorescence dye, was tested representing MNMs that are based on organic polymers. The uptake and distribution of nPS in the mussel soft tissue were observed using a fluorescence microscope. Following exposure to metal and metal oxides we were able to determine BAF_{ss} and BCF_{ss} values. BAF_{ss} values of 31 and 128 for two NM 300K concentrations (0.624 and 6.177 µg Ag/L) and of 6,150 and 9,022 for two NM 105 concentrations (0.099 and 0.589 µg TiO₂/L) showed that the BAF_{ss} depends on the exposure concentration. Also for AgNO₃, concentration depending BCF_{ss} of 31 and 711 were estimated for the higher and lower concentration, respectively. The analysis of metals in the soft tissue of previously exposed mussels and the resulting compartment specific distribution factors provide clear indications, that the uptake of NPs was mainly driven by the simple ingestion of NPs rather than the accumulation of dissolved ions. This was supported by the measurement of particle concentrations in mussel tissue using single particle ICP-MS.

Kurzbeschreibung: Entwicklung einer Methode zur Bestimmung der Bioakkumulation von synthetischen Nanomaterialien in filtrierenden Organismen (Bivalvia)

Immer größer werdende Mengen an synthetischen Nanomaterialien (MNMs) werden für den industriellen Einsatz produziert und können während der Produktion, dem Einsatz der Produkte, sowie bei deren Entsorgung in die Umwelt gelangen. MNMs mit hohen Produktionsvolumina unterliegen einer Bioakkumulationsbewertung im Rahmen der EU REACH Verordnung, um potentielle Umweltbelastungen abschätzen zu können. Die hierbei für die Chemikalienbewertung klassischerweise verwendeten Methoden, etwa Durchflussstudien mit Fischen gemäß OECD TG 305, sind für das Testen von MNMs in aquatischen Medien jedoch nur bedingt geeignet. So neigen die meisten MNMs dazu, in aquatischen Systemen nur metastabile Suspensionen zu bilden und direkt nach dem Eintreten in das Medium oder im zeitlichen Verlauf zu sedimentieren. Eine konstante homogene Exposition im Testsystem wird somit stark erschwert. Für *Corbicula fluminea*, eine weit verbreitete Süßwassermuschel, wurde bereits in früheren Studien gezeigt, dass sie MNMs aus der Wasserphase durch Filtration aufnehmen kann. Im Rahmen dieses Projekts wurde die Eignung von *C. fluminea* für Bioakkumulationsstudien mit MNMs geprüft. Hierzu wurde ein neues Durchflusssystem entwickelt, welches eine konstante und homogene Exposition von MNMs ermöglicht. Zur Überprüfung wurden synthetische Nanomaterialien gewählt, welche jeweils MNMs mit bestimmten Eigenschaften repräsentieren. Das Silbernanopartikel NM 300K (Ag NP) wurde als Repräsentant der Gruppe der gut dispergierbaren und ionenfreisetzenden MNMs getestet und mit AgNO₃ als nicht nanopartikuläre Form desselben Elements verglichen. NM 105, ein Titandioxid NP, wurde für die Gruppe der nicht ionenfreisetzenden MNMs getestet. Für die Gruppe der MNMs, welche auf organischen Polymeren basieren, wurde das Polystyrol NP Fluoro-Max™ getestet, welches mit einem Fluoreszenzfarbstoff markiert war. Somit konnte die Aufnahme und Verteilung des NPs im Weichkörper der Muscheln u.a. mittels Fluoreszenzmikroskop untersucht werden. Für die Ag und TiO₂ Behandlungen konnten nach Messung der Gewebekonzentrationen BAF bzw. BCF Werte im Konzentrationsgleichgewicht ermittelt werden. BAF_{ss} Werte von 31 und 128 für die beiden NM 300K Konzentrationen (0,624 und 6,177 µg Ag/L) und 6150 und 9022 für die beiden NM 105 Konzentrationen (0,099 und 0,589 µg TiO₂/L) zeigten, dass BAF_{ss} Werte für die untersuchten MNMs abhängig von der jeweiligen Expositionskonzentration sind. Für die AgNO₃ Behandlung wurden ebenso konzentrationsabhängige BCF_{ss} Werte von 31 und 711 für die höhere und niedrigere Konzentrationen ermittelt. Die Kinetik der gemessenen Partikelkonzentrationen in den Muschelgeweben (sp-ICP-MS) wie auch die ermittelten Distributionsfaktoren für einzelne Kompartimente lieferten Hinweise, dass die untersuchten MNMs zwar aufgenommen, aber nicht inkorporiert wurden.

Table of content

| | |
|---|----|
| Table of content | 7 |
| List of figures | 11 |
| List of tables | 13 |
| List of abbreviations | 15 |
| Summary | 16 |
| Zusammenfassung..... | 20 |
| 1 Introduction..... | 25 |
| 2 Objectives of the research project and project realization..... | 27 |
| 2.1 Objectives of the research project | 27 |
| 2.2 Project structure..... | 27 |
| 3 Selection of test species and nanomaterials..... | 28 |
| 3.1 Selection of test species and husbandry | 28 |
| 3.2 Selection of nanomaterials..... | 28 |
| 4 Nanomaterials: Elucidation of physical and chemical properties | 30 |
| 4.1 Zinc oxide nanomaterial NM 110 | 30 |
| 4.1.1 Solubility test | 30 |
| 4.1.1.1 Test design | 30 |
| 4.1.1.2 Analytics..... | 30 |
| 4.1.1.3 Mass balance | 31 |
| 4.1.1.4 Results..... | 32 |
| 4.1.1.5 Conclusion..... | 33 |
| 4.2 Titanium dioxide NM 105 | 34 |
| 4.2.1 Stability test (I) NM 105 - in test media..... | 34 |
| 4.2.1.1 Test design | 34 |
| 4.2.1.2 Analytics..... | 34 |
| 4.2.1.3 Results..... | 35 |
| 4.2.1.4 Conclusion..... | 35 |
| 4.2.2 Stability test (II) NM 105 - in test media and ultra-pure water | 36 |
| 4.2.2.1 Test design | 36 |
| 4.2.2.2 Analytics..... | 37 |
| 4.2.2.3 Results..... | 37 |
| 4.2.2.4 Conclusion..... | 37 |
| 4.3 Silver nitrate, AgNO ₃ | 38 |

| | | |
|---------|---|----|
| 4.3.1 | Stability test | 38 |
| 4.3.1.1 | Test design | 38 |
| 4.3.1.2 | Analytics..... | 38 |
| 4.3.1.3 | Results..... | 38 |
| 4.3.1.4 | Conclusion..... | 39 |
| 4.4 | Silver NM 300K | 40 |
| 4.4.1 | Stability test | 40 |
| 4.4.1.1 | Test design | 40 |
| 4.4.1.2 | Analytics..... | 40 |
| 4.4.1.3 | Results..... | 40 |
| 4.4.1.4 | Conclusion..... | 41 |
| 4.4.2 | Solubility test | 41 |
| 4.4.2.1 | Test design | 41 |
| 4.4.2.2 | Analytics..... | 41 |
| 4.4.2.3 | Results..... | 41 |
| 4.4.2.4 | Conclusion..... | 42 |
| 4.5 | Polystyrene nanoparticles | 43 |
| 4.5.1 | Stability test | 43 |
| 4.5.1.1 | Test design | 43 |
| 4.5.1.2 | Analytics..... | 43 |
| 4.5.1.3 | Results..... | 43 |
| 4.5.1.4 | Conclusion..... | 44 |
| 5 | Establishment of the new test system | 45 |
| 5.1 | Description of the flow-through system | 45 |
| 5.2 | Feeding study | 47 |
| 5.2.1 | Study design..... | 47 |
| 5.2.2 | Results..... | 47 |
| 5.2.3 | Conclusion..... | 47 |
| 6 | Investigations on the bioaccumulation of the selected nanomaterials | 49 |
| 6.1 | Preliminary studies..... | 49 |
| 6.1.1 | Preliminary study AgNO ₃ | 49 |
| 6.1.1.1 | Study design..... | 49 |
| 6.1.1.2 | Results..... | 49 |
| 6.1.1.3 | Evaluation | 51 |

| | | |
|---------|---|----|
| 6.1.2 | Preliminary study NM 300K | 52 |
| 6.1.2.1 | Study design..... | 52 |
| 6.1.2.2 | Results..... | 52 |
| 6.1.2.3 | Evaluation | 53 |
| 6.1.3 | Preliminary study nPS | 54 |
| 6.1.3.1 | Study design..... | 54 |
| 6.1.3.2 | Results..... | 54 |
| 6.1.3.3 | Evaluation | 54 |
| 6.2 | Main studies | 54 |
| 6.2.1 | Bioaccumulation study AgNO ₃ | 54 |
| 6.2.1.1 | Study design..... | 54 |
| 6.2.1.2 | Results..... | 54 |
| 6.2.1.3 | Evaluation | 59 |
| 6.2.2 | Bioaccumulation study NM 300K..... | 60 |
| 6.2.2.1 | Study design..... | 60 |
| 6.2.2.2 | Results..... | 60 |
| 6.2.2.3 | Evaluation | 65 |
| 6.2.3 | Bioaccumulation study NM 105..... | 65 |
| 6.2.3.1 | Study design..... | 65 |
| 6.2.3.2 | Results..... | 65 |
| 6.2.3.3 | Evaluation | 70 |
| 6.2.4 | Investigations on particle number and distribution of total concentrations in the soft tissue | 70 |
| 6.2.4.1 | Study design..... | 70 |
| 6.2.4.2 | Results..... | 71 |
| 6.2.4.3 | Evaluation | 79 |
| 6.2.5 | Bioaccumulation study nPS..... | 80 |
| 6.2.5.1 | Study design..... | 80 |
| 6.2.5.2 | Results..... | 80 |
| 7 | General discussion..... | 82 |
| 7.1 | Dietary tests | 82 |
| 7.2 | Uptake, elimination and accumulation of Ag..... | 82 |
| 7.3 | Uptake, elimination and accumulation of TiO ₂ | 84 |
| 7.4 | Uptake, elimination and accumulation of nPS | 85 |

| | | |
|-----|--|----|
| 7.5 | Suitability of the test system and the suggested endpoints | 85 |
| 8 | List of references | 87 |

List of figures

| | | |
|------------|--|----|
| Figure 1: | <i>Corbicula fluminea</i> | 29 |
| Figure 2: | Husbandry of <i>Corbicula fluminea</i> in a mesocosm | 29 |
| Figure 3: | TiO ₂ concentrations during the 0.1 mg TiO ₂ /L stability test..... | 35 |
| Figure 4: | TiO ₂ concentrations during the 1 mg TiO ₂ /L stability test..... | 35 |
| Figure 5: | TiO ₂ concentrations during stability test (II): 0.1 mg/L in UHQ and tap water | 36 |
| Figure 6: | TiO ₂ concentrations during stability test (II): 1 mg/L in UHQ and tap water | 36 |
| Figure 7: | AF4-FLD-fractogram of samples at different sampling times: Fluorescence intensity during the nPS stability test | 44 |
| Figure 8: | Schematic presentation of the bivalvia flow-through system..... | 45 |
| Figure 9: | Bivalvia flow-through system | 46 |
| Figure 10: | <i>Corbicula fluminea</i> on steel grids | 46 |
| Figure 11: | Bivalvia test system during the feeding study, top-left: <i>Spirulina</i> , top-right: stinging-nettle powder, bottom-left: fish food tablet, bottom-right: no food..... | 48 |
| Figure 12: | Preliminary study with AgNO ₃ : total Ag concentrations in test media | 51 |
| Figure 13: | Preliminary study with AgNO ₃ : total Ag concentrations in <i>C.f.</i> tissue..... | 51 |
| Figure 14: | Preliminary study with NM 300K: total Ag concentrations in test media | 53 |
| Figure 15: | Preliminary study with NM 300K: total Ag concentrations in <i>C.f.</i> tissue..... | 53 |
| Figure 16: | Bioaccumulation study with AgNO ₃ - low concentration: total Ag concentrations in test media..... | 56 |
| Figure 17: | Bioaccumulation study with AgNO ₃ - low concentration: total Ag concentrations in test media at several levels (depths) of the flow-through system | 56 |
| Figure 18: | Bioaccumulation study with AgNO ₃ – low concentration: total Ag concentrations in <i>C.f.</i> tissue | 57 |
| Figure 19: | Bioaccumulation study with AgNO ₃ - high concentration: total Ag concentrations in test media..... | 58 |
| Figure 20: | Bioaccumulation study with AgNO ₃ - high concentration: total Ag concentrations in test media at several levels (depths) of the flow-through system | 58 |
| Figure 21: | Bioaccumulation study with AgNO ₃ – high concentration: total Ag concentrations in <i>C.f.</i> tissue | 59 |
| Figure 22: | Bioaccumulation study with NM 300K – low concentration: total Ag concentrations in test media | 62 |

| | | |
|------------|--|----|
| Figure 23: | Bioaccumulation study with NM 300K – low concentration: total Ag concentrations in test media at several levels (depths) of the flow-through system..... | 62 |
| Figure 24: | Bioaccumulation study with NM 300K – low concentration: total Ag concentrations in <i>C.f.</i> tissue..... | 63 |
| Figure 25: | Bioaccumulation study with NM 300K – high concentration: total Ag concentrations in test media | 64 |
| Figure 26: | Bioaccumulation study with NM 300K – high concentration: total Ag concentrations in test media at several levels (depths) of the mussel device of the flow-through system..... | 64 |
| Figure 27: | Bioaccumulation study with NM 300K – high concentration: total Ag concentrations in <i>C.f.</i> tissue..... | 64 |
| Figure 28: | Bioaccumulation study with NM 105 – low concentration: total TiO ₂ concentrations in test media | 67 |
| Figure 29: | Bioaccumulation study with NM 105 – low concentration: total TiO ₂ concentrations in test media at several levels (depths) of the flow-through system | 67 |
| Figure 30: | Bioaccumulation study with NM 105 – low concentration: total TiO ₂ concentrations in <i>C.f.</i> tissue..... | 67 |
| Figure 31: | Bioaccumulation study with NM 105 – high concentration: total TiO ₂ concentrations in test media..... | 69 |
| Figure 32: | Bioaccumulation study with NM 105 – high concentration: total TiO ₂ concentrations in test media at several levels (depths) of the flow-through system | 69 |
| Figure 33: | Bioaccumulation study with NM 105 – high concentration: total TiO ₂ concentrations in <i>C.f.</i> tissue | 69 |
| Figure 34: | Compartments dissected from <i>Corbicula fluminea</i> | 71 |
| Figure 35: | Particle concentrations in the soft tissue during uptake and depuration phase of NM 300K | 72 |
| Figure 36: | Calculated median particle size in the soft tissue - NM 300K | 72 |
| Figure 37: | Calculated median particle size in media - NM 300K | 73 |
| Figure 38: | Particle concentrations in the different compartments at the end of the uptake phase - NM 300K..... | 73 |
| Figure 39: | Calculated median particle size in the different compartments at the end of the uptake phase - NM 300K | 74 |
| Figure 40: | Concentrations of presumed particles in the soft tissue during uptake and depuration phase of AgNO ₃ | 74 |
| Figure 41: | Calculated median particle size in the soft tissue – AgNO ₃ | 75 |
| Figure 42: | Calculated median particle size in media – AgNO ₃ | 75 |
| Figure 43: | Concentrations of presumed particles in the different compartments at the end of the uptake phase – AgNO ₃ | 76 |

| | | |
|------------|--|----|
| Figure 44: | Calculated median size for the presumed particles in the different compartments at the end of the uptake phase – AgNO ₃ | 76 |
| Figure 45: | Particle concentrations in the soft tissue during uptake and depuration phase of NM 105 | 77 |
| Figure 46: | Calculated median particle size in the soft tissue – NM 105..... | 77 |
| Figure 47: | Calculated median particle size in media – NM 105 | 77 |
| Figure 48: | Particle concentrations in the different compartments at the end of the uptake phase – NM 105 | 78 |
| Figure 49: | Calculated median particle size in the different compartments at the end of the uptake phase – NM 105 | 78 |
| Figure 50: | Distribution factors of total content of Ag/TiO ₂ based on the total content of calculated complete soft tissue bodies | 79 |
| Figure 51: | Feces of <i>C.f.</i> from the nPS bioaccumulation study under a fluorescence lamp, showing different intensities of fluorescence | 81 |
| Figure 52: | Whole soft tissue of an animal sampled after the uptake phase (top) and an animal sampled after 24 h of depuration (bottom), left: fluorescence lamp, right: daylight..... | 81 |
| Figure 53: | Pictures (fluorescence microscope) of different compartments of <i>C.f.</i> sampled after the uptake phase (top) and after 24 h of depuration (bottom)..... | 81 |

List of tables

| | | |
|-----------|--|----|
| Table 1: | Samplings zinc solubility test..... | 31 |
| Table 2: | Total concentrations zinc solubility test in copper reduced tap water..... | 32 |
| Table 3: | Total, solved and non-solved part of zinc in the ZnO solubility test in copper reduced tap water | 32 |
| Table 4: | Mass balance of the ZnO solubility test | 33 |
| Table 5: | Total Ti concentrations during the NM 105 stability test (I) | 34 |
| Table 6: | Total concentrations of Ag during the AgNO ₃ stability test in copper reduced tap water | 38 |
| Table 7: | Total Ag concentrations during the NM 300K stability test in copper reduced tap water | 40 |
| Table 8: | Total Ag concentrations in the filtrate of the NM 300K solubility test in copper reduced tap water | 41 |
| Table 9: | Calculated nPS concentrations of the test media in the nPS stability test | 43 |
| Table 10: | Endpoints of the feeding study. Water parameters after 192 h | 48 |
| Table 11: | Sampling scheme preliminary study with AgNO ₃ , *end of the uptake phase | 50 |

| | | |
|-----------|--|----|
| Table 12: | Preliminary study with AgNO ₃ : total Ag concentrations in test media and <i>C.f.</i> tissue, *end of the uptake phase | 50 |
| Table 13: | Preliminary study with NM 300K: total Ag concentrations in test media and <i>C.f.</i> tissue, *end of the uptake phase | 52 |
| Table 14: | Bioaccumulation study with AgNO ₃ – low concentration: total Ag concentrations in test media and <i>C.f.</i> tissue, *end of the uptake phase | 55 |
| Table 15: | Bioaccumulation study with AgNO ₃ – high concentration: total Ag concentrations in test media and <i>C.f.</i> tissue, *end of the uptake phase | 57 |
| Table 16: | Bioaccumulation study with NM 300K – low concentration: total Ag concentrations in test media and <i>C.f.</i> tissue, *end of the uptake phase | 61 |
| Table 17: | Bioaccumulation study with NM 300K – high concentration: total Ag concentrations in test media and <i>C.f.</i> tissue, *end of the uptake phase | 63 |
| Table 18: | Bioaccumulation study with NM 105 – low concentration: total TiO ₂ concentrations in test media and <i>C.f.</i> tissue, *end of the uptake phase | 66 |
| Table 19: | Bioaccumulation study with NM 105 – high concentration: total TiO ₂ concentrations in test media and <i>C.f.</i> tissue, *end of the uptake phase | 68 |

List of abbreviations

| | |
|----------------------|--|
| AF4-FLD-MALLS | Flourescence light detector coupled with asymmetrical flow field-flow fractioned and with multi-angle laser light scattering |
| BAF | Bioaccumulation factor |
| BCF | Bioconcentration factor |
| BMF | Biomagnification factor |
| C.f. | <i>Corbicula fluminea</i> |
| ICP-MS | Inductively coupled plasma – mass spectroscopy |
| ICP-OES | Inductively coupled plasma – optical emission spectroscopy |
| ICP-QQQ-MS | Triple Quadrupole – inductively coupled plasma mass spectroscopy |
| MNMs | Manufactured nanomaterials |
| MT | Metallothionein |
| NP | Nanoparticle |
| nPS | Nanoparticulate polystyrene |
| OECD | Organisation for Economic Co-operation and Development |
| PBT | Persistent, bioaccumulative, toxic |
| SDS | Sodium dodecyl sulfate |
| sp-ICP-MS | Single particle Inductively coupled plasma – mass spectroscopy |
| TWA | Time-weighted average |
| UBA | Umweltbundesamt |
| UHQ | Ultra High Quality Water |
| vPvB | Very persistent, very bioaccumulative |

Summary

The European Commission estimated the global production of produced manufactured nanomaterials (MNMs) to be 11.5 million tons per year which corresponds to a market value of 20 bn € (European Commission, 2012). Further industrialization and economic expansion of industrial countries and economies will further increase the production and usage of MNMs. MNMs are released into the environment during their production, their use and the disposal of nano functionalized products (Benn and Westerhoff, 2008; Mueller and Nowack, 2008; Gottschalk and Nowack, 2011). The increasing production of MNMs leads inevitably to a larger environmental burden and a reliable environmental risk assessment of MNMs is thus required (Levard *et al.*, 2012).

Due to their high annual production, several MNMs are subject to bioaccumulation assessment as required under the European Chemicals Registration REACH (European Parliament Council, 2006), the Japanese Chemical Substance Control Act “Kashinho” or others e.g. HPV, TCFCA or KKDIK (USEPA, 2004; Korea Ministry of Government Legislation, 2008; Naiki, 2010; Ministry of Environment and Urbanization(MoEU) of Turkey, 2017).

Under REACH, the bioconcentration factor (BCF) represents the most important endpoint for bioaccumulation assessment (ECHA, 2017). The BCF is mostly determined by fish flow-through studies in accordance to OECD test guideline 305 (de Wolf *et al.*, 2007; Organisation for Economic Co-operation and Development (OECD), 2012) which was developed for water-soluble test items. However, most MNMs tend to sediment in aquatic environments leading to problems with respect to the maintenance of stable and continuous exposure conditions during classic flow-through studies with MNMs. By this, the establishment of suitable experimental conditions for bioaccumulation studies is difficult. Thus, there is the need to develop suitable test methods adapted to the specific needs for testing nanomaterials (Aschberger *et al.*, 2011; Hankin *et al.*, 2011).

In 2018 a tiered testing approach to meet the requirements of MNM bioaccumulation testing was presented that also includes bioaccumulation tests with invertebrates which may provide indications allowing to waive further studies using fish as test organism (Handy *et al.*, 2018).

This is in accordance with the REACH Guidance on Information Requirements and Chemical Safety Assessment describing that other taxonomic groups than fish are allowed to be used to gain data for the assessment of the B criteria. In this context, the mussel bioconcentration test of the ASTM was suggested as a possible alternative (American Society for Testing and Materials, 2003; ECHA, 2017).

Marine, as well as fresh water bivalves have been widely used as bioindicators for pollution in aquatic systems, e.g. due to their ability to accumulate high concentrations of heavy metals in their tissue (Regoli and Orlando, 1994; Cossu *et al.*, 1997; Doyotte *et al.*, 1997; Vidal, Bassères and Narbonne, 2001; Geret, Serafim and Bebianno, 2003). Moreover, bivalves have been used for the determination of the bioavailability and the effects of xenobiotics and genotoxic compounds (Narbonne *et al.*, 1999; Vidal, Bassères and Narbonne, 2001; Legeay *et al.*, 2005). Filter-feeding bivalves considerably increase the pelagic-benthic coupling e.g. by the ingestion of particulate materials that are concentrated in feces or pseudofeces (Gergs, Rinke and Rothhaupt, 2009; Basen *et al.*, 2012). As described for AuNPs (Hull *et al.*, 2011), these particulate materials could be MNMs that are dispersed in the water. The filter-feeding behavior of bivalves and their benthic habitat make bivalves a group of organisms predominantly exposed to MNMs (Moore, 2006; Baun *et al.*, 2008; Griffitt *et al.*, 2008; Tedesco *et al.*, 2010; Baker, Tyler and Galloway, 2014). Mesocosm studies by Ferry *et al.* (2009) showed that bivalves represent an important

sink for MNMs, similar results were presented by Cleveland *et al.* (2012). Due to the fact that the feces and pseudofeces of bivalves represent an important part of the diet of benthic invertebrates, they may play a key role regarding the transfer of MNMs into the aquatic food chain (Karatajev, Burlakova and Padilla, 1997; Roditi, Strayer and Findlay, 1997). Bivalves may also represent a link between the aquatic and terrestrial environment being part of the diet of water birds (Custer and Custer, 1996; van Nes *et al.*, 2008). Mussels also represent an important route into the human food chain. Different species of marine and freshwater bivalves e.g. the mussels *Mercenaria mercenaria*, *Mytilus edulis* or *Corbicula fluminea* are on the menu in many countries worldwide (McMahon, 1983; Ferry *et al.*, 2009).

The fresh water bivalve *C. fluminea* is an invasive species that is, due to its ability to tolerate a wide range of environmental conditions and their extreme adaptability, widely spread in Africa, North and South America, Europe and the Pacific Islands (Phelps, 1994; Rajagopal, van der Gelde and bij de Vaate, 2000; Darrigran, 2002; Karatajev *et al.*, 2009). Due to the high filtration rate of *C. fluminea*, this species has a high potential to be used in bioaccumulation tests (Sousa, Guilhermino and Antunes, 2005). The euryoecious characteristics of this species enable *C. fluminea* to be used in test systems that are adjustable to meet the requirements of the wide spectrum of different MNMs.

The development of a suitable test system for bioaccumulation studies of MNMs with fresh water bivalves was the central aim of this project. Therefore, a flow-through system was developed that allows a continuous and constant exposure of MNMs to determine the bioavailability and bioaccumulation of MNMs in bivalves using *C. fluminea* as test species. The new test system provides optimal experimental conditions for the performance of bioaccumulation studies with bivalves. Good oxygen supply, moderate pH values and an acceptable burden of ammonia, nitrite and nitrate were recorded during the studies.

Test animals used in laboratory bioaccumulation studies were collected from the field, due to the long reproductive cycle and the high amount of animals required for bioaccumulation testing. A method for the husbandry of the animals was developed and allowed us to keep up to 2,000 mussels in 1.5 m³ microcosms, in which the mussels were housed in stainless steel baskets. Animals could be maintained for more than 12 months under this conditions leading to only moderate mortality. All main studies of this research project were carried out with animals from a single batch of mussels, which was collected in October 2017.

Based on the available literature, three MNMs (plus one ionic control substance) were chosen based on featuring differences in their major characteristics and tested for their bioaccumulation potential.

a) the silver nanoparticle NM 300K (AgNP)

NM 300K was tested as representative of MNMs that are well dispersible and release ions. AgNPs are some of the most used and commercialized MNMs, e.g. due to their antibacterial properties (Fabrega *et al.*, 2011; Bone *et al.*, 2012; Cleveland *et al.*, 2012; Vale *et al.*, 2016; Zhang, Hu and Deng, 2016; McGillicuddy *et al.*, 2017). The antibacterial effects are based on released Ag⁺ ions (Ag⁺) that cause disruptions of the respiratory chain of the cells, the deactivation of proteins and the disturbance of membrane transport processes (Bragg and Rainnie, 1974; Schreurs and Rosenberg, 1982; Feng *et al.*, 2000).

b) silver nitrate

AgNO₃ was used as test item representing the same element as NM 300K but in a non-nanoparticulate form allowing to compare the bioavailability, accumulation and fate of dissolved and particulate Ag.

c) the titanium dioxide nanomaterial NM 105 (TiO₂NP)

In contrast to AgNPs, TiO₂NPs such as MNM NM 105 are nearly chemical inert and are one of the most commonly used MNMs (Piccinno *et al.*, 2012) representing non- ion-releasing and highly sedimenting MNMs. TiO₂NPs are of great ecotoxicological interest due to their potential to alter the bioavailability and thus the toxicity of co-existing contaminants like heavy metals or organic compounds in aquatic organisms like fishes and bivalves (Zhang *et al.*, 2007; Zhu, Zhou and Cai, 2011; Balbi *et al.*, 2014; Vale *et al.*, 2014; Farkas *et al.*, 2015; Fan *et al.*, 2017).

d) polystyrene nanoparticle Fluoro-Max™ (nPS)

The polystyrene nanoparticle Fluoro-Max™ represent MNMs that are based on organic polymers. The particles were homogenously spiked with a fluorescence dye to allow the detection of the NPs. In this way the bioavailability and accumulation of the nPS within the mussel's soft tissue could be determined using a fluorescence light detector coupled with asymmetrical flow field-flow fractionation and with multi-angle laser light scattering and fluorescence microscopy.

For the elucidation of the bioavailability, uptake and elimination of the tested metal and metal oxide based MNMs in the soft tissue of *C. fluminea*, total Ag and Ti concentrations were measured in the animal's soft tissue using inductively coupled plasma mass spectrometry or optical emission spectroscopy (ICP-MS or ICP-OES). Determination of particle concentrations in the soft tissue was carried out by single particle coupled plasma mass spectrometry (sp-ICP-MS).

The bioaccumulation studies for the different MNMs were conducted with two concentrations each. An exception was the nPS material that was tested with just one concentration due to the high test concentration (approx. 5 mg nPS/L) required to allow the measurement of the test item. The tissue was examined by fluorescence microscopy.

The main study on the bioaccumulation of nPS was carried out using common aquaria in a semi-static setting due to the easier handling and limited amount of nPS. During the exposure with nPS, the animals showed the strongest filtration activity observed in all exposure studies carried out in this project. A high production rate of feces and pseudofeces was observed. The nPS were not only ingested very rapidly and accumulated in the feces, they were also eliminated quickly. Highest fluorescence levels were found in the viscera, the gastrointestinal tract and the feces in which the nPS seemed to accumulate. The strong elimination of the ingested nPS by defecation highlighted the role of filter feeders in the aquatic food web.

In the case of the other MNMs, we were able to estimate BAF values under steady state conditions and gained clear kinetics for the uptake and elimination of the MNMs or ions. For AgNO₃, BCF estimates could be determined. Comparable values were gained for total Ag concentrations in mussel tissue following exposure to NM 300K and AgNO₃. For the higher test concentrations BAF_{ss} and BCF_{ss} values of approx. 31 were calculated. The BAF_{ss} and BCF_{ss} values calculated for the lower test concentrations were broadly of the same magnitude but showed a higher deviation with a BAF_{ss} and BCF_{ss} of approx. 130 and 711 for NM 300K and AgNO₃, respectively. The different values may have been the result of different filtration activities induced by free Ag⁺ ions representing a protective behaviour. The calculated distribution factors of accumulated Ag for the different tissue compartments (mantle, foot, muscle and viscera) were similar for both exposure scenarios (NM 300K vs. AgNO₃). In both cases the viscera and mantle showed the highest Ag concentration, whereas the muscle tissue showed the lowest concentration. This might be explained by the expression of metallothioneins (MT) and their Ag⁺ binding properties. MTs are known to be mainly present in the gills as part of the viscera and the mantle (Hardivillier *et al.*, 2006).

In the bioaccumulation studies with NM 105, only the viscera showed a higher distribution factor. BAF_{ss} values of 6,150 and 9,022 were estimated for the low and high concentrated treatments, respectively. In comparison to the Ag treatments no filtration reduction was observed during exposure and the elimination of the measured Ti content in the soft tissue decreased very fast within a few hours of the depuration phases.

The observed fast elimination of the nanoforms as well as the distribution, concentrated in the viscera, clearly indicate that the MNMs were not really incorporated and only ingested by the animals. Therefore, the time required to eliminate the previously ingested material and to reach a body burden that is comparable to the start conditions was suggested as an alternative endpoint for bioaccumulation assessment of MNMs that is more meaningful than the BAF_{ss}.

The bioaccumulation studies with the fresh water bivalve *C. fluminea* demonstrated the suitability of the new test system. During all studies a continuous exposure with stable MNM concentrations was achieved. The elucidation of bioavailability, uptake and elimination as well as accumulation of the test items was possible on the level of total and particle concentrations for the whole soft body as well as the single tissue compartments. By this, the fate of MNMs within the body and at the level of different tissues could be further clarified. However, methods like correlative microscopy using transmission electron microscope are required for the absolute evidence if MNMs are really incorporated into the tissue or penetrated into cells. Nevertheless, the results obtained with this test system can be used to generate useful information required for regulatory purposes and could be included in a tiered bioaccumulation testing strategy for MNMs as suggested by Handy *et al.*, 2018.

Even if MNMs are not really bioaccumulated by the freshwater bivalve *C. fluminea*, the estimated BAF_{ss} represent a valuable indication for a mobilization of MNMs by bivalves leading to a transfer of MNMs into the aquatic food chain via predators or benthic invertebrates that feed on bivalve feces and / or pseudo feces (Karatayev, Burlakova and Padilla, 1997; Roditi, Strayer and Findlay, 1997; Gergs, Rinke and Rothhaupt, 2009). The transfer of MNMs into the human diet needs to be discussed further (McMahon, 1983). The concentration of the test item in the feces or pseudo feces of the bivalves and the time needed to eliminate most of the previously accumulated material may provide the basis for improved regulatory endpoints.

Generally, pretests need to be carried out for bioaccumulation studies with MNMs to ensure the homogenous distribution of the test item in the test system and to estimate a suitable exposure concentration to avoid protective behavior of the bivalves as described for Ag⁺.

Zusammenfassung

Die EU schätzt, dass die jährliche Produktionsrate von Nanomaterialien (MNM) weltweit bei etwa 11,5 Mio. Tonnen und einem Marktwert von 20 Mrd. € liegt (European Commission, 2012). Die Produktion sowie der Einsatz von MNMs werden weiter zunehmen. Hierdurch gelangen mehr und mehr MNMs in die Umwelt. Dies geschieht sowohl während ihrer Produktion, der Verwendung, als auch bei der Entsorgung (Benn und Westerhoff, 2008; Mueller und Nowack, 2008; Gottschalk und Nowack, 2011). Somit führt die steigende Produktion von MNMs unweigerlich zu einer höheren Umweltbelastung und macht damit eine verlässliche Risikobewertung für die Umwelt unerlässlich (Levard *et al.*, 2012).

Aufgrund ihrer hohen jährlichen Produktionsrate unterliegen verschiedene MNMs einer Bewertung ihres Bioakkumulationspotenzials, etwa im Rahmen des Europäischen Chemikalienrechts REACH (European Chemicals Registration REACH) (European Parliament Council, 2006), dem japanischen „Chemical Substance Control Act Kashinho“ (Naiki, 2010) oder anderen wie HPV, TCFCA oder KKDIK (USEPA, 2004; Korea Ministry of Government Legislation, 2008;; Ministry of Environment and Urbanization(MoEU) of Turkey, 2017).

Im Rahmen von REACH repräsentiert der Biokonzentrationsfaktor (BCF) den wichtigsten Endpunkt der Bewertung des Bioakkumulationspotenzials von Chemikalien (ECHA, 2017). Der BCF wird üblicherweise in Durchflussstudien mit Fischen gemäß der OECD Test Richtlinie 305 ermittelt, welche für wasserlösliche Testsubstanzen entwickelt und optimiert wurde (de Wolf *et al.*, 2007; Organisation for Economic Co-operation and Development (OECD), 2012).

Die meisten MNMs tendieren jedoch dazu, in aquatischer Umgebung zu sedimentieren, was zu Problemen hinsichtlich stabiler und kontinuierlicher Expositionskonzentrationen bei Anwendung des klassischen Studiendesigns führt. Somit können die für die Bewertung erforderlichen validen und plausiblen Testbedingungen kaum erreicht werden. Daher ist es notwendig, angemessene Testmethoden zu entwickeln, die an die spezifischen Anforderungen der Untersuchung von MNMs angepasst sind (Aschberger *et al.*, 2011; Hankin *et al.*, 2011).

Ein gestuftes Testverfahren zur Bewertung des Bioakkumulationspotentials von MNMs wurde kürzlich präsentiert (Handy *et al.*, 2018), das die besonderen Eigenschaften und Anforderungen von MNMs berücksichtigt und Bioakkumulationstests mit Invertebraten einbezieht. Diese Tests sollen Hinweise liefern, ob Fische als Testtiere in der weiteren Bewertung verzichtbar sind.

Dieser Ansatz ist vereinbar mit den Leitlinien zu den Informationsanforderungen und zur Stoffsicherheitsbeurteilung der REACH Verordnung, welche angibt, dass andere taxonomische Gruppen als die der Fische verwendet werden können, um Daten zur Beurteilung des B-Kriteriums zu generieren, sofern andere Organismen relevantere Zielorganismen darstellen. In diesem Zusammenhang wird etwa der Muschelbiokonzentrationstests der ASTM angeführt (American Society for Testing and Materials, 2003; ECHA, 2017).

Marine, aber auch Süßwassermuscheln sind aufgrund ihrer Eigenschaft, hohe Konzentrationen an Schwermetallen zu akkumulieren, als Bioindikatoren für Belastungen in Gewässern etabliert (Regoli und Orlando, 1994; Cossu *et al.*, 1997; Doyotte *et al.*, 1997; Vidal, Bassères und Narbonne, 2001; Geret, Serafim und Bebianno, 2003). Darüber hinaus werden Muscheln zur Bestimmung der Bioverfügbarkeit und Untersuchung schädigender Effekte von Xenobiotika und genotoxischer Verbindungen verwendet (Narbonne *et al.*, 1999; Vidal, Bassères und Narbonne, 2001; Legeay *et al.*, 2005). Filtrierende Muscheln tragen erheblich zur Kopplung der benthischen und pelagischen Bereiche in aquatischen Lebensräumen bei. Etwa indem sie Schwebstoffe und suspendierte Teilchen aufnehmen und in konzentrierter Form über ihren Fäzes ausscheiden und somit den Transfer in die aquatische Nahrungskette verstärken (Gergs, Rinke und Rothhaupt,

2009; Basen *et al.*, 2012). Dieser Vorgang wurde für im Wasser suspendierte Teilchen in Form von AuNPs beschrieben (Hull *et al.*, 2011). Sowohl das Filtrationsverhalten der Muscheln (zum Zweck der Nahrungsaufnahme und der Atmung), als auch ihre benthische Lebensweise machen Muscheln zu einer Gruppe von Organismen, die im Besonderen von der Exposition mit MNMs in der Umwelt betroffen sein kann (Moore, 2006; Baun *et al.*, 2008; Griffitt *et al.*, 2008; Tedesco *et al.*, 2010; Baker, Tyler und Galloway, 2014). In Mesokosmenstudien wurde bereits gezeigt, dass Muscheln eine der Hauptsinken für MNMs in aquatischen Lebensräumen darstellen (Ferry *et al.*, 2009; Cleveland *et al.*, 2012). Aufgrund der Tatsache, dass der Fäzes der Muscheln eine wichtige Nahrungsgrundlage für benthische Invertebraten darstellt, könnten filtrierende Muscheln eine Schlüsselrolle für den Transfer von MNMs in die aquatische Nahrungskette spielen (Karatayev, Burlakova, Padilla, 1997; Roditi, Strayer und Findlay, 1997). Als Bestandteil der Nahrung von Wasservögeln stellen Bivalvia zudem eine Verbindung zwischen der aquatischen und terrestrischen Umwelt dar (Custer und Custer, 1996; van Nes *et al.*, 2008).

Verschiedene marine und Süßwassermuschelarten wie z.B. *Mercenaria mercenaria*, *Mytilus edulis* oder *Corbicula fluminea* werden weltweit in vielen Ländern als Speisemuscheln genutzt und repräsentieren somit eine potentielle Route für MNMs in die menschliche Nahrung (McMahon, 1983; Ferry *et al.*, 2009). Die Süßwassermuschel *C. fluminea* ist eine invasive Art, welche aufgrund ihrer euryöken Toleranzbereiche wie auch der enormen Anpassungsfähigkeit in Afrika, Nord- und Südamerika, Europa und den Pazifischen Inseln weit verbreitet ist (Phelps, 1994; Rajagopal, van der Gelde und bij de Vaate, 2000; Darrigran, 2002; Karatayev *et al.*, 2009). Ihre hohe Filtrationsrate macht sie zu einem geeigneten Kandidaten für den Einsatz von Muscheln im Rahmen von Bioakkumulationsstudien (Sousa, Guilhermino and Antunes, 2005). Ihre weiten Toleranzbereiche bezüglich zahlreicher Umweltfaktoren ermöglichen ihren Einsatz in Systemen mit hohen Anpassungsmöglichkeiten wie sie benötigt werden, um ein weites Spektrum an MNMs testen zu können.

Die Entwicklung eines solchen Systems zur Untersuchung der Bioakkumulation von MNMs in Süßwassermuscheln war das zentrale Ziel dieses Forschungsvorhabens. Ein Durchflusssystem wurde entwickelt, welches konstante Expositionen von MNMs unter homogenen Konzentrationsbedingungen erlaubt. Somit kann die Bioverfügbarkeit und das Bioakkumulationspotenzial von MNMs in Bivalvia unter Verwendung von *C. fluminea* als Testspezies bestimmt werden. Das neue Testsystem stellt optimale Versuchsbedingungen für die Versuchsdurchführung von Bioakkumulationsstudien mit Muscheln dar: gute Sauerstoffversorgung, moderate pH-Werte und akzeptable Belastungen durch Ammonium, Nitrit und Nitrat.

Aufgrund der hohen Anzahl an Tieren, die zur Durchführung aller Methodenentwicklungen, Vor- und Hauptstudien benötigt wurden, sowie aufgrund des langen Reproduktionszyklus der Tiere, wurden die Versuchstiere im Feld gesammelt. Eine Hälterungsmethode wurde entwickelt, welche die Hälterung von bis zu 2000 Tieren in 1.5 m³ Mikrokosmen ermöglicht. Die Tiere können auf diese Weise über 12 Monate im Labor gehältert werden und weisen unter diesen Bedingungen nur eine moderate Mortalität auf. Somit konnten alle Tiere, welche in den Hauptstudien dieses Vorhabens eingesetzt wurden, aus einer einzelnen Tiergruppe bezogen werden, die im Oktober 2017 gesammelt wurde.

Zur Bestimmung des Bioakkumulationspotenzials von MNMs anhand dieses Testsystems wurden repräsentative Vertreter von MNMs ausgewählt und getestet, die sich deutlich in ihren physikalisch-chemischen Eigenschaften unterscheiden und die eine hohe industrielle Relevanz aufweisen:

a) Silbernanopartikel NM 300K (AgNP)

NM 300K stellt sowohl einen Vertreter ionenfreisetzender MNMs wie auch der gut dispergierbaren MNMs dar. AgNPs gehören zu den am meisten verwendeten MNMs, z.B. aufgrund ihrer antibakteriellen Wirkung (Fabrega *et al.*, 2011; Bone *et al.*, 2012; Cleveland *et al.*, 2012; Vale *et al.*, 2016; Zhang, Hu und Deng, 2016; McGillicuddy *et al.*, 2017). Diese basiert auf ihrer Eigenschaft Ag⁺ Ionen (Ag⁺) freizusetzen, welche die Atmungskette der Zellen unterbrechen, Enzyme deaktivieren und Membrantransportprozesse stören (Bragg und Rainnie, 1974; Schreurs und Rosenberg, 1982; Feng *et al.*, 2000).

b) Silbernitrat

AgNO₃ wurde als Testsubstanz eingesetzt, um ein identisches Element in nicht nanostruktureller Form zu testen. Dies ermöglicht den Vergleich der Ergebnisse zur Bioverfügbarkeit, der Akkumulation und des Schicksals des Ag aus rein gelöster Form (AgNO₃), sowie aus nanopartikulärer (AgNP) und daraus gelöster Form (Ag⁺), in diesem Fall freigesetzt durch NM 300K.

c) Titandioxidnanopartikel NM 105 (TiO₂NP)

Im Gegensatz zu AgNPs sind TiO₂NPs nahezu chemisch inert und stellen ebenfalls eine der meist verwendeten MNMs dar (Piccinno *et al.*, 2012). NM 105 repräsentierte im Vorhaben somit nicht ionenfreisetzende MNMs sowie stark sedimentierende MNMs. TiO₂NPs sind von großem ökotoxikologischen Interesse, z.B. aufgrund ihres Potenzials die Bioverfügbarkeit und damit auch die Toxizität anderer Schadstoffe wie Schwermetalle oder organische Verbindungen bei Co-Exposition gegenüber aquatischen Organismen, wie Fischen oder Muscheln, zu beeinflussen (Zhang *et al.*, 2007; Zhu, Zhou und Cai, 2011; Balbi *et al.*, 2014; Vale *et al.*, 2014; Farkas *et al.*, 2015; Fan *et al.*, 2017).

d) Polystyrolnanopartikel Fluoro-Max™ (nPS)

Das Polystyrolnanopartikel Fluoro Max™ stellte im Vorhaben den Vertreter solcher MNMs dar, welche auf organischen Polymeren basieren. Die getesteten nPS waren homogen mit einem Fluoreszenzfarbstoff markiert, der es erlaubte, die Bioverfügbarkeit, die Akkumulation und Lokalisierung der nPS im Weichkörper der Muscheln z.B. mittels Fluoreszenzdetektor und -mikroskop zu erfassen.

Zur Bestimmung der Bioverfügbarkeit, Aufnahme, Elimination und Bioakkumulation der getesteten Metall- oder Metalloxid MNMs sowie von Ag⁺ im Weichkörper der Tiere wurde der Totalgehalt der Metalle mittels Massenspektrometrie mit induktiv gekoppeltem Plasma (ICP-MS) oder optischer Emissionsspektrometrie mit induktiv gekoppeltem Plasma (ICP-OES) ermittelt. Die Bestimmung der Einzelpartikelkonzentrationen im Weichgewebe erfolgte mittels Einzelpartikel ICP-MS (sp-ICP-MS).

Mit Ausnahme des nPS wurden alle MNMs in den Hauptstudien mit zwei Konzentrationen getestet. Polystyrolnanopartikel (nPS) wurden mit einer deutlich höheren Konzentration (5 mg nPS/L) getestet, um eine ausreichend hohe Gewebekonzentration für die Detektoranalyse zu erzielen. Das Weichgewebe sowie die einzelnen Gewebekompartimente wurden mittels Fluoreszenzmikroskop untersucht.

Die Hauptstudie mit nPS wurde im semi-statischen Design durchgeführt, da die Menge an verfügbaren nPS nicht für eine mehrtägige Durchflussstudie ausgereicht hätte. Die Studien wurden zudem in regulären Aquarien durchgeführt, da ein semi-statischer Ansatz mit einem verringerten Medienvolumen in der neuen Testanlage deutlich aufwendiger gewesen wäre. Während der Exposition mit nPS wurde die stärkste Filtrationsaktivität der Tiere im Rahmen

aller in diesem Projekt durchgeführten Studien beobachtet. Diese ging einher mit einer deutlich verstärkten Produktion und Freisetzung von Fäzes und Pseudofäzes. Hierbei wurden die nPS nicht nur sehr schnell aufgenommen, sondern auch sehr schnell eliminiert, was sich auch in den Fluoreszenzmessungen zeigte. Das Viszeralgewebe, der Gastrointestinaltrakt sowie der Fäzes stellten sich bei der Gewebeanalyse als Orte hoher Fluoreszenzintensität dar. Die schnelle Eliminierung kann durch Defäkation erklärt werden

Für die anderen MNMs und das AgNO_3 konnten BAF bzw. BCF Werte unter Konzentrationsgleichgewichtszuständen sowie kinetische Verläufe für die Aufnahme und Elimination der Substanzen ermittelt werden.

Für NM 300K und AgNO_3 wurden bezüglich der Anreicherung von Silber vergleichbare Werte ermittelt. In beiden Studien wurden für die höheren Ag Konzentrationen BCF/BAF Werte von rund 31 ermittelt. Die Werte, die bei den geringeren Konzentrationen ermittelt wurden, lagen in derselben Größenordnung mit einem BAF_{ss} von rund 130 für NM 300K und einem BCF_{ss} von rund 710 für AgNO_3 , zeigten jedoch eine größere Abweichung voneinander. Diese unterschiedlichen Anreicherungsgrade könnten durch die unterschiedlich starken Filtrationsaktivitäten der Tiere als Reaktion auf die erhöhten Ag^+ Konzentrationen im Wasser erklärt werden, welche zu reduzierten Filtrationsraten als Schutzmechanismus führten. Die ermittelten Distributionsfaktoren für Ag in den verschiedenen Kompartimenten (Mantel, Fuß, Adduktorenmuskel und Viszeralmasse) waren für beide Formen der Silberexposition (partikulär und gelöst) vergleichbar und wiesen bei beiden Expositionsformen die höchsten Werte für das Viszeral- und Mantelgewebe auf. Dies könnte durch die verstärkte Präsenz von Metallothioneinen in den Kiemen (zur Viszera gehörend) und dem Mantel erklärt werden (Hardivillier *et al.*, 2006).

Im Fall der NM 105 Exposition wies nur das Viszeralgewebe im Vergleich zu den anderen Geweben einen höheren Distributionsfaktor auf. BAF_{ss} von 6150 und 9022 wurden jeweils für die niedrigere und die höhere Testkonzentration ermittelt. Bei der NM 105 Exposition wurde keine veränderte Filtrationsaktivität beobachtet. Die Titandioxidgewebekonzentrationen zeigten einen rapiden Abfall in der Depurationsphase und erreichten innerhalb weniger Stunden das Anfangsniveau.

Sowohl die schnelle Elimination als auch die ermittelten Distributionsfaktoren der MNMs weisen darauf hin, dass diese zwar physikalisch aufgenommen, aber nicht wirklich physiologisch verfügbar waren und demnach nur den Gastrointestinaltrakt durchwanderten. Daher wurde die Zeit bis zum Erreichen der Gewebeausgangskonzentration ab Beginn der Depurationsphase als alternativer Endpunkt und Ergänzung zum BAF_{ss} vorgeschlagen.

Die Bioakkumulationsstudien mit *C. fluminea* zeigten, dass das neue Testsystem geeignet ist, um die Bioverfügbarkeit und das Bioakkumulationspotenzial von MNMs unter konstanten Konzentrationsbedingungen zu ermitteln. Die Konzentrationsbestimmung im Gewebe konnte für den ganzen Weichkörper wie auch für die einzelnen Gewebekompartimente sowohl auf Ebene des Totalgehalts als auch auf Ebene der Einzelpartikel durchgeführt werden. Dennoch sollten gerade bei der analytischen Betrachtung weitere Methoden wie die korrelative Mikroskopie in Betracht gezogen werden, um genaue Informationen zur Lokalisierung der Partikel zu erhalten: angelagert an Membranen oder eingedrungen in einzelne Zellen? Unabhängig davon kann das entwickelte System wertvolle Daten für erforderliche regulatorische Prozesse liefern und auch in gestufte Teststrategien für MNMs integriert werden (Handy *et al.*, 2018).

Auch wenn einige MNMs nicht wirklich bioakkumulieren, stellt der gewonnene BAF_{ss} Wert eine wertvolle Grundlage zur Abschätzung des Transfers von MNMs durch Bivalvia in die benthische

Nahrungskette dar (Karatayev, Burlakova und Padilla, 1997; Roditi, Strayer und Findlay, 1997; Gergs, Rinke und Rothhaupt, 2009). Die Konzentration von MNMs im Fäzes/Pseudofäzes der Muscheln und die erforderliche Zeit zur vollständigen Elimination der zuvor aufgenommenen MNMs liefern wichtige Hinweise zum Bioakkumulationspotential von MNMs und könnten als ergänzende Endpunkte für die regulatorische Bewertung eingesetzt werden. Der Transfer von MNMs in die menschliche Nahrungskette bedarf weiterer Untersuchungen (McMahon, 1983).

Insgesamt bleibt festzuhalten, dass die Durchführung von Vortests zu Bioakkumulationsstudien mit Bivalvia zu empfehlen ist, um die homogene Verteilung der zu testenden MNMs im Testsystem sicherzustellen und die Eignung der im Haupttest eingesetzten Testkonzentration zu überprüfen. Dabei ist insbesondere auf eine angemessene Dosierung zu achten, die das Auslösen des "Schutzverhaltens" der Muscheln, wie für Ag⁺ beobachtet, ausschließt.

1 Introduction

The identification and scientific assessment of compounds that bioaccumulate in organisms and biomagnify in food webs play a key role within the PBT- assessment. The bioaccumulation potential of compounds is commonly expressed as bioconcentration factors (BCF) determined in flow-through studies with fish.

An experimentally determined BCF of > 2,000 (classification as PBT-compound) or > 5,000 (classification as vPvB-compound) is used as threshold value for bioaccumulation assessment (European Parliament Council, 2006). The uptake of the test item by the body surface (e.g. gills) is thus decisive. BCF-tests (exposition via the water) are mainly carried out according to OECD TG 305 (OECD, 2012) as flow-through tests using fishes.

Bioconcentration studies estimate the increase of the test item concentration in the whole organism or specific tissues of the test animal in relation to the concentration of the test item in the surrounding media. During exposure, the concentration of the test item in the test system should not vary more than $\pm 20\%$ from the average concentration measured over the exposition phase.

Bioaccumulation studies with manufactured nanomaterials (MNMs) are difficult to carry out due to the lack of suitable test systems that allow a permanent and constant exposure to the test item. In contrast to organic compounds, the behaviour of MNMs in the environment and biological media is mainly influenced by processes like (hetero-) aggregation, sedimentation, adsorption of other compounds, adhesion to surfaces, transformation and dissolution of the MNMs. Those processes are caused by the characteristics of the particles (size, geometry, surface properties) as well as by the environmental conditions (e.g. pH-value, salinity, content of total organic carbon).

There are currently no test systems available that allow a constant exposure to MNMs. Biomagnification studies (exposition by the food) according to OECD 305 (OECD, 2012) could be an alternative, but the unrealistic exposure scenario (commercial carp or trout food enriched with the test item) may cause artificial results.

Due to the MNMs' property to sediment, depending on their density and agglomeration processes, they will be mainly present at the bottom of the aquatic ecosystem and less in the water phase. Therefore, it may be expected that the MNMs are primarily taken up by benthic species (Voelker *et al.*, 2015). Therefore, it is important to look for MNM's impact on organisms that live on or in the sediment. At the Horizontal meeting in Berlin, 2013, it was recognized that there is a lack of information about the impact of MNMs on such organisms including filter feeders (OECD, 2014).

In North America the fresh water amphipod *Hyaella azteca* (*H.a.*) has been established as standard test organism for aquatic toxicity tests. Due to its special kind of feeding by grazing on the sediment surface, *H.a.* could be a suitable test organism for test items which tend to accumulate in the sediment (Othman and Pascoe, 2001). *H.a.* has been successfully used in studies on metal uptake and bioaccumulation (e.g. Kühr *et al.*, 2018; Shuhaimi-Othman and Pascoe, 2007; Borgmann, 1998; Ball, Borgmann and Dixon, 2006; Norwood, Borgmann and Dixon, 2007; Alves, Borgmann and Dixon, 2009).

Mussels are able to live in high densities on the ground of aquatic systems if suitable sediments are available. They filtrate high amounts of water through their gill system to gain oxygen and to extract plankton which represents an important part of their diet. Different studies have shown that mussels are able to ingest and to incorporate MNMs suspended in water (Ward and Kach,

2009; Hull *et al.*, 2011; Conway *et al.*, 2014). Cilia filtrate the particles from the water and transport them, attached to mucus, to the mouth (Amler, Fischer and Rogalla, 2000). For soluble compounds such as AgNPs, the uptake of dissolved material from the surrounding media and the uptake of particulate matter cannot be differentiated by this kind of uptake pathway. Therefore, using filtering mussels as test organism only allows to investigate the overall accumulation of test material. Only the less specific bioaccumulation factor (BAF) reflecting the bioaccumulation of dissolved and particulate material can be determined. However, analysis of single particle numbers and total concentration distribution in the soft tissue can provide complementary information on the bioaccumulation potential of MNMs.

Standardized test methods to investigate the bioaccumulation of substances in mussels are available, but have been developed and optimized for soluble, non-particulate substances (e.g. American Society for Testing and Materials, 2003). Therefore, the development of a test system allowing to apply MNMs at constant exposure concentrations was required.

2 Objectives of the research project and project realization

2.1 Objectives of the research project

The aims of this research project were:

- a. Development of a suitable test system to determine the bioaccumulation of MNMs using filtering organisms (Bivalvia)
- b. Determination of the bioaccumulation potential of selected MNMs featuring differences in their major characteristics
- c. Estimation of suitable endpoints for bioaccumulation assessment of MNMs
- d. Identification of limiting factors for test performance and optimizing the test system and design

2.2 Project structure

The research project was divided in six parts. In the first part, MNMs featuring specific characteristics and a suitable test species (freshwater bivalve) were selected. In the second part, the relevant physical and chemical properties of the selected MNMs were specified. The third part comprised the measurement and characterization of single particles in the test media using inductively coupled plasma mass spectroscopy (sp-ICP-MS). The fourth part included the development, testing and establishment of the new test system allowing constant exposure conditions. The experimental investigations on the bioaccumulation of the selected MNMs were carried out in the fifth part. A discussion of the results and recommendations for a specific test implementation are provided (part six).

3 Selection of test species and nanomaterials

3.1 Selection of test species and husbandry

The Asian clam *Corbicula fluminea* (C.f.) and the zebra mussel *Dreissena polymorpha* were considered as potential species for bioaccumulation testing. Both species are exotic invaders commonly found in Germany / Europe. The sampling of *Dreissena polymorpha* is difficult due to the increasing abundance of the Quagga mussel *Dreissena bugensis* which is morphological difficult to discern from *Dreissena polymorpha*. Therefore, C.f. (Fig. 1) was selected as test species used in this project. Animals used in this project were collected from the field, due to their long reproduction cycle and the high amount of animals required for bioaccumulation testing.

Because of the high demand of test animals required for the studies and pre-tests carried out in this project, locations for field collection of C.f. were identified based on monitoring data from the North Rhine-Westphalia State Agency for Nature, Environment and Consumer Protection. Animals used in the studies were collected from the river Niers (47669, Wachtendonk) which contains a dense population of C.f.. Due to the high amount of animals required for bioaccumulation testing, collected animals were kept in 1.5 m³ microcosms prior to be used in the experiments. Up to 2,000 mussels were placed in stainless steel baskets within the microcosms (Fig. 2) with frequent water exchange (every three weeks), aeration and slight water circulation. Animals were fed with a suspension of fine milled stinging nettle leaves. Animals could be maintained for at least 12 months under this conditions. Only moderate mortality was observed. All main studies of this research project were carried out with animals from the same batch of animals, collected in October 2017. All experimental animals were kept in the mesocosms for at least 14 days before they were used in the bioaccumulation test. During this time the mussels could depurate previously accumulated contaminants.

3.2 Selection of nanomaterials

Based on the available literature, four groups of MNMs were differentiated by their major characteristics.

- a) MNMs that release ions
- b) MNMs with no ion release
- c) MNMs that are well dispersible
- d) MNMs that are based on organic polymers

For each group one representative compound was selected:

The following MNMs were selected:

- a) Zinc oxide nanomaterial NM 110
- b) Titanium dioxide nanomaterial NM 105 (TiO₂NPs)
- c) Silver nanomaterial NM 300K (AgNPs). Silver nitrate (AgNO₃) was used (fifth test item), representing the same element in non-nanoparticulate form
- d) Polystyrene nanoparticle Fluoro-Max™ (nPS)

Figure 1: *Corbicula fluminea*



Source: Fraunhofer IME

Figure 2: Husbandry of *Corbicula fluminea* in a mesocosm



Source: Fraunhofer IME

4 Nanomaterials: Elucidation of physical and chemical properties

Different tests were carried out to determine the key chemical and physical properties of the test items which are essential to be considered to ensure the preparation of stable stock solutions or suspensions for bioaccumulation testing.

4.1 Zinc oxide nanomaterial NM 110

4.1.1 Solubility test

4.1.1.1 Test design

A solubility test for the zinc oxide nanomaterial NM 110 was carried out to elucidate the solubility of the compound in the test media (copper-reduced tap water). Glass products like Erlenmeyer flasks or glass beakers were cleaned with high purity grade acids (aqua regia) before usage in the test to avoid distortion of the analytical measurements by contamination. The acid treatment was supplied overnight, followed by rinses with nitric acid (HNO₃) and ultra-high quality water (UHQ). Stock suspensions with two different concentrations, separated by factor 10, were produced by adding weighed aliquots of NM 110 to copper reduced tap water. The suspensions were transferred into Erlenmeyer flasks and shaken at 100 rpm by a shaking device. Media samples were taken at the start (day d0) and at the following three days (d1-d3, Tab. 1). Zinc was measured as equivalent to zinc oxide (ZnO). Samples for the determination of the total zinc content were acidified using high purity grade HNO₃ to guarantee that the whole zinc oxide was dissolved. Additional samples were taken and transferred into Sartorius Viva Spin® ultrafiltration units with a pore size of 3,000 Dalton. Samples were centrifuged at 3,500 rpm (2851 x g) for 60 minutes. The filtrates were acidified with HNO₃. The supernatant was rinsed with aqua regia to allow the quantification of the non-dissolved / particulate ZnO. An additional sample was handled in an analogous way, whereby the supernatant was rinsed with copper reduced tap water. The obtained sample was not acidified to allow sp-ICP-MS measurements. In addition, samples for the sp-ICP-MS measurements were taken directly from the Erlenmeyer flask.

4.1.1.2 Analytics

The measurement of the total Zn concentration was carried out using an Agilent 8900 Triple Quadrupole ICP-MS (ICP-QQQ-MS). Calibration solutions were prepared in the range of 1, 5, 10, 25 and 50 µg/L using certified standard solutions diluted in HNO₃ (10 %). To avoid interference, the isotope ⁶⁴Zn was measured in the reaction mode with helium in addition to the no-gas mode. A certified water reference material was measured as quality control sample as well as duplicated calibration solution samples for evaluation of validity of the measurement. Additional blank samples were measured between samples to detect a possible carryover within the system. Additional rinses of the measurement system with hydrochloric acid (3 %) and nitric acid (10 %) were necessary to minimize the carryover. For the sp-ICP-MS measurements, the isotope ⁶⁴Zn was selected and measured in the helium mode.

Table 1: Samplings zinc solubility test

| Samplings [ml] | | |
|----------------|----|---------------------------------|
| d0 | 20 | Total concentration measurement |
| | 15 | Single-Particle |
| | 15 | Viva Spin sample water |
| | 15 | Viva Spin sample aqua regia |
| d1 | 20 | Total concentration measurement |
| | 15 | Single-Particle |
| | 15 | Viva Spin sample water |
| | 15 | Viva Spin sample aqua regia |
| d2 | 20 | Total concentration measurement |
| | 15 | Single-Particle |
| | 15 | Viva Spin sample water |
| | 15 | Viva Spin sample aqua regia |
| d3 | 20 | Total concentration measurement |
| | 15 | Single-Particle |
| | 15 | Viva Spin sample water |
| | 15 | Viva Spin sample aqua regia |

4.1.1.3 Mass balance

The total amount of zinc in the Erlenmeyer flasks was measured at test start to allow the establishment of a mass balance. The amount of zinc that was removed from the Erlenmeyer flask by the daily samplings was calculated (Tab. 1 & 2). The remaining suspension in the Erlenmeyer flasks after the last sampling was filled up to 250 ml using aqua regia. The solution was shaken to dissolve potentially adhered zinc oxide from the glass. After that samples were taken for determination of total zinc concentrations. A mass balance for zinc measured in the test system during the solubility test was calculated.

Table 2: Total concentrations zinc solubility test in copper reduced tap water

| Test day | Concentration 1 [mg/L] | Concentration 2 [mg/L] |
|----------|------------------------|------------------------|
| d0 | 1,395.62 | 135.09 |
| d1 | 753.76 | 100.07 |
| d2 | 643.30 | 92.46 |
| d3 | 640.76 | 76.20 |

4.1.1.4 Results

Initial concentrations of total zinc with 1,395.62 mg/L and 135.09 mg/L (for Conc. 1 and 2) were determined (Tab. 2). The percentage of dissolved, non-particulate zinc (measured concentration of the filtrate) in relation to the total Zn concentration increased from 17 % (Conc. 1) and 51 % (Conc. 2) at d0 to 75 % and 76 % at d3 (Tab. 3). The mass balance shows that the recovery has been acceptable: approx. 101 % for Conc. 1 and approx. 110 % for Conc. 2 (Tab. 4). Already at d0 no particles were detected in the supernatant or samples taken directly from the Erlenmeyer flasks for sp-ICP-MS analysis. However, a very high background of dissolved zinc was detected, comparable to the results of previous investigations.

Table 3: Total, solved and non-solved part of zinc in the ZnO solubility test in copper reduced tap water

| Conc. 1 | Total conc. in water (mg/L) | Total conc. in water (%) | Conc. of dissolved ZnO (mg/L) | Percentage of dissolved ZnO of the total ZnO (%) to total | Conc. of non-solved ZnO (mg/L) | Conc. of non-solved ZnO (%) to total | Supernatant + Filtrate total (solved) (mg/L) | Supernatant + Filtrate (%) to total |
|---------|-----------------------------|--------------------------|-------------------------------|---|--------------------------------|--------------------------------------|--|-------------------------------------|
| d0 | 1,395.62 | 100.00 | 243.20 | 17.43 | 654.54 | 72.91 | 897.74 | 64.33 |
| d1 | 753.76 | 54.01 | 329.66 | 54.22 | 278.34 | 45.78 | 608.00 | 80.66 |
| d2 | 643.30 | 46.09 | 337.26 | 73.19 | 123.56 | 26.81 | 460.82 | 71.63 |
| d3 | 640.76 | 45.91 | 381.82 | 75.35 | 124.92 | 24.65 | 506.74 | 79.08 |
| Conc. 2 | Total conc. in water (mg/L) | Total conc. in water (%) | Conc. of dissolved ZnO (mg/L) | Percentage of dissolved ZnO of the total ZnO (%) to total | Conc. of non-solved ZnO (mg/L) | Conc. of non-solved ZnO (%) to total | Supernatant + Filtrate total (solved) (mg/L) | Supernatant + Filtrate (%) to total |
| d0 | 135.09 | 100.00 | 69.41 | 51.38 | 60.48 | 44.77 | 129.89 | 96.15 |
| d1 | 100.07 | 74.08 | 71.64 | 71.58 | 30.25 | 30.22 | 101.88 | 101.81 |
| d2 | 92.46 | 68.44 | 54.45 | 58.89 | 8.56 | 9.25 | 63.00 | 68.14 |
| d3 | 76.20 | 56.41 | 58.13 | 76.29 | 2.27 | 2.97 | 60.40 | 79.26 |

Table 4: Mass balance of the ZnO solubility test

| Concentration 1: 1,395.62 mg/L | | Concentration 2: 135.09 mg/L | |
|---|------------------------|---|-------------------------|
| Initial mass after measurement d0 (mg) | 348.91 (100%) | Initial mass after measurement d0 (mg) | 33.77 (100%) |
| Reduction of the initial mass due to loss by the daily samplings for the concentration measurement (mg) | 177.84 (51.0%) | Reduction by samplings (mg) | 20.25 (60.0%) |
| Residual mass of the initial amount after the daily samplings (mg) | 175.12 (50.2%) | Reduction remaining mass from remaining volume (mg) | 16.71 (49.5%) |
| Balance (mg) | 4.05 (1.2%) | Balance (mg) | -3.19 (9.5%) |
| Recovery (%) | 101.2 | | 109.5 |

4.1.1.5 Conclusion

The high solubility of the NM 110 NPs in copper reduced tap water would require the usage of very high NM 110 concentrations to reach representative amounts of particulate nano ZnO in the test media. These high concentrations may induce toxicity effects caused by dissolved Zn, which may not be distinguished from those induced by the NPs.

Furthermore, the use of ZnO as test item is challenging due to high carryover effects observed between the measurements of single samples in the analytical system during the analytical procedure as well as the adherence of the material to glass ware. Those effects may also appear during the exposure phase of bioaccumulation studies and may induce artefacts with respect to the determination of the bioaccumulation potential of NM 110 (ZnO).

In consultation with the UBA project coordinators NM 110 was excluded from the list of suggested test items. Therefore, only silver nanoparticle NM 300K was tested as representative of the ion releasing group of MNMs (Group a). Investigations on tissue distribution of silver and titanium concentrations in *C.f.* exposed to the NPs were carried out as replacement for the cancelled studies with NM 110.

4.2 Titanium dioxide NM 105

4.2.1 Stability test (I) NM 105 - in test media

4.2.1.1 Test design

The used glassware was cleaned before test start as described above (Part 4.1.1). Two stock suspensions with concentrations separated by factor 10 were produced by adding weighed aliquots of NM 105 to UHQ water. The stock suspensions were added to copper reduced tap water and sonicated to gain the test suspensions. Each test suspension was transferred into two glass beakers (1,000 mL). The glass beakers were used for a stirred and non-stirred test, respectively. The stirred suspension was continuously stirred by a magnet stirrer at 300 rpm. Samples of 20 ml were taken at the onset of the stability test (d0) and at the following five days d1-d5. Titanium was measured as equivalent to titanium oxide (TiO₂). The sampling procedure and the sampling position in the test system was identical for both tests (stirred and non-stirred) and all sampling days.

4.2.1.2 Analytics

A MLS Ultra Clave microwave was used for hydrofluoric acid digestion of the samples to ensure that the whole TiO₂ was solved. The digestion was carried out at 220°C and 95 bar, using HNO₃ (69 %) and hydrofluoric acid (HF) (40 %) at a ratio of 4:1. Boric acid (4 %) was used to dilute the solution and to complex non-reacted HF before the solution was analyzed for its total amount of titanium. The measurement of the titanium concentration was carried out by inductively coupled plasma optical emission spectrometry (ICP-OES) using an Agilent 720 ICP-OES. Calibration solutions were produced in the range of 1, 2.5, 5, 7.5, 10, 25, 50, 75 100 and 250 µg/L prepared by dilution of a certified titanium standard solution in nitric acid (10 %). A certified reference water sample was measured as well as duplicated calibration solutions to control the quality of the measurement process. Measurements were carried out at the wavelengths 307.52, 308.8, 323.45, 334.94 and 338.38 nm.

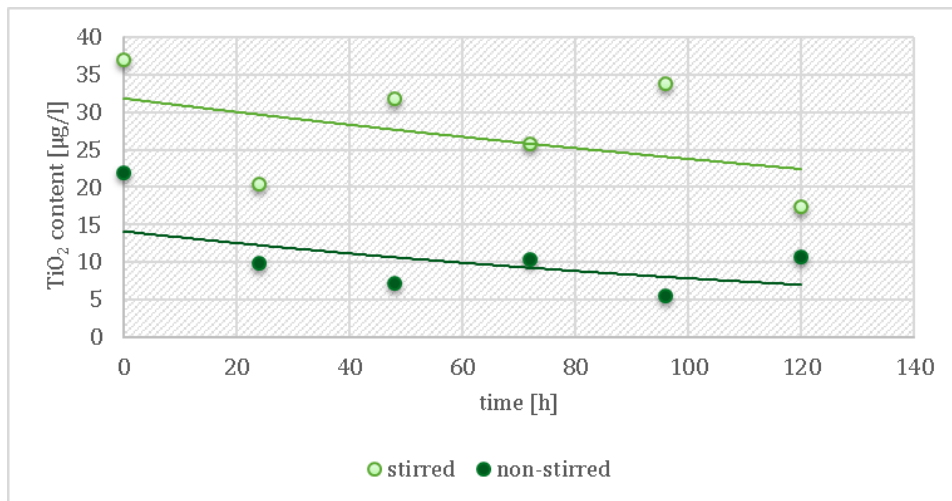
Table 5: Total Ti concentrations during the NM 105 stability test (I)

| Sampling day | Concentration 1 stirred (µg/L) | Concentration 1 non-stirred (µg/L) | Concentration 2 stirred (µg/L) | Concentration 2 non-stirred (µg/L) |
|--------------|--------------------------------|------------------------------------|--------------------------------|------------------------------------|
| d0 | 368.92 | 365.64 | 36.89 | 21.98 |
| d1 | 19.85 | 168.13 | 20.40 | 9.79 |
| d2 | 14.80 | 136.89 | 31.74 | 7.18 |
| d3 | 364.51 | 89.31 | 25.83 | 10.44 |
| d4 | 519.66 | 72.10 | 33.78 | 5.53 |
| d5 | 247.91 | 68.74 | 17.39 | 10.73 |

4.2.1.3 Results

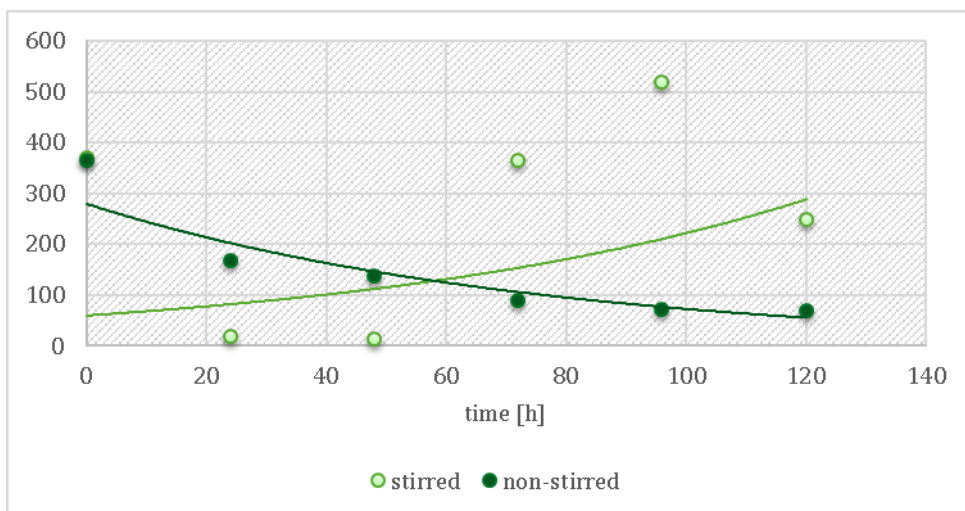
The detectable concentrations of titanium decreased strongly within the first 24 h, whereby the trend of decreasing concentrations weakened during the experimental period and seemed to stabilize at low concentration levels. The trend of concentration changes observed for the stirred suspensions was less clear: A measured concentration decreased over a period of 48 hours but then increased after additional 24 and 48 hours to levels higher than the initial start concentration (Fig. 3 & 4, Tab. 5).

Figure 3: TiO_2 concentrations during the 0.1 mg TiO_2/L stability test



Source: own diagram, Fraunhofer IME

Figure 4: TiO_2 concentrations during the 1 mg TiO_2/L stability test



Source: own diagram, Fraunhofer IME

4.2.1.4 Conclusion

In both assays only about 40 % of the used TiO_2 could be recovered directly after preparation of the suspension, whereby the concentration ratio of the measured concentrations was the same as that of the target concentrations. To reveal errors from the weighing process or losses from sorption or strong sedimentation processes, defined quantities of NM 105 were weighed directly in the Teflon reaction vials for the HF digestion. Also in this case only 40 % could be recovered.

Over all assays and independent of the concentrations applied, a trend to decreasing concentrations could be observed over time in the test systems. This general trend can be explained by the sedimentation of the NM 105 particles. For the stirred assays less visible trends with even higher concentrations in comparison to the initial concentrations were observed. The stirring process may have induced or supported the agglomeration of the nanoparticles. This may explain the high variance of the test media concentrations due to a heterogeneous distribution of the NPs.

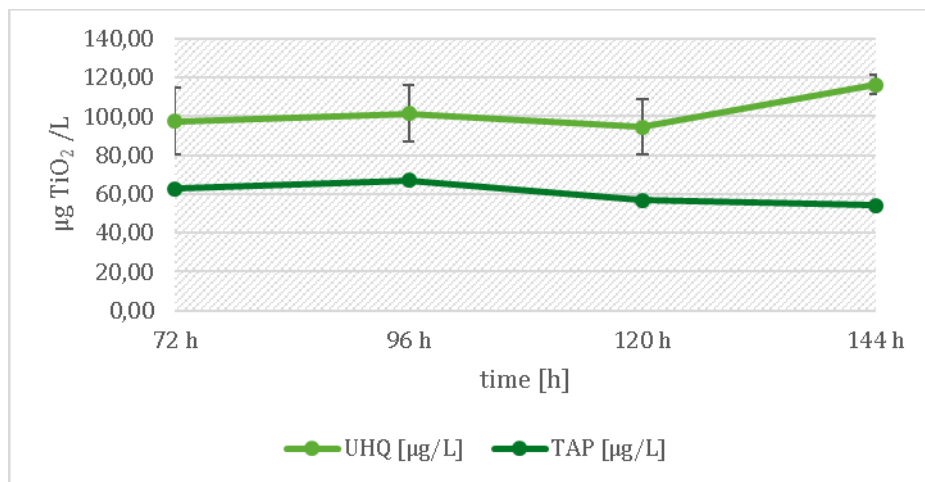
4.2.2 Stability test (II) NM 105 - in test media and ultra-pure water

4.2.2.1 Test design

Another stability test was carried out with NM 105 to elucidate the impact of the dilution medium on the stability of NM 105 stock suspensions. The same test design was used as described above (Part 4.2.1.1). However, no stirring was carried out and an additional assay using UHQ water instead of copper reduced water was added.

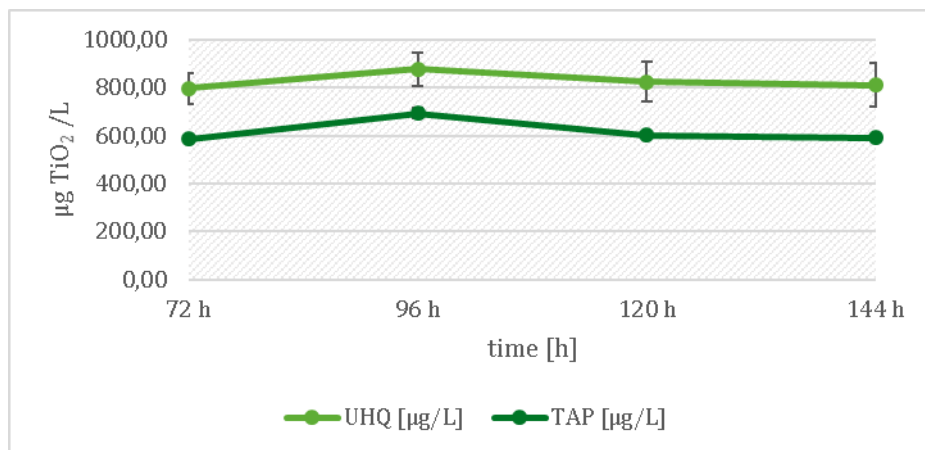
Due to the fact that a trend towards stable concentrations (equilibration) was observed after 72 h in the former stability test, the sampling process started after 72 h of incubation. Further samples were then taken every 24 h up to a total of 144 h.

Figure 5: TiO_2 concentrations during stability test (II): 0.1 mg/L in UHQ and tap water



Source: own diagram, Fraunhofer IME

Figure 6: TiO_2 concentrations during stability test (II): 1 mg/L in UHQ and tap water



Source: own diagram, Fraunhofer IME

4.2.2.2 Analytics

The samples were measured directly after sample collection without any processing or chemical digestion. The measurements were carried out as described above (Part 4.2.1.2).

4.2.2.3 Results

Stable concentrations (equilibrium) were observed in both assays (UHQ and copper reduced tap water) from 72 h up to 144 h (Fig. 5 & 6). The equilibrated concentrations (around 100 and 800 $\mu\text{g TiO}_2/\text{L}$ for 0.1 and 1.00 mg TiO_2/L target concentrations (nominal)) of the UHQ water assay were higher than those of the copper reduced tap water assays (around 60 and 600 $\mu\text{g TiO}_2/\text{L}$).

4.2.2.4 Conclusion

In comparison to copper reduced tap water, the UHQ water seems to be the more suitable medium for the preparation of NM 105 stock suspensions, due to the higher concentration level measured in the equilibrated NM suspensions. The lower stability of the NM 105 suspension in copper reduced tap water may be caused by the higher ionic strength. This may counteract the stabilizing effect of the repulsive forces between the NM 105 NPs leading to agglomeration and increased sedimentation in the test system.

A lower recovery was also observed for the higher concentration tested in UHQ water (around 80 vs 100%). This effect may also be explained by the higher rate of agglomeration which may be supported by the increased particle numbers of NPs at the higher concentration. A comparable effect was not observed in the copper reduced tap water assay. At both concentrations the recovery level was at around 60 %. Nevertheless, the recovery was still higher than that of the method using HF-digestion (40 %) described above.

Based on this results, we decided to generate the NM 105 stock suspensions (using UHQ water), required for the flow-through studies, which were allowed to equilibrate for at least 72 h before usage. The working suspension was obtained by decantation of the equilibrated stock suspension.

4.3 Silver nitrate, AgNO₃

4.3.1 Stability test

4.3.1.1 Test design

The used glassware was cleaned before test start as described above (Part 4.1.1.1). Weighed aliquots of silver nitrate (AgNO₃, ≥ 99 %, Ph.Eur. reinst, Carl Roth®) were dissolved in copper reduced tap water to generate two solutions with concentrations separated by factor 10. The solutions were stirred in amber glass bottles at 300 rpm using a magnetic stirrer. For each concentration a stirred and non-stirred assay was carried out. The solutions were transferred into glass beakers, covered with aluminium foil to avoid exposure to light. Samples were taken at the test start (d0) and every 24 hours until d5. Samples were stabilized by adding 200 µl concentrated HNO₃ (68 %, supra pure) and stored protected from light.

4.3.1.2 Analytics

The measurement of total Ag concentrations was carried out by inductively coupled plasma mass spectroscopy using an Agilent 7700 ICP-Q-MS. Ag solutions with concentrations of 0.1, 0.25, 0.5, 1, 2.5, 5, 7.5, 10, 25, 50, 75 and 100 µg/L were prepared for the calibration by diluting a certified Ag stock solution with HNO₃ (10 %). Samples were also diluted with HNO₃ (10 %) in the ratio 1:10 or 1:2 before measurement. To avoid interferences during the measurement, the isotopes ¹⁰⁷Ag and ¹⁰⁹Ag were measured in the no-gas mode and two additional collision modes with helium. A reference water was measured as well as duplicated calibration solutions to control the quality of the measurement process.

4.3.1.3 Results

A slight trend to decreasing Ag concentrations was observed over the test period (Tab. 6). The non-stirred and stirred assays with the high concentration showed only small deviation from the initial concentration with 2 % and 6 % respectively. A higher deviation was observed for the lower test concentrations (about 23 % for 49.15 µg Ag/L and about 15 % for 49.04 µg Ag/L).

Table 6: Total concentrations of Ag during the AgNO₃ stability test in copper reduced tap water

| Sampling day | Concentration 1 stirred (µg/L) | Concentration 1 non-stirred (µg/L) | Concentration 2 stirred (µg/L) | Concentration 2 non-stirred (µg/L) |
|--------------|--------------------------------|------------------------------------|--------------------------------|------------------------------------|
| d0 | 520.84 | 525.37 | 49.04 | 49.15 |
| d1 | 512.40 | 515.80 | 43.77 | 44.04 |
| d2 | 516.45 | 540.30 | 42.82 | 43.25 |
| d3 | 508.75 | 515.15 | 42.68 | 41.44 |
| d4 | 503.47 | 523.18 | 42.99 | 41.19 |
| d5 | 490.76 | 516.92 | 41.61 | 37.80 |

4.3.1.4 Conclusion

The assays with the higher concentrations seemed to be more stable than those with a 10 times lower concentration. The observed decrease of the Ag concentrations may have been caused by minimal precipitation of Ag^+ - ions (Ag^+) as silver chloride (AgCl) or silver carbonate (AgCO_3) or by the reduction of Ag^+ to $\text{Ag}_{(s)}$ and may explain the greater deviations from the initial concentrations observed in those assays.

Therefore, the higher concentrated solutions were selected for the performance of the bioaccumulation studies.

4.4 Silver NM 300K

4.4.1 Stability test

4.4.1.1 Test design

The used glassware was cleaned before the test start as described above (Part 4.1.1.1). Fresh material of NM 300K was filled up to 10 ml using UHQ water and sonicated to obtain a stock solution. Aliquots of the stock solution were taken to generate working suspensions of two concentrations divided by factor 10. The stock solution was added to copper reduced water in glass beakers and directly stirred to generate the working suspension. For each concentration a stirred and non-stirred assay was tested. A sample of each assay was taken directly (d0) to determine the initial concentration of Ag. Further samples were taken every 24 hours until d5. Samples were stabilized by adding 200 µl concentrated HNO₃ (68%, supra pure) and stored protected from light.

4.4.1.2 Analytics

The measurement of total concentrations of Ag was carried out by inductively coupled plasma mass spectrometry as described above (Part 4.3.1.2).

4.4.1.3 Results

The target concentrations were not reached in all assays. The measured concentrations were separated by nearly factor 2 and not 10 (Tab. 7), as targeted. In all assays a small trend to decreasing concentrations was observed over the test period. The highest deviation (16 %) was found in the non-stirred assays with the higher initial concentration (109.97 µg Ag/L). A smaller deviation (5 %) of the measured concentrations over the test period in relation to the initial concentration was observed in the stirred assay with the higher concentration (95.40 µg Ag/L). This deviation was comparable to those in the lower concentrated stirred assay (4.5 %). Whereas the lower concentrated non-stirred assay showed a higher deviation (8 %).

Table 7: Total Ag concentrations during the NM 300K stability test in copper reduced tap water

| Sampling day | Concentration 1 stirred (µg/L) | Concentration 1 non-stirred (µg/L) | Concentration 2 stirred (µg/L) | Concentration 2 non-stirred (µg/L) |
|--------------|--------------------------------|------------------------------------|--------------------------------|------------------------------------|
| d0 | 95.40 | 109.97 | 58.87 | 57.93 |
| d1 | 93.51 | 96.26 | 56.17 | 57.01 |
| d2 | 93.59 | 93.26 | 57.12 | 55.96 |
| d3 | 96.06 | 92.14 | 58.33 | 56.43 |
| d4 | 90.42 | 92.84 | 56.91 | 53.28 |
| d5 | 92.25 | 107.37 | 56.42 | 54.64 |

4.4.1.4 Conclusion

The NM 300K suspension seemed to be stable with respect to the selected test concentrations. Deviations between the concentrations and the different treatments (stirring or non-stirring) were negligible.

4.4.2 Solubility test

4.4.2.1 Test design

The potential of NM 300K NPs to release ions was investigated in a solubility test. Samples were also taken from the assays of the previously described stability test. Samplings were carried out every 24 hours from d0 until d5. Media samples from the NM 300K assays of the stability tests were transferred directly in Sartorius Viva Spin® ultrafiltration units with a pore size of 3,000 Dalton and handled as described above (Part 4.1.1.1). Filtrates were stabilized by adding 200 µL concentrated HNO₃ (68 %, supra pure) and stored protected from light.

4.4.2.2 Analytics

The measurements of the total Ag content in the media samples were carried out as described in Part 4.4.1.2.

4.4.2.3 Results

The measured concentrations in the filtrates of the higher concentrations were within the same range. In the stirred assay with the higher concentration around 22.4 % of the Ag was present as dissolved Ag, the percentage of dissolved Ag in the non-stirred assay was comparable with 19.8 % (Tab. 8). The percentage of dissolved Ag was lower in the assays with lower Ag concentrations (3.9 % stirred, 3.2 % non-stirred). During the test period a trend to increasing percentages of dissolved Ag was observed.

Table 8: Total Ag concentrations in the filtrate of the NM 300K solubility test in copper reduced tap water

| Sampling day | Concentration 1 stirred (µg/L) | Concentration 1 non-stirred (µg/L) | Concentration 2 stirred (µg/L) | Concentration 2 non-stirred (µg/L) |
|-------------------|--------------------------------|------------------------------------|--------------------------------|------------------------------------|
| d0 | 21.45 | 18.25 | 2.38 | 1.63 |
| d1 | 20.31 | 20.23 | 1.73 | 1.53 |
| d2 | 20.97 | 19.26 | 1.77 | 1.51 |
| d3 | 20.17 | 19.15 | 2.37 | 1.41 |
| d4 | 21.21 | 19.68 | 2.43 | 1.75 |
| d5 | 21.78 | 19.86 | 2.86 | 2.78 |
| Ø solved part [%] | 22.4 | 19.8 | 3.9 | 3.2 |

4.4.2.4 Conclusion

The MNM NM 300K meets the criteria to be used as an ion-releasing MNM without showing too high dissolution rates. The recommended exchange rate for the working suspensions used in the bioaccumulation studies was estimated to be between every 24 to 120 hours to allow bioaccumulation of Ag following ingestion of AgNPs.

4.5 Polystyrene nanoparticles

4.5.1 Stability test

4.5.1.1 Test design

A test suspension was generated having a target concentration of 5 mg nPS/L. Green fluorescent Fluoro-Max™ nPS stock solution was added to an equivalent amount of copper reduced tap water in a glass beaker. Samples were taken at the start (0 h), after 12 h and 24 h.

4.5.1.2 Analytics

The measurement of the fluorescence in the test suspension was carried out using a fluorescence light detector coupled to an asymmetrical flow field-flow fractionation system also coupled to multi-angle laser light scattering (AF4-FLD-MALLS). The system was calibrated by measurement of nPS suspensions of different concentrations and a calibration function was established. Quantification of nPS in media samples was performed on the basis of estimated peak areas (Fig. 7)

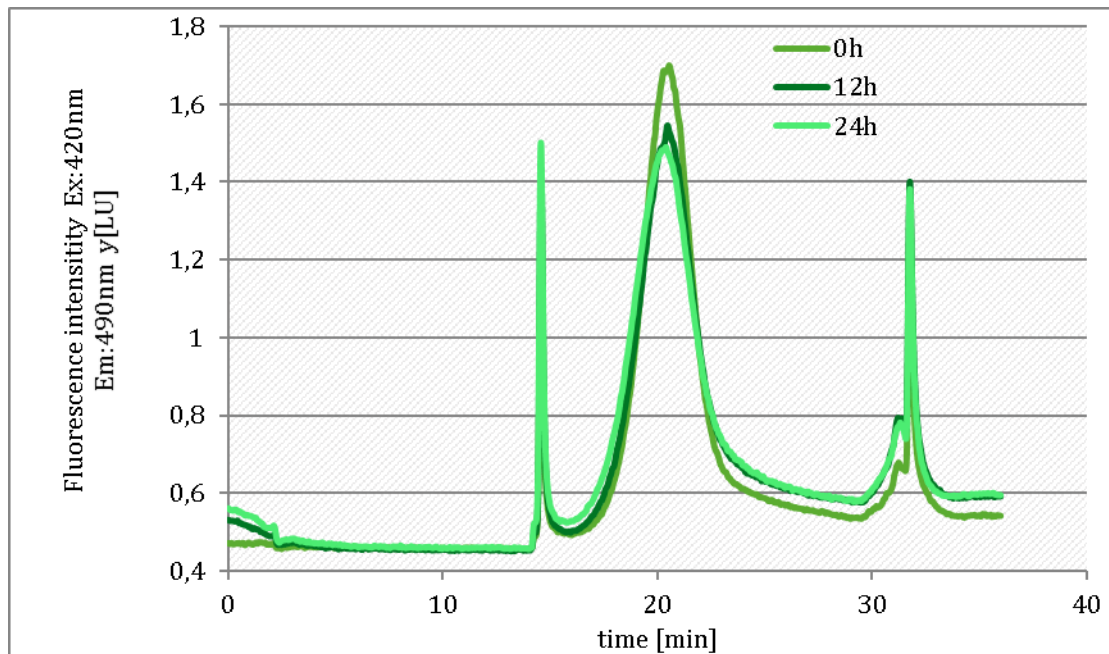
4.5.1.3 Results

The measured initial concentration of the stability test was 4.1 mg nPS/L. The concentration decreased to 3.8 mg nPS/L after 12 h, and remained stable within the next 12 h (Tab. 9, Fig. 7).

Table 9: Calculated nPS concentrations of the test media in the nPS stability test

| Duration of the test [h] | Calculated concentration nPS [mg/L] |
|--------------------------|-------------------------------------|
| 0 | 4.1 |
| 12 | 3.8 |
| 24 | 3.8 |

Figure 7: AF4-FLD-fractogram of samples at different sampling times: Fluorescence intensity during the nPS stability test



Source: own diagram, Fraunhofer IME

4.5.1.4 Conclusion

The nPS suspension showed to be stable over a period of 24 hours. A target concentration of 5 mg nPS/L led to detectable concentrations also after 24 hours of incubation. Therefore, the following studies were carried out with concentrations of at least 5 mg nPS/L to ensure detectable concentrations.

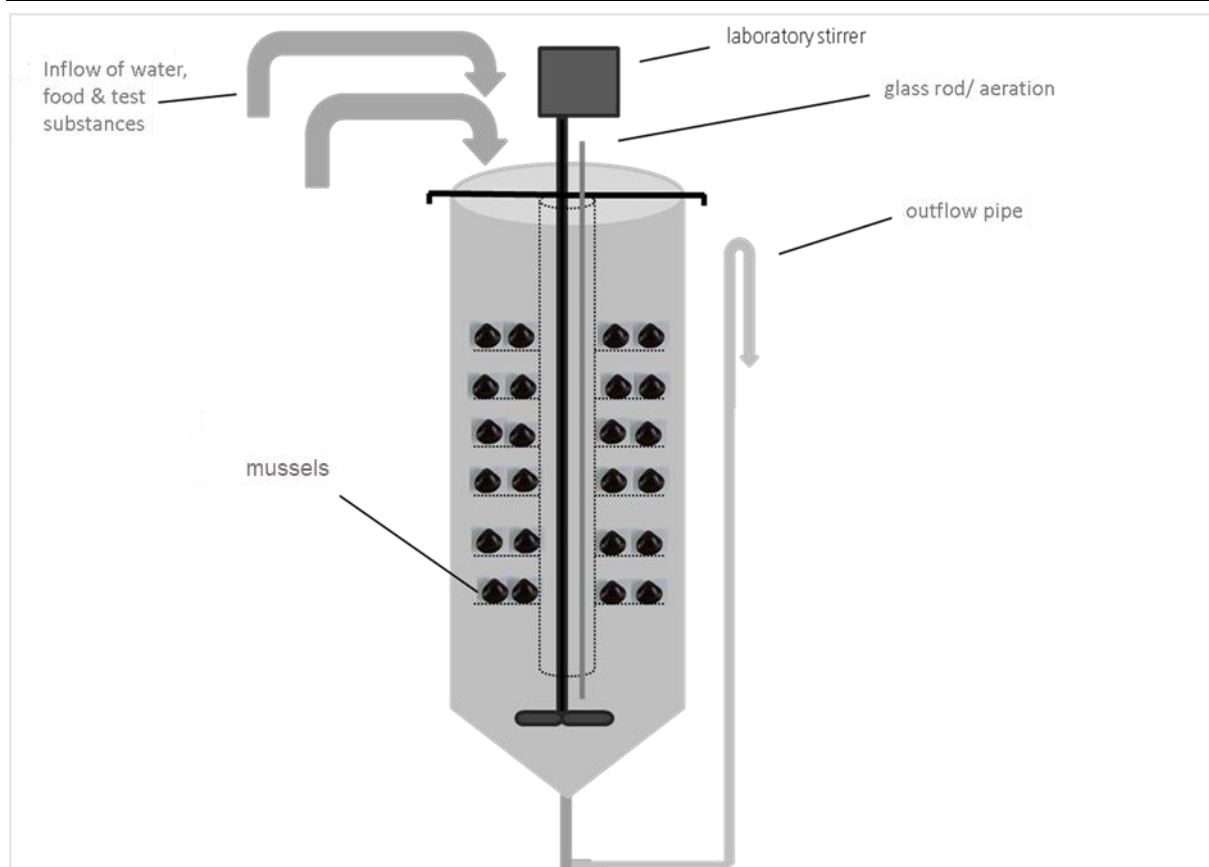
5 Establishment of the new test system

5.1 Description of the flow-through system

A flow-through system was developed to allow continuous exposure of MNMs containing test media at constant concentrations. The new test system was designed to comply with specific requirements caused by the properties of the MNMs. On the one hand the system allows a wide range of adjustments (e.g. aeration, intensity of stirring or the flow rate) to make testing of test items with different properties possible. On the other hand the system was designed to be easy to handle and to clean. The use of glass and stainless steel (V4A) parts allows to clean the experimental units with strong acids.

The central part of the new test system is a zuger glass jar with a volume of 8 L used as test vessel. Within this vessel a V4A rack allows to place up to 170 bivalves (in a size of 2 - 2.5 cm) on perforated shelves. The test system includes an adjustable aeration as well as a stirrer with adjustable spin rates from 2 to 40 rpm. Test media (nanomaterial suspension) and food suspension are applied into a mixing vessel using peristaltic pumps (IPC High Precision Multichannel Dispenser, ISMATEC®) and further diluted with copper reduced tap water supplied by a membrane pump (gamma / X, ProMinent®) that delivers copper reduced tap water to the mixing vessel to produce the test media. The test medium is supplied into the zuger glass jar by TYGON® tubes (E-3603, TYGON®). The whole system allows a flowrate from < 0.5 L/h (or static conditions) to > 20 L/h. The test media leave the test system at the bottom of the zuger glass jar by an overflow pipe (Fig. 8 - 10).

Figure 8: Schematic presentation of the bivalvia flow-through system



Source: Fraunhofer IME

Figure 9: Bivalvia flow-through system



Source: Fraunhofer IME

Figure 10: *Corbicula fluminea* on steel grids



Source: Fraunhofer IME

5.2 Feeding study

5.2.1 Study design

A feeding study lasting 192 hours was carried out to identify a suitable experimental diet for bioaccumulation studies. Five treatments were tested: *Spirulina spec.* (SP), grounded stinging nettle (SN), grounded plant based fish food tablets (FFT) (www.ms-tierbedarf.de), a combination of ground stinging nettle and fish food tablets (SN+FFT), were compared with a no food treatment (/). The test system was running for 24 h before the test started to allow equilibration of experimental conditions.

For the feeding study flow-through units (one unit / treatment) were stocked with 50 animals which were pre-conditioned in microcosms for several weeks. Prior to the study the animals were brushed and transferred into a clean microcosm without any food source to allow defecation. After 24 h the cleaning procedure was repeated, animals were transferred into a second microcosm for defecation. Before the animals were transferred into the test vessels, their length was measured and their valves were dried using paper towels before the animal's weight was determined. During the feeding study the test systems were set to a flow rate of 4 L/h, whereby each litre of test media contained 16 ml of a food suspension (equivalent to 400 mg dry mass/L). Temperature, dissolved oxygen as well as the pH were measured daily. Measurements of ammonia, nitrite and nitrate were carried out at the start and end of the test. During the feeding study the valve opening and filtration activity were observed. At the end of the feeding study, the animal valves were cleaned and dried, and each animal was weighed again.

5.2.2 Results

The average weight of the animals used in the dietary test was 6.68 g (± 0.79), their average length was estimated to be 26.84 mm (± 1.23) (anterior-posterior) and 17.07 mm (± 0.77) (ventral-dorsal). The temperature in the single treatments units ranged from 17.7 to 19.0 °C over all test vessels. The pH values ranged from 7.5 to 7.9. The average oxygen level and saturation ranged from 8.2 mg/l and 93 % in the SP and FFT treatments to 97 % in the “no food” treatment (/), which also showed the best water chemical parameters whereas the SP treatment showed the lowest water quality as shown in Tab. 10. Mortality rates after 192 h ranged from 4 % in the SN treatment to 10 % in the SP treatment. In all treatments filtration activity of the test animals was observed, whereas animals in the no food treatment showed very low filtration activity. The strongest pollution of the test vessels caused by e.g. (pseudo) feces or biofilms appeared in the SP treatment, whereas nearly no pollution was detectable in the no food treatment (Tab. 10, Fig. 11).

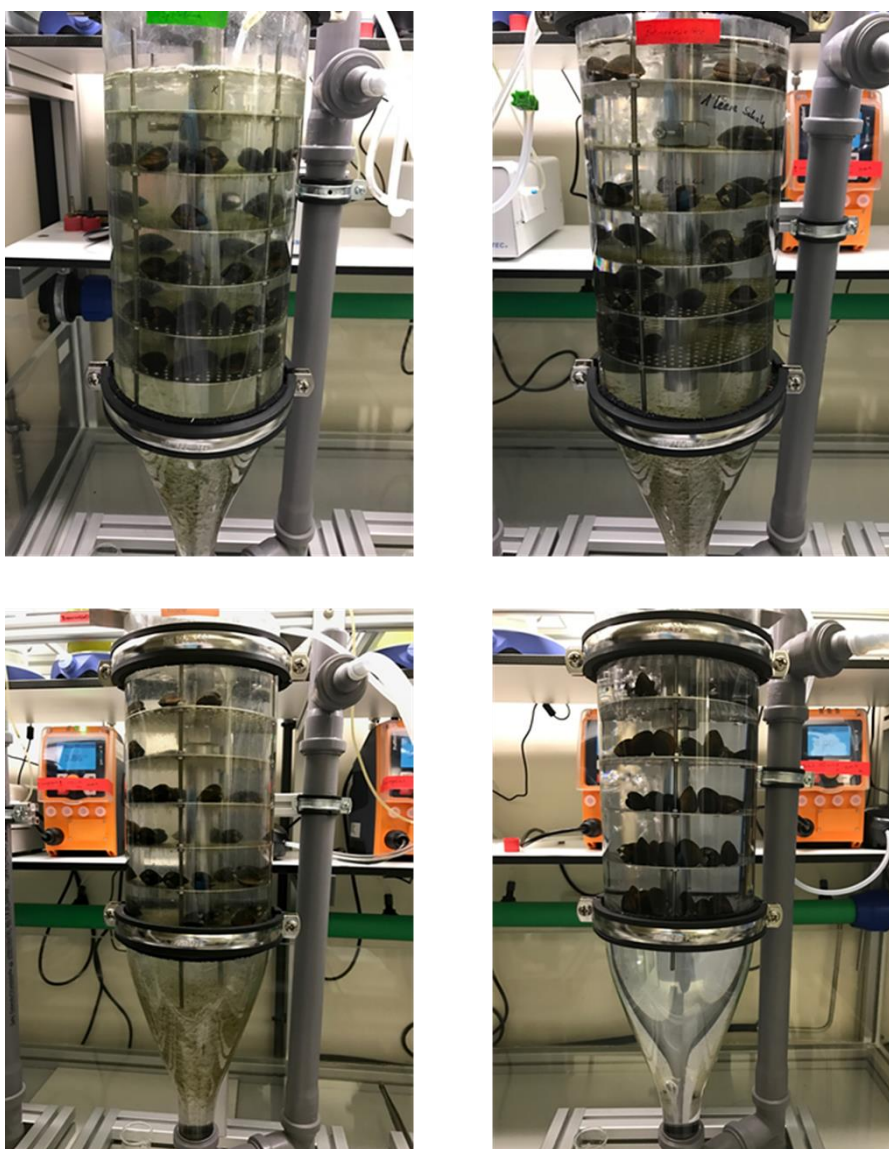
5.2.3 Conclusion

During the feeding study ground stinging nettle (SN treatment) showed, apart from the no food treatment (/), the lowest water burden with respect to ammonia, nitrite and nitrate concentration. Good oxygen saturation levels and moderate pH values in this treatment resulted in the lowest mortality rate (4 %) over 192 h of all treatments. However, it is not clear if the higher mortality rates were induced by the different food sources or by the impaired water quality. Considering the fact that in comparison to the other food sources less pollution was observed in the test vessels like feces or biofilms, grounded stinging nettle appeared to be the best food source of the tested treatments. Generally, the amount of food should be supplied on a very low level to avoid sorption processes of the NPs to the food, but still high enough to allow sufficient nutrient uptake during the bioaccumulation studies.

Table 10: Endpoints of the feeding study. Water parameters after 192 h

| Treatment | Ammonium [mg/L] | Nitrate [mg/L] | Nitrite [mg/L] | Oxygen [mg/L] | Oxygen [%] | pH | Mortality [%] |
|------------------------------------|-----------------|----------------|----------------|---------------|------------|------|---------------|
| No food | 0.2 | 7 | 0.11 | 8.5 | 96.7 | 7.81 | 8 |
| <i>Spirulina</i> | 0.9 | 8 | 0.37 | 8.2 | 93.0 | 7.68 | 10 |
| Fish food tablet | 0.7 | 7 | 0.26 | 8.2 | 92.7 | 7.65 | 6 |
| Stinging nettle | 0.6 | 7 | 0.22 | 8.3 | 94.7 | 7.73 | 4 |
| Fish food tablet + stinging nettle | 0.8 | 8 | 0.24 | 8.3 | 95.4 | 7.76 | 8 |

Figure 11: Bivalvia test system during the feeding study, top-left: *Spirulina*, top-right: stinging-nettle powder, bottom-left: fish food tablet, bottom-right: no food



Source: Fraunhofer IME

6 Investigations on the bioaccumulation of the selected nanomaterials

6.1 Preliminary studies

Preliminary tests were carried out to determine optimized conditions for the performance of bioaccumulation studies. Key parameters such as concentration levels, amount of food, flow rates, duration of the exposure phase and the animal's behaviour during the test period were considered.

6.1.1 Preliminary study AgNO_3

6.1.1.1 Study design

A solution of AgNO_3 was tested to estimate the optimal test concentration. The test system was used as described above (Part 5.2). The AgNO_3 stock solution of 833 $\mu\text{g Ag/L}$ was renewed every 48 hours and stirred at 300 rpm. The food stock suspension was renewed every 24 hours. Stock solution and food suspension were transferred into a mixing chamber where they were diluted with copper reduced tap water. The medium in the mixing chamber was stirred at 300 rpm and finally rinsed through TYGON® tubes (E-3603, TYGON®) into the zuger glass. A flow rate of 1 L/h was used. The system was aerated continuously and was allowed to equilibrate prior to the start of the experiment. The animals were added to the systems after three sequential samples (taken in intervals not less than 3 h), to prove that concentrations did not vary more than 20 % from each other. The test started (0 h) when the mussels were placed in the zuger glass. Samples of the animals were taken as specified in the sampling scheme (Tab. 11). The collection of duplicated samples of animals was combined with a media sampling (triplicates). The media samples were stabilized by addition of 200 μL conc. HNO_3 as described above. The duration of the uptake phase was 72 hours, after that time the remaining mussels were taken from the test system, rinsed with tap water and transferred into a new clean test system running under the same conditions but without test medium. During the depuration phase animals were sampled as described in the sampling scheme (Tab. 11). Test medium remaining in the bivalves was removed after the shells were opened and each animal was rinsed two times in two water bowls containing clean tap water. After that the soft tissue was removed from the shells using clean disposable scalpels. The soft tissues were blotted using lint free lab towels, weighed and stored at -20 °C until chemical analysis. For the measurement of the total Ag content the animals were weighed again and transferred to quartz glass vials for the microwave digestion using HNO_3 . 5 ml of concentrated HNO_3 were added to the samples following vortexing for a few seconds before the samples were digested at 220 °C, 95 bar for 1 hour using a MLS ULTRA Clave microwave. The resulting solution was filled up to 15 ml using UHQ water and measured as described in Part 4.3.

6.1.1.2 Results

The media concentration decreased slowly during the uptake phase from initial 8.85 $\mu\text{g Ag/L}$ at 0 h to 5.29 $\mu\text{g Ag/L}$ at 72 h. The tissue concentration increased from 0.12 mg Ag/kg (fresh weight based) at 2 h to 0.22 mg Ag/kg at the end of the uptake phase (72 h). The tissue concentration decreased during the depuration phase to 0.09 – 0.11 mg Ag/kg after 168 and 192 h (based on the whole test duration) (Tab. 12, Fig. 12 & 13). The calculated time weighted average concentration (TWA) of the media was 6.18 $\mu\text{g Ag/L}$.

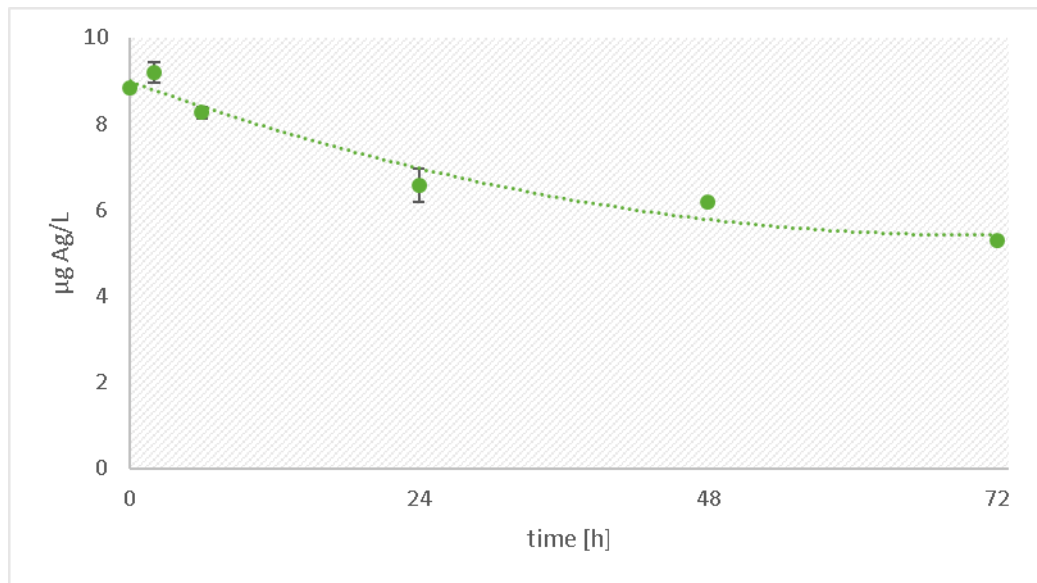
Table 11: Sampling scheme preliminary study with AgNO₃, *end of the uptake phase

| Time [h] | Animal sampling | Media sampling |
|----------|----------------------|----------------|
| 0 | Control 3 x4 animals | 3 x |
| 2 | 2 x 2-3 animals | 3 x |
| 6 | 2 x 2-3 animals | 3 x |
| 24 | 2 x 2-3 animals | 3 x |
| 48 | 2 x 2-3 animals | 3 x |
| 72* | 2 x 2-3 animals | 3 x |
| 74 | 2 x 2-3 animals | 3 x |
| 78 | 2 x 2-3 animals | 3 x |
| 96 | 2 x 2-3 animals | 3 x |
| 144 | 2 x 2-3 animals | 3 x |

Table 12: Preliminary study with AgNO₃: total Ag concentrations in test media and *C.f.* tissue, *end of the uptake phase

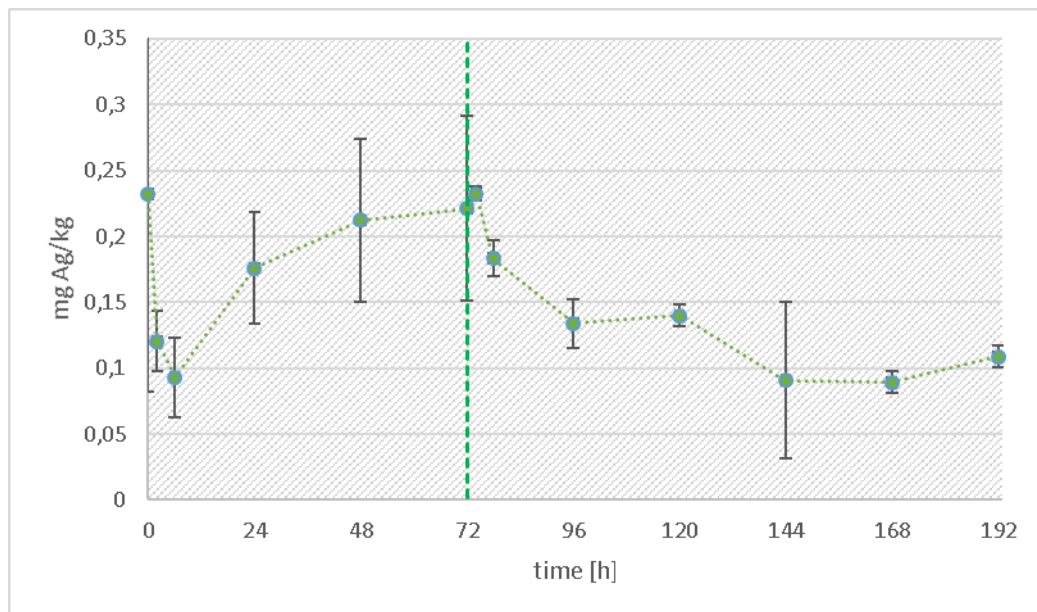
| Time [h] | Media concentration [µg Ag/L] | Tissue concentration [mg Ag/kg] |
|----------|----------------------------------|------------------------------------|
| 0 | 8.85 | 0.23 |
| 2 | 9.20 | 0.12 |
| 6 | 8.26 | 0.09 |
| 24 | 6.57 | 0.18 |
| 48 | 6.18 | 0.21 |
| 72* | 5.29 | 0.22 |
| 74 | | 0.23 |
| 78 | | 0.18 |
| 96 | | 0.13 |
| 120 | | 0.14 |
| 144 | | 0.09 |
| 168 | | 0.09 |
| 192 | | 0.11 |
| TWA | 6.18 | |

Figure 12: Preliminary study with AgNO_3 : total Ag concentrations in test media



Source: own diagram, Fraunhofer IME

Figure 13: Preliminary study with AgNO_3 : total Ag concentrations in *C.f.* tissue



Source: own diagram, Fraunhofer IME

6.1.1.3 Evaluation

During the test period a slight increase of chloride was detected in the copper reduced tap water, which may explain the trend of decreasing Ag^+ concentrations in the test media during the uptake phase by precipitation of silver chloride in the mixing chamber (Fig. 12). The increase of the Ag concentration in the soft body from 0.12 mg Ag/kg to 0.22 mg Ag/kg could be explained by the accumulation of dissolved Ag from the test media. Due to the fact that the concentration was still increasing at 72 h, it can be assumed that the concentration equilibration, and thus the steady state was not reached. The Ag content in the soft tissue of the mussels decreased during the depuration phase until it reached a level of (0.09 mg Ag/kg) which was comparable to the test start (Fig. 13). Considering a steady state concentration of 0.22 - 0.25 mg Ag/kg (72 h), the calculated TWA of 6.18 µg Ag/L would result in a BAF_{ss} value of 37.2 - 42.

6.1.2 Preliminary study NM 300K

6.1.2.1 Study design

A suspension of NM 300K was tested in a preliminary test carried out as described above for AgNO₃ (Chapter 6.1.1). The NM 300K stock suspension was generated as described in part 4.4.1 and renewed every 48 hours. Samplings of the animals were taken as described in the sampling scheme (Tab. 11). Samplings and measurements were carried out as described for the preliminary test with AgNO₃ (Chapter 6.1.1).

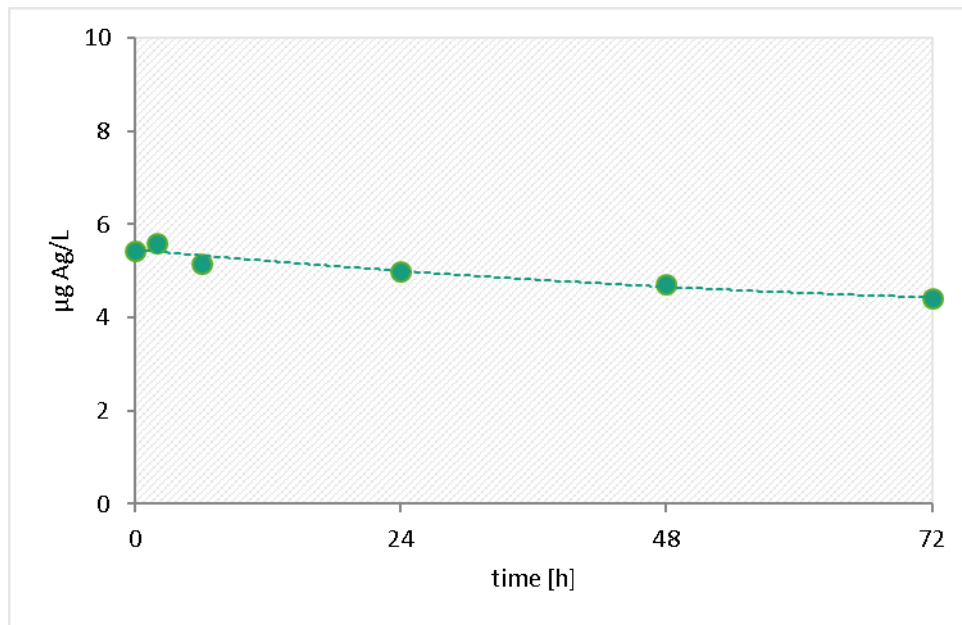
6.1.2.2 Results

The test media concentration decreased slowly over the uptake phase from 5.42 µg Ag/L at 0 h to 4.41 µg Ag/L at 72 h. The tissue concentration increased slightly from 0.15 mg Ag/kg (fresh weight based) after 2 h to 0.19 mg Ag/kg at the end of the uptake phase (72 h) (Tab.13, Fig. 14 & 15). The Ag concentration in the soft tissue decreased during the depuration phase to 0.16 µmg Ag/kg. The calculated TWA was 4.73 µg Ag/L.

Table 13: Preliminary study with NM 300K: total Ag concentrations in test media and *C.f.* tissue, *end of the uptake phase

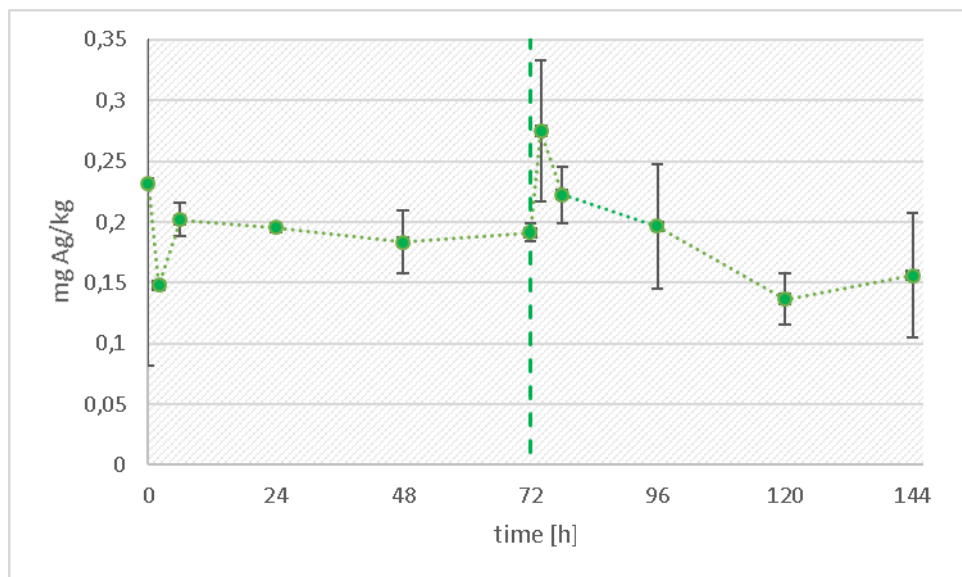
| Time [h] | Media concentration [µg Ag/L] | Tissue concentration [mg Ag/kg] |
|----------|----------------------------------|------------------------------------|
| 0 | 5.42 | 0.23 |
| 2 | 5.59 | 0.15 |
| 6 | 5.17 | 0.20 |
| 24 | 4.99 | 0.20 |
| 48 | 4.71 | 0.18 |
| 72* | 4.41 | 0.19 |
| 74 | | 0.27 |
| 78 | | 0.22 |
| 96 | | 0.20 |
| 120 | | 0.14 |
| 144 | | 0.16 |
| TWA | 4.73 | |

Figure 14: Preliminary study with NM 300K: total Ag concentrations in test media



Source: own diagram, Fraunhofer IME

Figure 15: Preliminary study with NM 300K: total Ag concentrations in *C.f.* tissue



Source: own diagram, Fraunhofer IME

6.1.2.3 Evaluation

It can be only speculated why decreasing media concentrations occurred during the uptake. It is assumed that decreasing concentrations resulted due to sorption of AgNPs to the algae suspended in the test media that were replaced as food source in following studies due to the results of the dietary test that was carried out after the preliminary study.

The increase of the Ag body burden from 0.15 mg Ag/kg to 0.2 mg Ag/kg within 2 to 6 h could be explained by the accumulation of Ag or AgNPs from the test media. The equilibration of the body burden at a level of 0.2 mg Ag/kg for the following samples indicates that steady state conditions were reached. The decreasing Ag content in the soft tissue of the mussels during the depuration phase reached concentrations at the end of the depuration at the same level at test start. Based on the calculated TWA of 4.73 µg Ag/L a BAF_{ss} value of 42.3 was calculated.

6.1.3 Preliminary study nPS

6.1.3.1 Study design

The preliminary test using nPS was carried out as a semi-static approach due to limited availability of the test material. Animals were transferred into a glass beaker (1 L) containing 700 ml of test medium, consisting of copper reduced tap water mixed with nPS at a concentration of 5 mg/L and food in the same range as in the other preliminary tests. Animals were exposed for 24 h. Samples of the test media were taken at the test start and after 24 hours, animals and feces were also sampled after 24 hours.

6.1.3.2 Results

The exposed animals showed an increased fluorescence compared to animals in the husbandry or in the other preliminary tests, with respect to their filtration behaviour. The fluorescence measurement showed a strongly decreased nPS concentration in the test media after 24 hours. The sampled feces were strongly fluorescent under daylight without special stimulation. In contrast, no fluorescence was detectable in the animal's tissue.

6.1.3.3 Evaluation

Media replacement should be carried out at least every 12 hours due to the fact that nearly no fluorescence was detectable in the media after 24 hours. In addition, samples of feces should be taken and also measured to elucidate the transfer of nPS in the test system.

6.2 Main studies

6.2.1 Bioaccumulation study AgNO₃

6.2.1.1 Study design

The main studies on the bioaccumulation of AgNO₃ were carried out as described for the preliminary tests, whereby some parameters were adjusted to take observations into account made during the preliminary tests. The number of animals used per test was increased to 170 individuals, to allow triplicated samples at each sampling point consisting of three animals each. In addition, the length of the uptake phase was extended to 144 hours to ensure that steady state conditions were reached during the uptake phase. Animals remaining in the test system at the end of the uptake phase were cleaned and transferred to new, uncontaminated test systems to investigate the depuration of previously accumulated test material over additional sampling points (Tab. 14). Two concentrations, separated by factor 10, were tested in two independent treatments allowing investigations on the concentration dependency of the resulting BAF_{ss} values. The flowrates in the test systems were set to 4 L/h.

6.2.1.2 Results

The measured total Ag concentrations in the test media and *C.f.* tissue are summarized in the Tab. 14 & 15 and visualized in Fig. 16 to 21. The calculated TWA concentrations applied in the first and second study were 0.682 and 7.791 µg Ag/L. The filtration behaviour of the animals exposed to both concentrations was reduced discernibly, whereby the filtration activity of the animals at the higher concentration was more reduced compared to the low test concentration. Within the single test systems homogenous concentrations were measured at different sampling depths (Fig. 17 & 20). The total Ag concentrations measured in the soft tissue are shown in Fig. 18 & 21. At the low test concentration (TWA 0.682 µg Ag/L) the media concentration decreased slightly under 0.6 µg Ag/L within the first 72 hours, after 72 hours the concentration

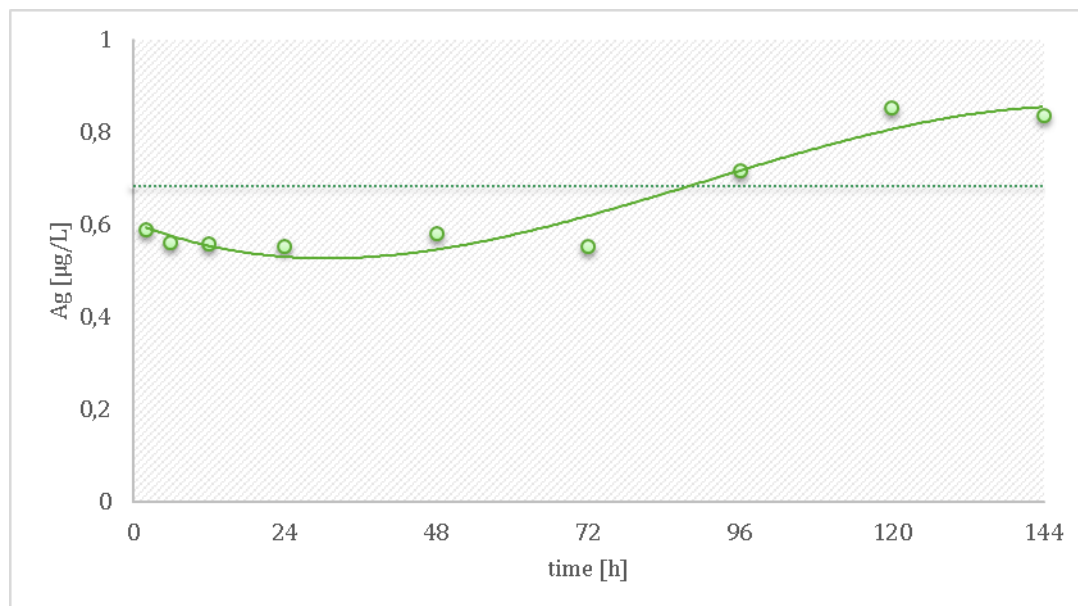
ranged from 0.72 to 0.84 µg Ag/L. The total Ag concentrations in the soft tissue increased from 0.06 mg Ag/kg (0 h) to around 0.5 mg Ag/kg after 72 h to 144 h of exposure. The total Ag concentration in the soft tissue decreased during the following depuration phase to a level of around 0.25 mg Ag/kg.

Table 14: Bioaccumulation study with AgNO₃ – low concentration: total Ag concentrations in test media and *C.f.* tissue, *end of the uptake phase

| Time [h] | Media concentration [µg Ag/L] | Tissue concentration [mg Ag/kg] |
|-----------------|-------------------------------|---------------------------------|
| Control animals | | 0.06 |
| 2 | 0.59 | 0.07 |
| 6 | 0.56 | 0.12 |
| 12 | 0.56 | 0.15 |
| 24 | 0.55 | 0.17 |
| 48 | 0.58 | 0.30 |
| 72 | 0.55 | 0.49 |
| 96 | 0.72 | 0.47 |
| 120 | 0.85 | 0.51 |
| 144* | 0.84 | 0.47 |
| 146 | | 0.44 |
| 150 | | 0.37 |
| 156 | | 0.35 |
| 168 | | 0.29 |
| 192 | | 0.33 |
| 216 | | 0.27 |
| 240 | | 0.25 |
| 264 | | 0.26 |
| 288 | | 0.25 |
| TWA | 0.68 | |

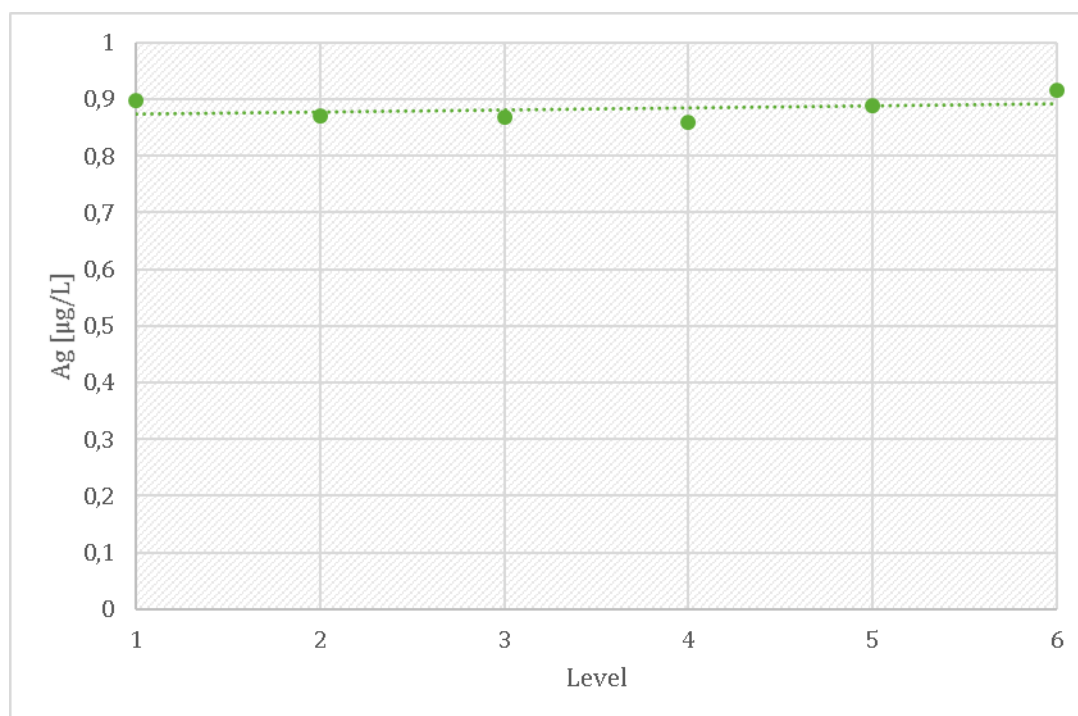
At the higher test concentration (TWA 7.791 $\mu\text{g Ag/L}$) the media concentration ranged from 7.04 to 8.71 $\mu\text{g Ag/L}$ during the uptake phase. The soft tissue concentration in the animals increased from 0.06 mg Ag/kg at 0h to 0.24 mg Ag/kg at 24 h and was stable at this level until the end of the exposure phase (144 h). During the depuration phase concentrations decreased to a level of 0.18 mg Ag/kg after two hours of depuration.

Figure 16: Bioaccumulation study with AgNO_3 - low concentration: total Ag concentrations in test media



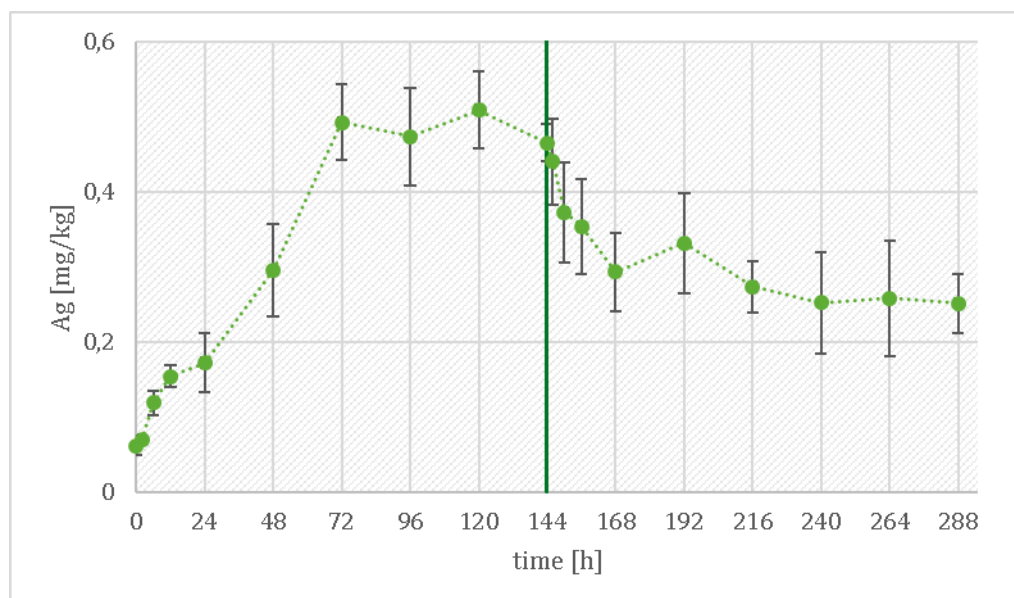
Source: own diagram, Fraunhofer IME

Figure 17: Bioaccumulation study with AgNO_3 - low concentration: total Ag concentrations in test media at several levels (depths) of the flow-through system



Source: own diagram, Fraunhofer IME

Figure 18: Bioaccumulation study with AgNO₃ – low concentration: total Ag concentrations in *C.f.* tissue

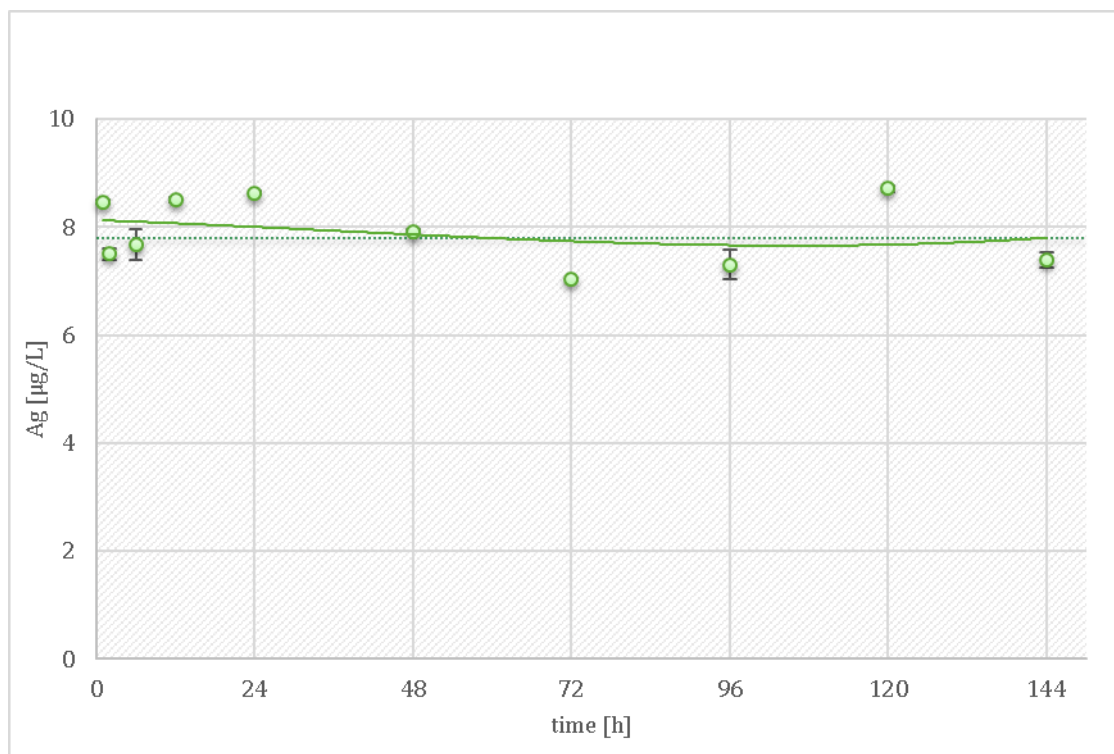


Source: own diagram, Fraunhofer IME

Table 15: Bioaccumulation study with AgNO₃ – high concentration: total Ag concentrations in test media and *C.f.* tissue, *end of the uptake phase

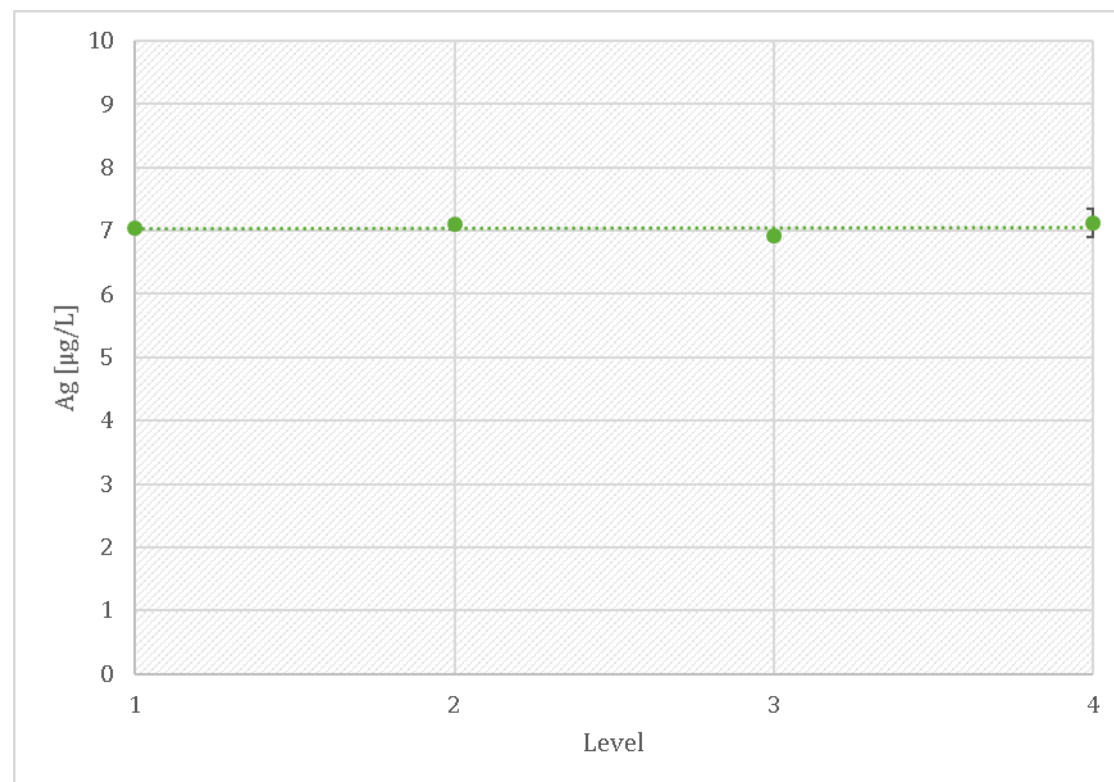
| Time [h] | Media concentration [µg Ag/L] | Tissue concentration [mg Ag/kg] |
|-----------------|-------------------------------|---------------------------------|
| Control animals | | 0.06 |
| 1 | 8.47 | 0.11 |
| 2 | 7.51 | 0.12 |
| 6 | 7.67 | 0.16 |
| 12 | 8.51 | 0.18 |
| 24 | 8.64 | 0.24 |
| 48 | 7.92 | 0.24 |
| 72 | 7.04 | 0.23 |
| 96 | 7.30 | 0.23 |
| 120 | 8.71 | 0.24 |
| 144* | 7.39 | 0.24 |
| 146 | | 0.18 |
| TWA | 7.79 | |

Figure 19: Bioaccumulation study with AgNO_3 - high concentration: total Ag concentrations in test media



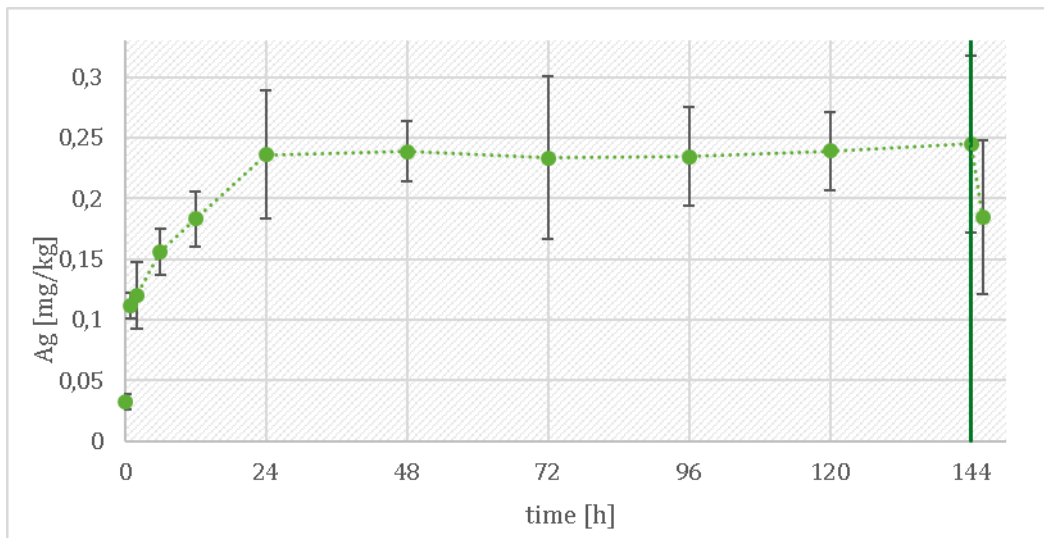
Source: own diagram, Fraunhofer IME

Figure 20: Bioaccumulation study with AgNO_3 - high concentration: total Ag concentrations in test media at several levels (depths) of the flow-through system



Source: own diagram, Fraunhofer IME

Figure 21: Bioaccumulation study with AgNO₃ – high concentration: total Ag concentrations in *C.f.* tissue



Source: own diagram, Fraunhofer IME

6.2.1.3 Evaluation

The reduced filtration activity of the test animals observed during the uptake phase may be explained by a protective mechanism. Different studies showed that *C.f.* reduce their filtration activity and the time of shell opening in response to the concentration of dissolved metal cations or other pollutants (e.g. Rodgers *et al.*, 1980; Doherty and Cherry, 1988). Those effects are in accordance with our observations with a stronger reduction of filtration activity observed at the higher AgNO₃ concentration.

The fluctuation of the test concentration at the beginning of the low-dosage test treatment cannot be fully explained. Presumable deviations in the Cl⁻ content in the copper reduced tap water may have led to precipitation and thus to reduction of the detectable total Ag concentration in the test media. Nevertheless, Ag concentrations in the test media increased after 72 h when a steady state of Ag concentrations was reached in the tissue samples. It could not be verified if the increase of the Ag concentrations in the media was caused by a reduced ingestion rate of Ag from the media due to saturation of the mussel tissues.

Of particular note is that the time to steady state as well as the Ag concentration at steady state obviously depend on the exposure concentration. At the higher concentration a lower steady state concentration (0.24 mg Ag/kg) was reached after just 24 hours, whereas the lower Ag exposition led to a higher steady state concentration (0.485 mg Ag/kg) which was reached only after 72 hours. A closer look at the depuration phase of the test with the lower Ag concentration showed, that the tissue concentration did not reach the initial concentration (around 0.06 mg Ag/kg). A tissue concentration of around 0.25 mg Ag/kg was reached within 240 hours and remained stable until the end of the depuration phase. Due to a lack of samples, an extended depuration period was not possible to be applied.

Using the calculated TWA concentrations and the estimated total Ag concentrations in the soft tissue we were able to calculate BAF_{ss} values. The low exposure concentration (TWA 0.682 µg Ag/L) resulted in a BAF_{ss} of 710.7, whereas the high exposure concentration (TWA 7.791 µg Ag/L) was leading to a BAF_{ss} of 30.5. The higher BAF_{ss} value at the lower concentration treatment may be explained by the higher Ag storage capacity due to the binding of the Ag to MT proteins resulting in a higher steady state concentration and leading to a reduced Ag elimination.

6.2.2 Bioaccumulation study NM 300K

6.2.2.1 Study design

The main studies on the bioaccumulation of NM 300K were carried out as described for the AgNO₃ studies. Two concentrations, separated by factor 10, were tested in two treatments. The test concentrations were chosen to be comparable to those from the AgNO₃ studies. This should allow a comparison between ionic and particulate based uptake and/or bioaccumulation of Ag.

6.2.2.2 Results

Total Ag concentrations in the test media and *C.f.* tissue are summarized in Tab. 16 & 17 and visualized in Fig. 22 to 27. As observed in the AgNO₃ studies the filtration activity of the mussels was reduced at the highest concentration even though the reduction was on a lower level than in the AgNO₃ studies.

The calculated TWA concentrations of the two treatments were 0.624 and 6.177 µg Ag/L. Within the single test systems homogenous concentrations were measured (Fig. 23 & 26).

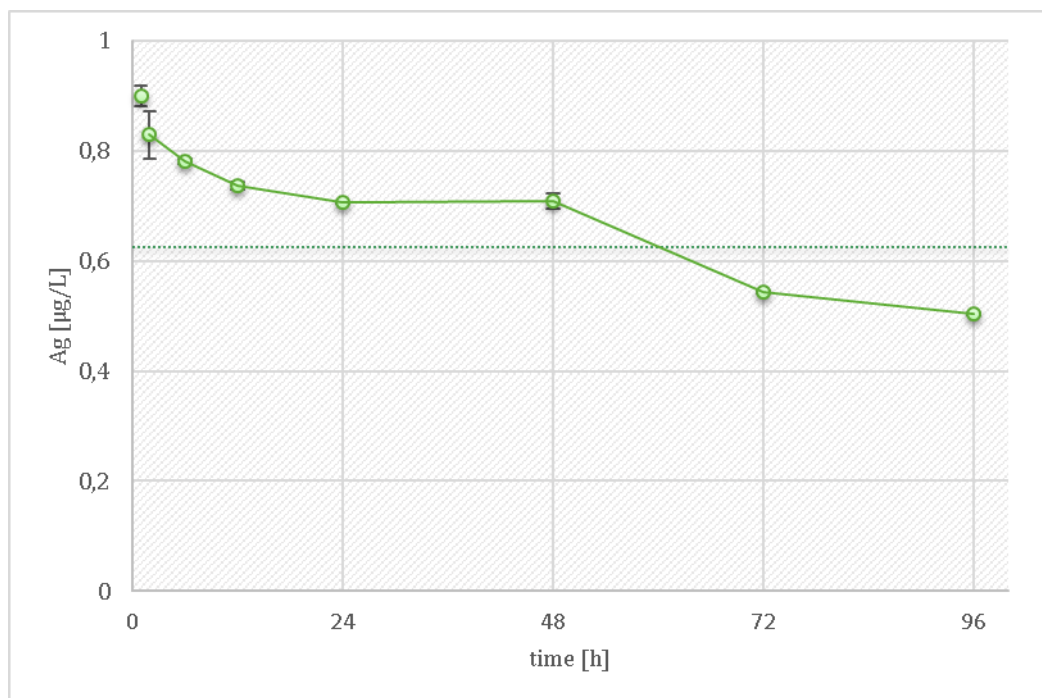
At the lower test concentration (TWA of 0.62 µg Ag/L) the initial media concentration was slightly higher (0.90 µg Ag/L) compared to the average concentration but decreased over the exposure period to 0.50 µg Ag/L at the end of the uptake phase at 96 h. The total Ag concentrations in the soft tissue increased from initial 0.03 mg Ag/kg (0 h) to 0.08 mg Ag/kg at 24 h and stayed on this level until the end of the uptake phase (96 h). The total Ag concentration in the soft tissue decreased during the depuration phase to a level of around 0.04 mg Ag/kg which is comparable to the start concentration (0.03 mg Ag/kg). This concentration was reached after 12 hours of depuration and was stable until the end of depuration phase after 48 hours of depuration.

At the high test concentration (TWA of 6.18 µg Ag/L) the media concentration ranged from 9.11 to 7.67 µg Ag/L within the first 24 hours and from 5.75 to 4.95 within the last 24 hours of the uptake phase. The soft tissue concentration of the animals increased from 0.03 mg Ag/kg at 0 h to around 0.20 mg Ag/kg at 24 h and was stable until the end of the exposure phase (96 h). Additional samplings during the depuration phase showed that tissue concentrations, decreased to 0.05 mg Ag/kg after 12 hours of depuration.

Table 16: Bioaccumulation study with NM 300K – low concentration: total Ag concentrations in test media and *C.f.* tissue, *end of the uptake phase

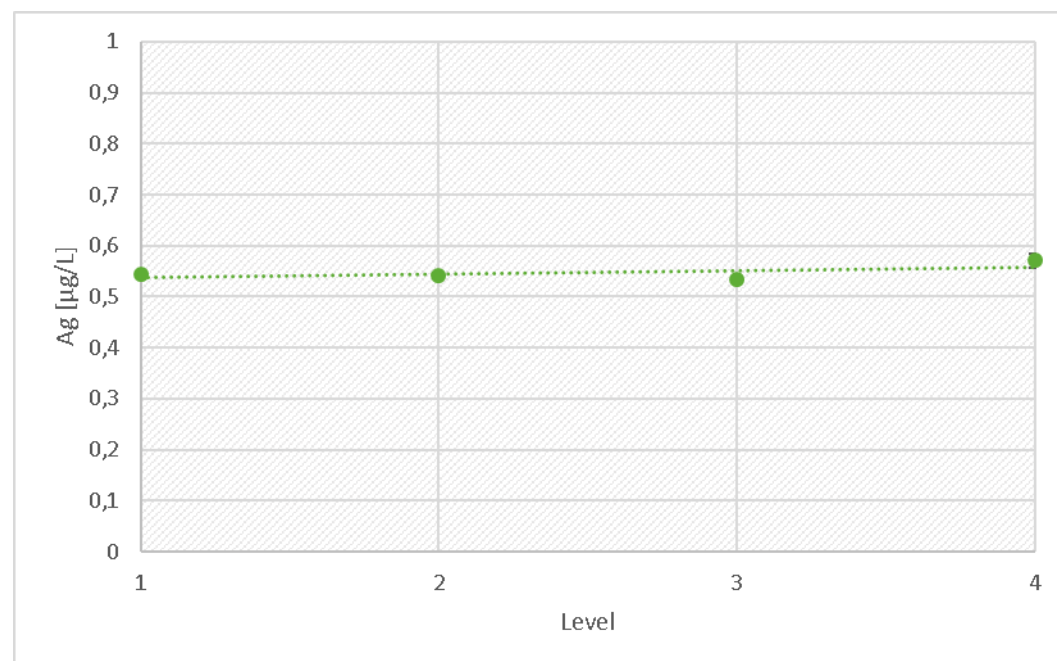
| Time [h] | Media concentration [µg Ag/L] | Tissue concentration [mg Ag/kg] |
|-----------------|----------------------------------|------------------------------------|
| Control animals | | 0.03 |
| 1 | 0.90 | 0.05 |
| 2 | 0.83 | 0.05 |
| 6 | 0.78 | 0.06 |
| 12 | 0.74 | 0.07 |
| 24 | 0.71 | 0.08 |
| 48 | 0.71 | 0.08 |
| 72 | 0.54 | 0.08 |
| 96* | 0.50 | 0.08 |
| 98 | | 0.07 |
| 100 | | 0.06 |
| 102 | | 0.06 |
| 108 | | 0.04 |
| 120 | | 0.04 |
| 144 | | 0.04 |
| TWA | 0.62 | |

Figure 22: Bioaccumulation study with NM 300K – low concentration: total Ag concentrations in test media



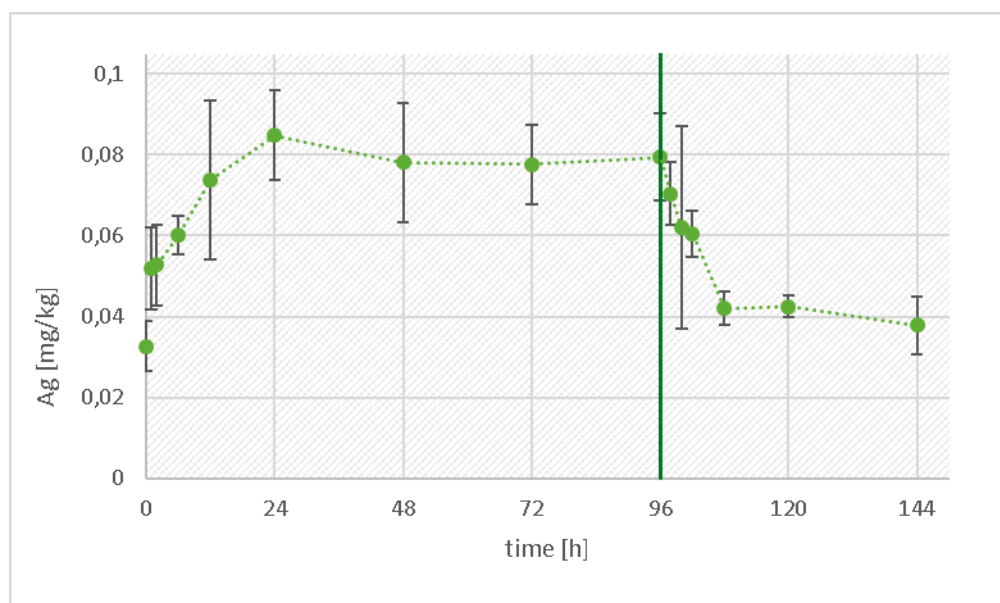
Source: own diagram, Fraunhofer IME

Figure 23: Bioaccumulation study with NM 300K – low concentration: total Ag concentrations in test media at several levels (depths) of the flow-through system



Source: own diagram, Fraunhofer IME

Figure 24: Bioaccumulation study with NM 300K – low concentration: total Ag concentrations in *C.f.* tissue

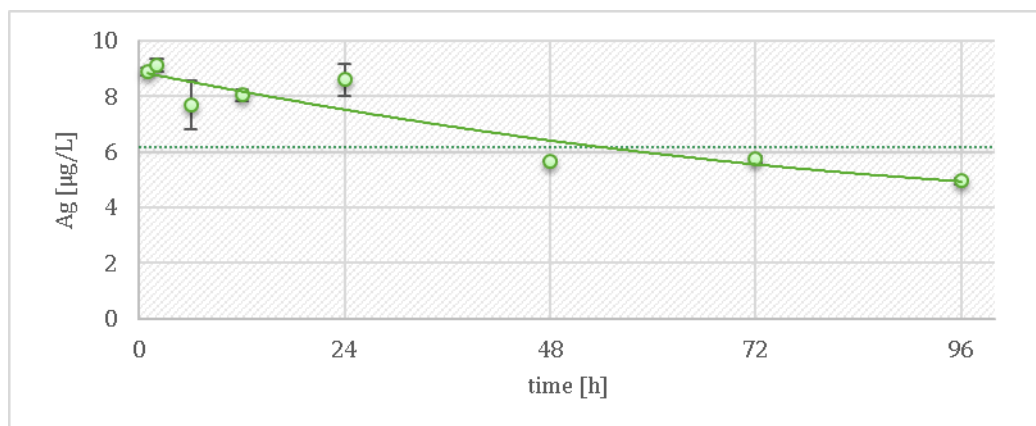


Source: own diagram, Fraunhofer IME

Table 17: Bioaccumulation study with NM 300K – high concentration: total Ag concentrations in test media and *C.f.* tissue, *end of the uptake phase

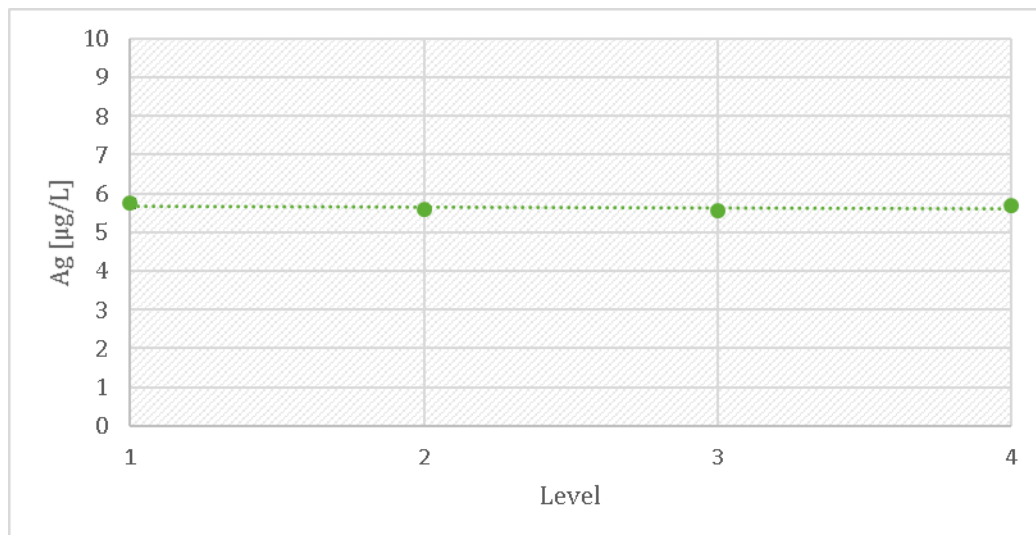
| Time [h] | Media concentration [µg Ag/L] | Tissue concentration [mg Ag/kg] |
|-----------------|----------------------------------|------------------------------------|
| Control animals | | 0.03 |
| 1 | 8.90 | 0.06 |
| 2 | 9.11 | 0.07 |
| 6 | 7.67 | 0.10 |
| 12 | 8.04 | 0.16 |
| 24 | 8.59 | 0.20 |
| 48 | 5.67 | 0.19 |
| 72 | 5.75 | 0.20 |
| 96* | 4.95 | 0.18 |
| 98 | | 0.09 |
| 100 | | 0.07 |
| 102 | | 0.06 |
| 108 | | 0.05 |
| TWA | 6.18 | |

Figure 25: Bioaccumulation study with NM 300K – high concentration: total Ag concentrations in test media



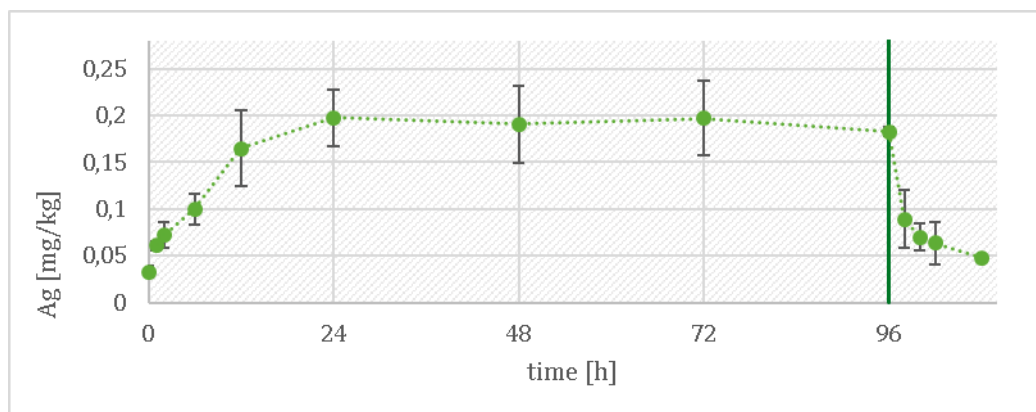
Source: own diagram, Fraunhofer IME

Figure 26: Bioaccumulation study with NM 300K – high concentration: total Ag concentrations in test media at several levels (depths) of the mussel device of the flow-through system



Source: own diagram, Fraunhofer IME

Figure 27: Bioaccumulation study with NM 300K – high concentration: total Ag concentrations in *C.f.* tissue



Source: own diagram, Fraunhofer IME

6.2.2.3 Evaluation

The decrease of the total Ag concentrations in the media observed during the uptake phase may be at least partly explained by sorption of particles to the surfaces of the zuger glass, the stainless steel device or the shells of the mussels.

The increase of the total tissue concentration during the uptake phase may be explained by the uptake of AgNPs and the accumulation of Ag⁺ released from NM 300K. The investigations using sp-ICP-MS showed that AgNPs were definitely ingested by the mussels (see part 6.2.4) whereas it remains unclear whether the AgNPs simply moved through the mussel body or whether they were really incorporated into different compartments or even penetrated single cells. A BAF_{ss} of 128 was calculated for the low test concentration (TWA of 0.62 µg Ag/L) and a BAF_{ss} of 31 for the high test concentration (TWA of 6.18 µg Ag/L). The difference in the BAF_{ss} values may be explained by the different filtration rates observed during the tests potentially induced by the previously discussed protection mechanism triggered by metal ion exposure. However, the effect was probably reduced compared to the study on AgNO₃ due to the lower presence of free Ag⁺ in the NM 300K media.

6.2.3 Bioaccumulation study NM 105

6.2.3.1 Study design

The main studies on the bioaccumulation of NM 105 were carried out as described for the studies with AgNO₃ (part 6.2.1). Two concentrations, separated by a factor of at least 5, were tested in two separate tests. The working suspension was generated by allowing a stock suspension with a concentration of 1 mg TiO₂/L (based on UHQ water) to equilibrate for 72 h in 2 L glass beakers at room temperature. Two thirds of the suspension volume were decanted and the equilibrated suspension used as working suspension. The NM 105 working suspension was supplied directly into the test vessel at 3 different spots to avoid agglomeration and sedimentation processes in the mixing vessel. Media samples were measured directly, tissue samples were measured after digestion as described in Chapter 4.2.1.2.

6.2.3.2 Results

The measured total Ti concentrations were summarized as calculated TiO₂ concentrations in Tab. 18 & 19 and visualized in Fig. 28 to 33. No reduced filtration activity of the mussels was observed in response to TiO₂ exposure.

The calculated TWA concentrations were 0.099 and 0.59 µg TiO₂/L, equivalent to a separation factor of around 6. Within the single test systems homogenous concentrations were measured at different depths (Fig. 29 & 32).

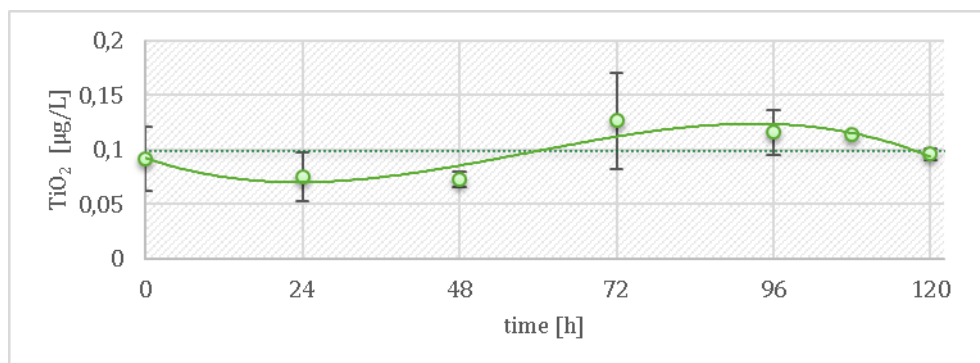
In both treatments the initial media concentrations were lower at the beginning (0.074 and 0.28 µg TiO₂/L), increased concentrations were observed after 72 h with 0.127 and 0.67 µg TiO₂/L). In both treatments the total TiO₂ concentrations in the soft tissue increased during the uptake phase.

At the low test concentration a soft tissue TiO₂ concentration of around 0.6 mg TiO₂/kg was reached after 24 h and was nearly stable until the end of the uptake phase (120 h). During the depuration phase a rapid decrease of the concentration was observed. After 6 h of depuration a concentration equivalent to the start concentration was reached (0.22 mg TiO₂/kg). During the remaining depuration time the concentration remained on this level.

Table 18: Bioaccumulation study with NM 105 – low concentration: total TiO₂ concentrations in test media and C.f. tissue, *end of the uptake phase

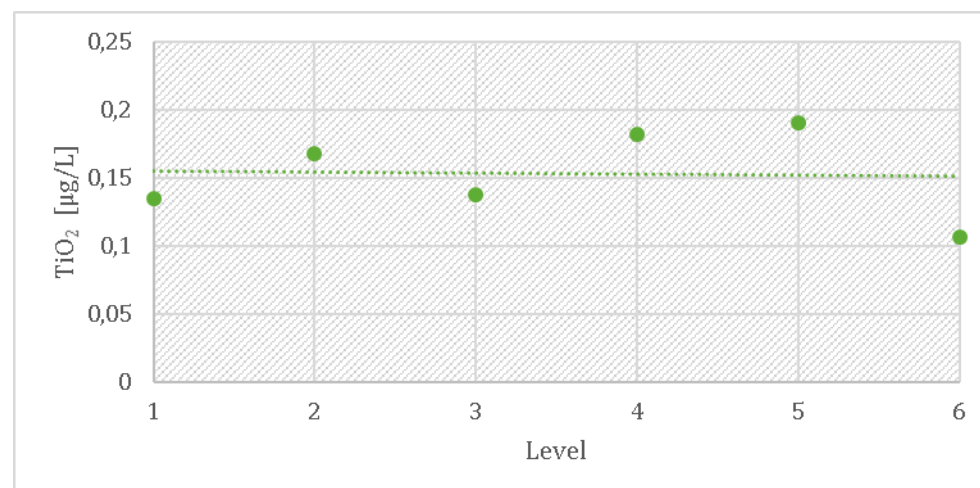
| Time [h] | Media concentration [µg TiO ₂ /L] | Tissue concentration [mg TiO ₂ /kg] |
|-----------------|---|---|
| Control animals | | 0.22 |
| 2 | 0.074 | 0.37 |
| 4 | | 0.42 |
| 6 | | 0.43 |
| 12 | | 0.47 |
| 24 | | 0.61 |
| 48 | 0.073 | 0.59 |
| 72 | 0.127 | 0.54 |
| 96 | 0.116 | 0.64 |
| 108 | 0.114 | 0.58 |
| 120* | 0.096 | 0.74 |
| 122 | | 0.47 |
| 124 | | 0.31 |
| 126 | | 0.22 |
| 132 | | 0.16 |
| 144 | | 0.17 |
| 168 | | 0.17 |
| 192 | | 0.19 |
| 216 | | 0.26 |
| 224 | | 0.16 |
| 240 | | 0.15 |
| 264 | | 0.13 |
| TWA | 0.099 | |

Figure 28: Bioaccumulation study with NM 105 – low concentration: total TiO_2 concentrations in test media



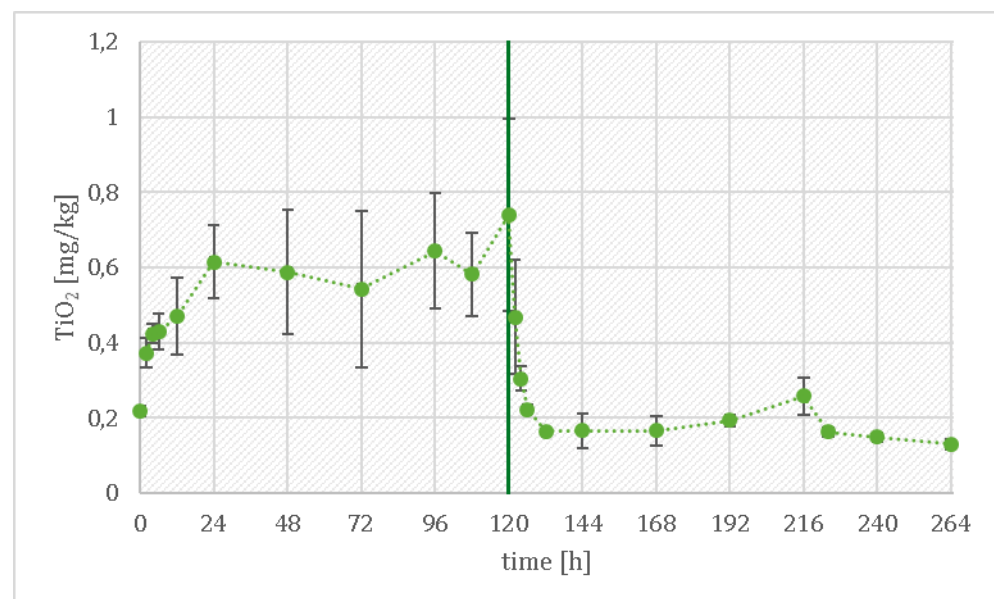
Source: own diagram, Fraunhofer IME

Figure 29: Bioaccumulation study with NM 105 – low concentration: total TiO_2 concentrations in test media at several levels (depths) of the flow-through system



Source: own diagram, Fraunhofer IME

Figure 30: Bioaccumulation study with NM 105 – low concentration: total TiO_2 concentrations in *C.f.* tissue



Source: own diagram, Fraunhofer IME

At the high test concentration a TiO₂ concentration of around 5.4 mg TiO₂/kg was reached in the soft tissue under steady state conditions and stayed on this level until the end of the uptake phase (Tab. 19). The elimination of TiO₂ was also very rapid like in the assay with the low TiO₂ concentration. A stable tissue concentration of 0.20 mg TiO₂/kg was reached after 24 hours of the depuration phase equivalent to the same low level measured at the start of the test (0 h).

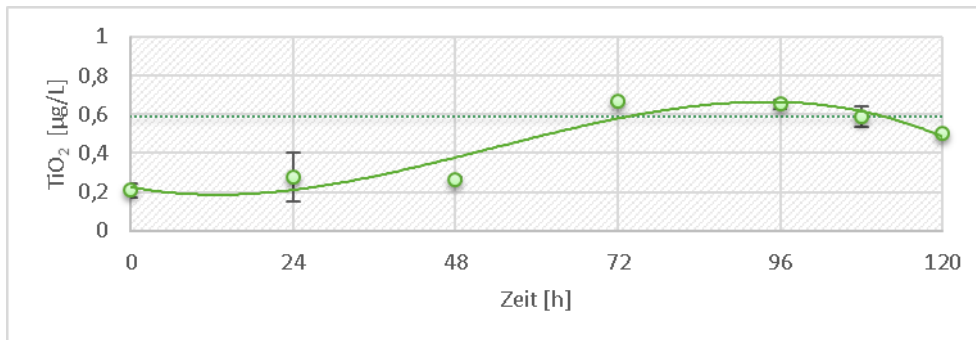
Table 19: Bioaccumulation study with NM 105 – high concentration: total TiO₂ concentrations in test media and C.f. tissue, *end of the uptake phase

| Time [h] | Media concentration [µg TiO ₂ /L] | Tissue concentration [mg TiO ₂ /kg] |
|-----------------|---|---|
| Control animals | | 0.22 |
| 2 | 0.28 | 0.67 |
| 4 | | 0.87 |
| 6 | | 1.13 |
| 12 | | 1.22 |
| 24 | | 1.57 |
| 48 | 0.27 | 2.66 |
| 72 | 0.67 | 4.99 |
| 96 | 0.65 | 5.36 |
| 108 | 0.59 | 5.30 |
| 120* | 0.50 | 5.61 |
| 122 | | 2.19 |
| 124 | | 1.10 |
| 126 | | 0.68 |
| 132 | | 0.50 |
| 144 | | 0.20 |
| 168 | | 0.27 |
| 192 | | 0.24 |
| 216 | | 0.30 |
| 224 | | 0.30 |
| 240 | | 0.17 |
| 264 | | 0.18 |

TWA

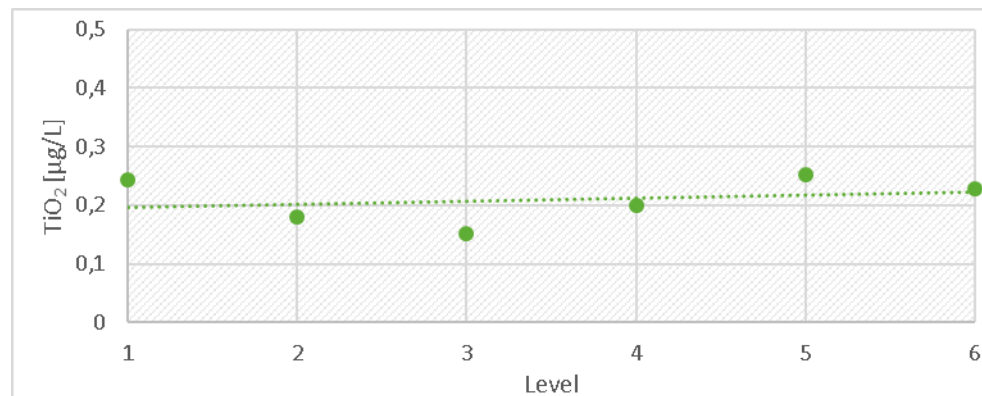
0.59

Figure 31: Bioaccumulation study with NM 105 – high concentration: total TiO_2 concentrations in test media



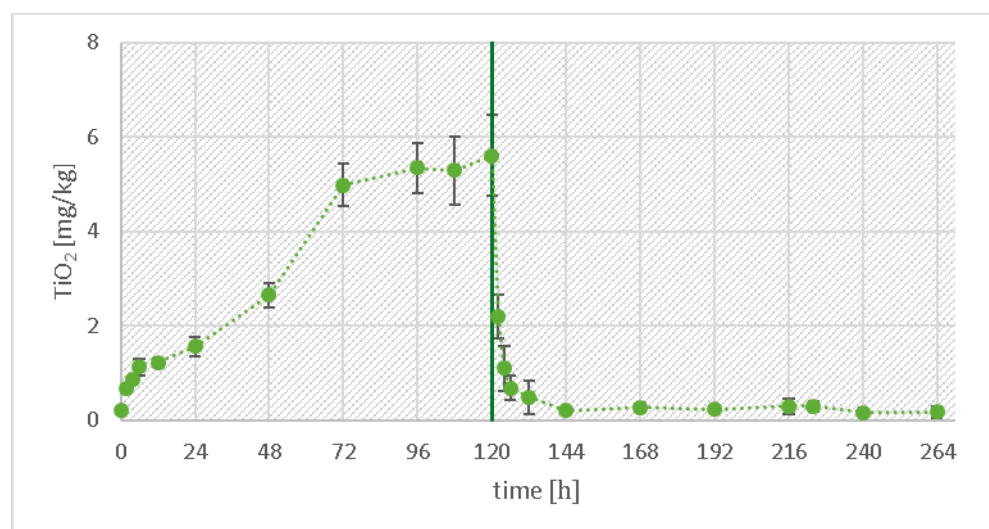
Source: own diagram, Fraunhofer IME

Figure 32: Bioaccumulation study with NM 105 – high concentration: total TiO_2 concentrations in test media at several levels (depths) of the flow-through system



Source: own diagram, Fraunhofer IME

Figure 33: Bioaccumulation study with NM 105 – high concentration: total TiO_2 concentrations in *C.f.* tissue



Source: own diagram, Fraunhofer IME

6.2.3.3 Evaluation

The heterogeneous concentration levels measured in the test medium during the uptake phase can be explained by the exchange of the NM 105 working suspension reservoir. Similar observations were made in both assays using the same stock suspension reservoir. The decrease in the total Ti or TiO₂ concentrations at the end of the uptake phase may be explained by sedimentation processes within the NM 105 working suspension reservoir.

The increase in the total Ti or TiO₂ tissue concentrations during the uptake phase could be explained by the uptake and potential accumulation of NM 105 NPs by the mussels from the media. However, the rapid decrease of the soft tissue concentrations during the depuration phase points to the quick elimination of the NPs. As mentioned for NM 300K it is not sure if the particles were just ingested or really incorporated into the tissue. The measured total concentrations may have been caused by particles localized in the digestive tract and in the viscera (see Chapter 6.2.4).

For the low concentration (TWA of 0.099 µg TiO₂/L) a BAF_{ss} value of 6,150 was calculated. The calculated BAF_{ss} value of 9,022 was calculated for the high concentration (TWA of 0.59 µgTiO₂/L). Due to the high standard deviation of the measured total tissue concentrations in the lower concentrated exposure the BAF_{ss} value of 6,150 should be handled with caution and the presence of a concentration depending BAF_{ss} could not be answered clearly.

6.2.4 Investigations on particle number and distribution of total concentrations in the soft tissue

6.2.4.1 Study design

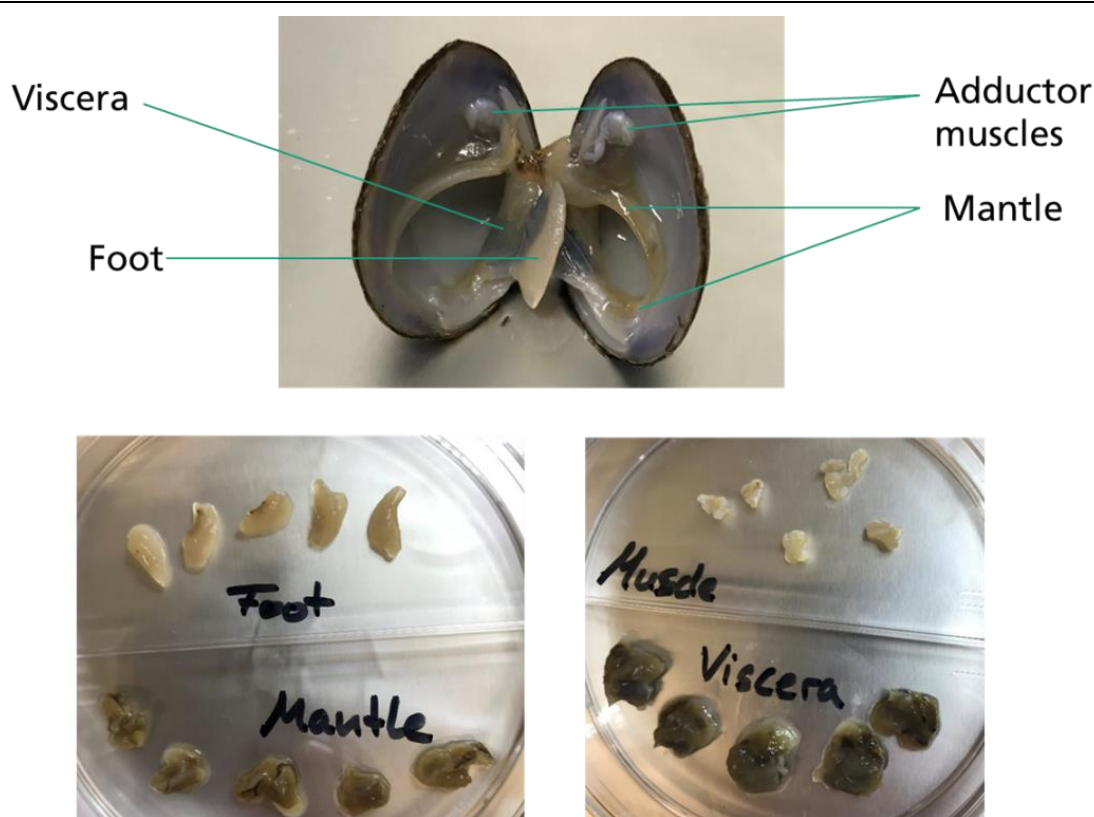
An additional study was carried out to elucidate the contribution of MNMs to the total concentrations measured in soft tissue, to elucidate potential particle size dependent uptake and elimination processes of the MNMs, and to investigate the distribution of MNMs in different compartments of the animals. Finally, the total concentrations of NM 300K, AgNO₃ and NM 105 measured in different compartments were compared.

The test systems were running under the same conditions as the systems used for the main study to investigate the bioaccumulation of the MNMs. The media with the highest test concentrations of those studies were applied. Animals were sampled during the uptake phase as well as during the depuration phase to show changes in the amount of incorporated NPs. Therefore, triplicated samples, each consisting of 3 animals, were sampled for the sp-ICP-MS measurements. The duration of the uptake phases was the same as in the main study to ensure that steady state conditions were reached. Samples used for the sp-ICP-MS measurements were directly frozen, using liquid nitrogen and stored at -20 °C. For the measurements, the samples were digested using the enzyme Proteinase K according to the method described by Loeschner *et al.*, 2013, and Schmidt *et al.*, 2011. The defrosted soft tissues were incubated with 10 ml of the digestion solution per 400 mg fresh weight for 3 hours at 50 °C and shaken at 100 rpm. The digestion solution was composed of 45 mg Proteinase K in 1 L puffer solution (0.5 % SDS + 50 mM NH₄HCO₃, pH 8.0 - 8.2). After the complete dissolution of the tissue, the solution was filtered using 0.45 µm syringe filters and measured using an ICP-QQQ-MS (Agilent 8900). The preparation of the calibration suspensions carried out at the day of measurement. Gold nanoparticles (AuNP, 60 nm, BBI Solutions) were used as reference material to determine the nebulization efficiency, a parameter needed for interconversion of measured particle event intensities into particle masses and sizes. Transient signals were recorded for 60 s for each

sample, using a dwell time of 100 μ s. Each sample was diluted to gain 200 - 2000 particle events per minute. According to Sannac *et al.* (2013) and Mitrano *et al.* (2014) this correlates to an element concentration in the range of ng/L. Ag was measured as the isotope ^{107}Ag . ^{48}Ti was measured in the NH_3 -reaction mode to minimize interferences with calcium. The used evaluation software calculated the particle size depending on the measured signals (for TiO_2 under consideration of the mass fraction of Ti in TiO_2).

Animals were sampled presumably under steady state conditions and dissected to investigate the total concentrations as well as particle distributions in the compartments (foot, mantle, muscle and viscera (Fig. 34). Five replicates, consisting of five animals each, were sampled. The samples were stored at -20°C and solved by acid digestion (Chapter 6.1.1.1) before being measured using ICP-MS as described above and directly frozen using liquid nitrogen in case of sp-ICP-MS analysis.

Figure 34: Compartments dissected from *Corbicula fluminea*



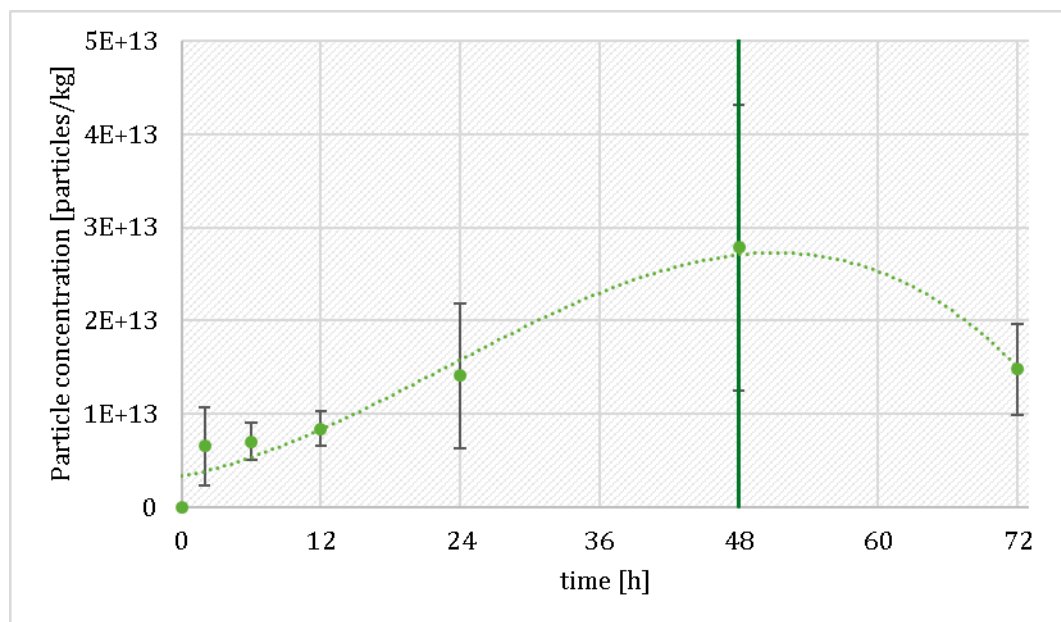
Source: Fraunhofer IME

6.2.4.2 Results

Results of the particle measurements

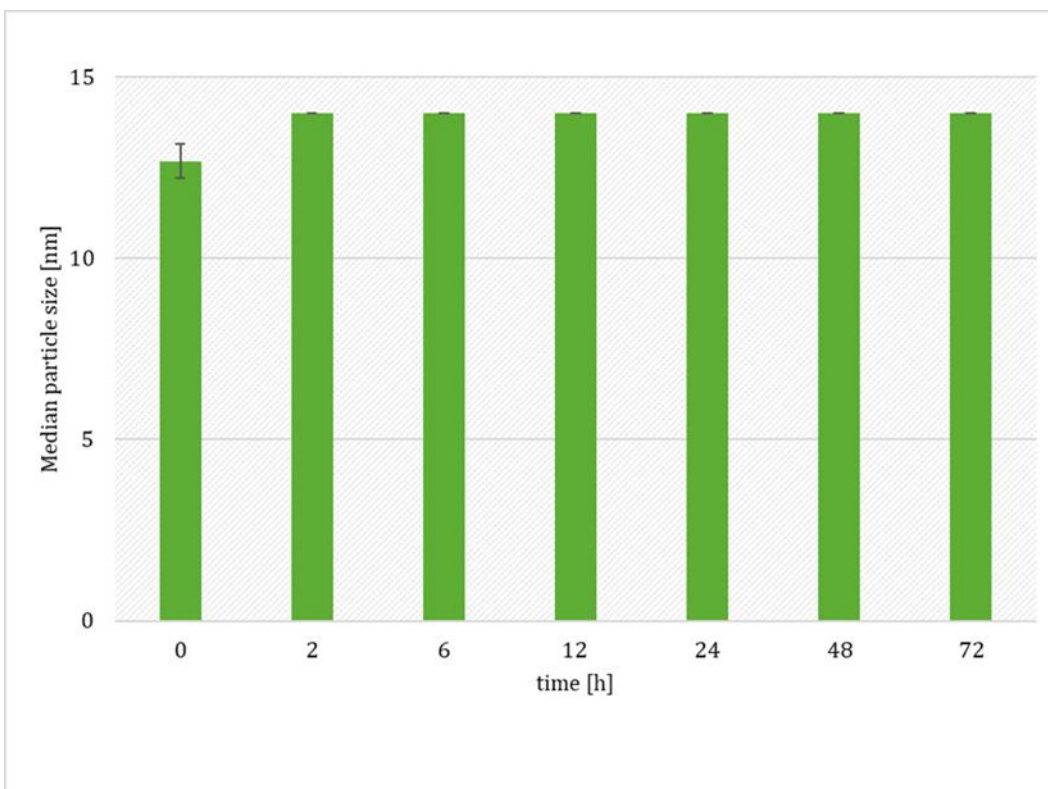
In the case of NM 300K a clear increase of particle concentration occurred in the soft tissue of *C.f.* during the uptake phase of 48 hours. The particle concentration in the soft tissue tended to decrease during the 24 hours lasting depuration phase as shown in Fig. 35. The determined median particle size in the soft tissue and in the media of around 14 nm was consistent over the whole test period, including uptake and depuration time (Fig. 36 & 37). However, no significant difference was observed between the particle sizes in the tissue over time and between the particles in the tissue and the medium. The size of NM 300K is near the particle detection limit for silver and the measured size distributions showed an overlap with the instrumental and ionic background.

Figure 35: Particle concentrations in the soft tissue during uptake and depuration phase of NM 300K



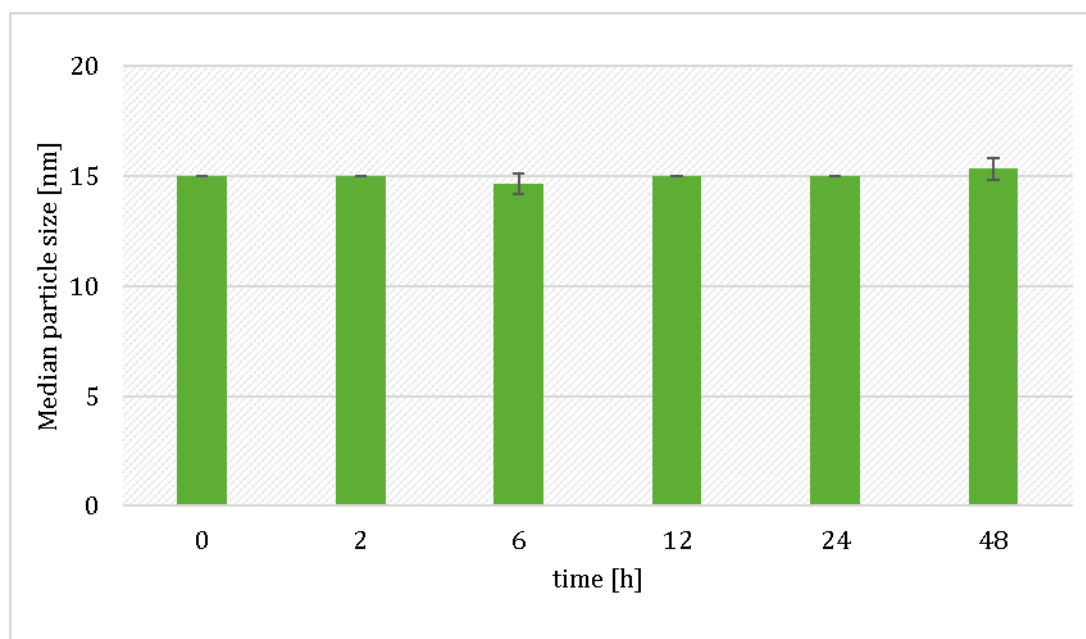
Source: own diagram, Fraunhofer IME

Figure 36: Calculated median particle size in the soft tissue - NM 300K



Source: own diagram, Fraunhofer IME

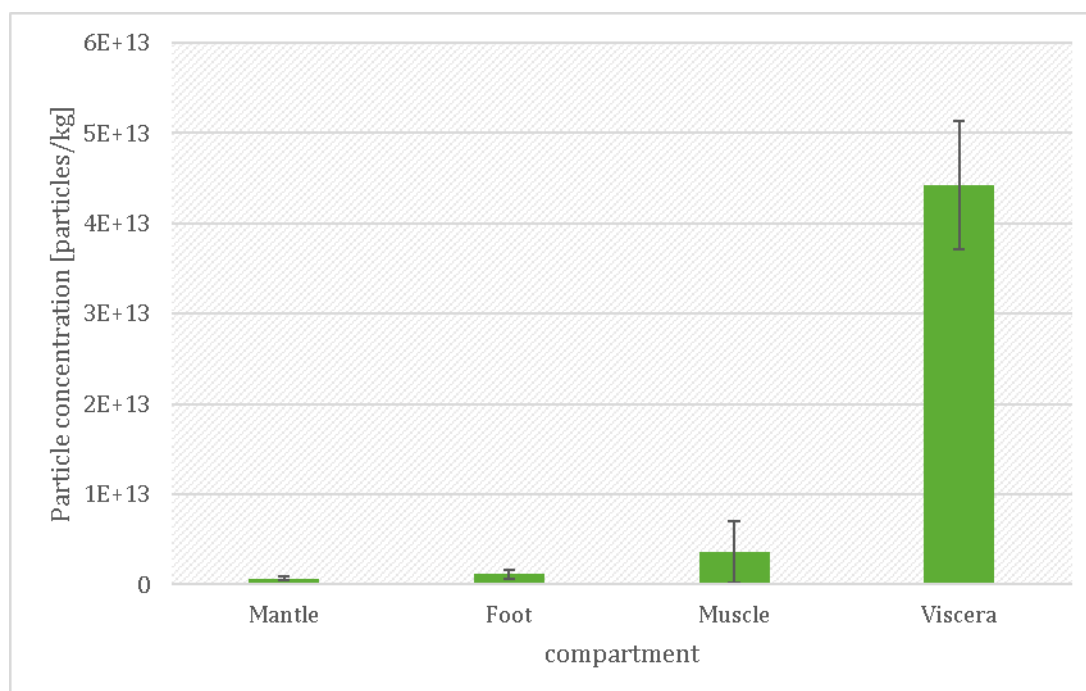
Figure 37: Calculated median particle size in media - NM 300K



Source: own diagram, Fraunhofer IME

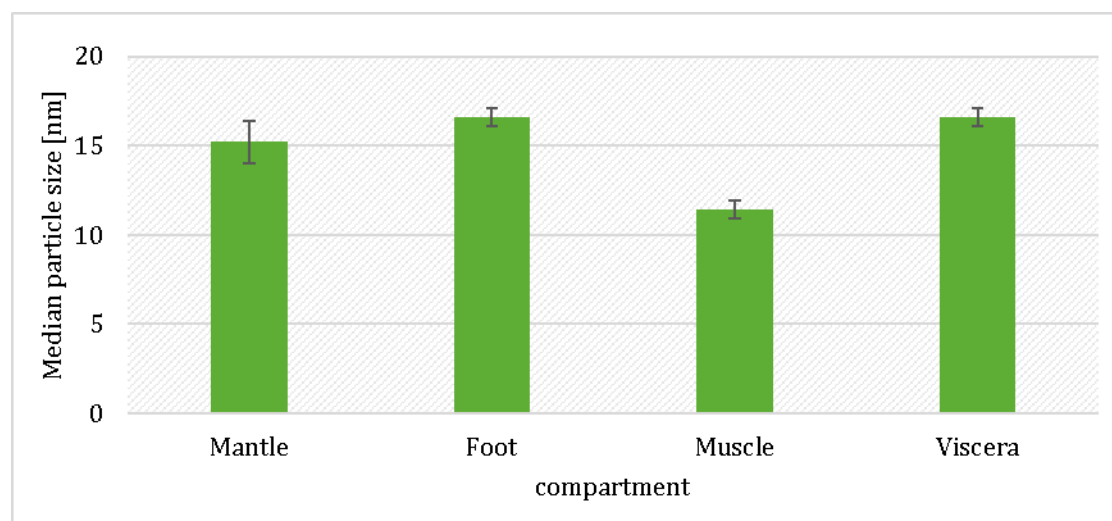
When looking at the different compartments of the mussel's soft tissue, the viscera showed the highest particle concentration of all compartments, with all particles being on a comparably low level with respect to their standard deviation (Fig. 38). The calculated median size of the particles ranged between 15 and 17 nm, only the median particle size of the particles in the muscle tissue was calculated to be on a lower level of 11 nm (Fig. 39).

Figure 38: Particle concentrations in the different compartments at the end of the uptake phase - NM 300K



Source: own diagram, Fraunhofer IME

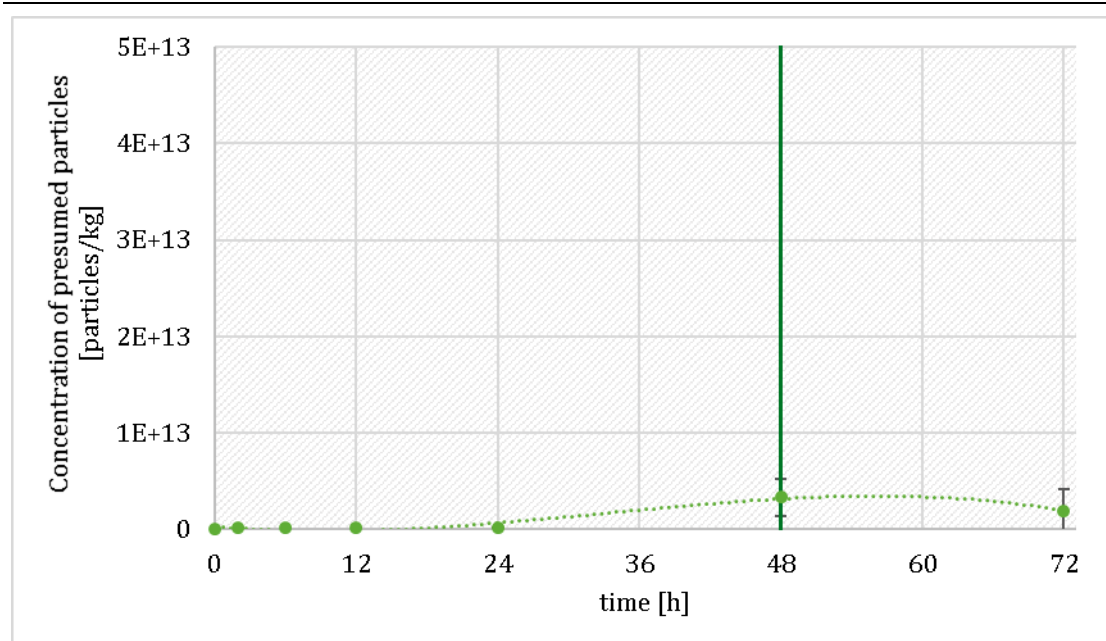
Figure 39: Calculated median particle size in the different compartments at the end of the uptake phase - NM 300K



Source: own diagram, Fraunhofer IME

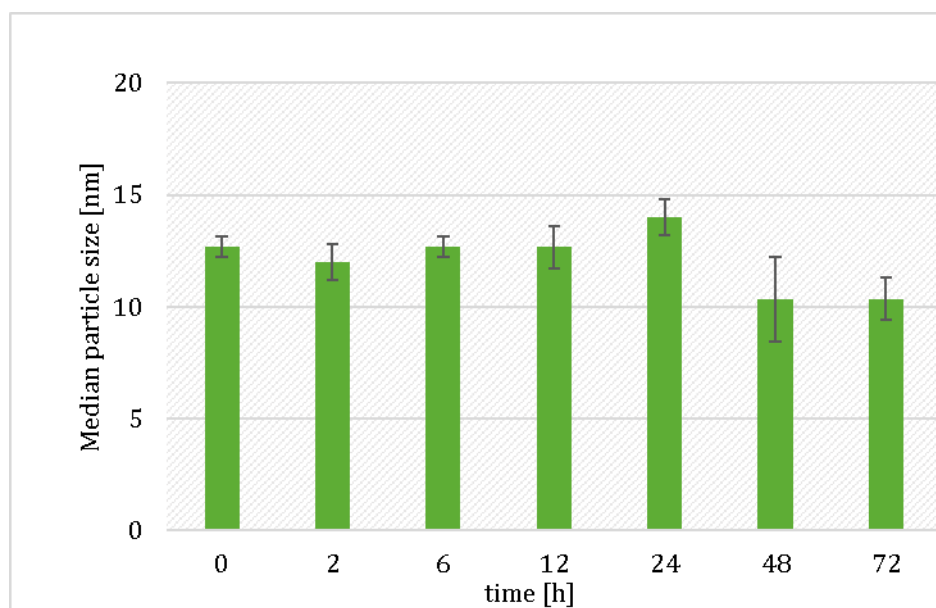
Also for soft tissue of animals exposed to AgNO_3 , sp-ICP-MS measurements were conducted. The data evaluation, with a setting of similar particle thresholds, showed also for these samples the presence of “particles”. This finding may be explained by the overlap of ionic background and particle domain due to the small size of NM 300K NPs near the analytical particle detection limit (background estimation diameter 7 - 10 nm). The increase of the presumed particle concentration during the uptake phase was much slower than that in the NM 300K exposure scenario. Similarly a slow decrease of the particle concentration was observed during the depuration phase (Fig. 40). The determined median size of the silver particles in the different tissues of the animals exposed to AgNO_3 was around 13 nm during the uptake phase and at 10 nm in the samples taken during the depuration phase (Fig. 41). The calculated median size of the particles in the media fluctuated around 14 nm during the uptake phase (Fig. 42).

Figure 40: Concentrations of presumed particles in the soft tissue during uptake and depuration phase of AgNO_3

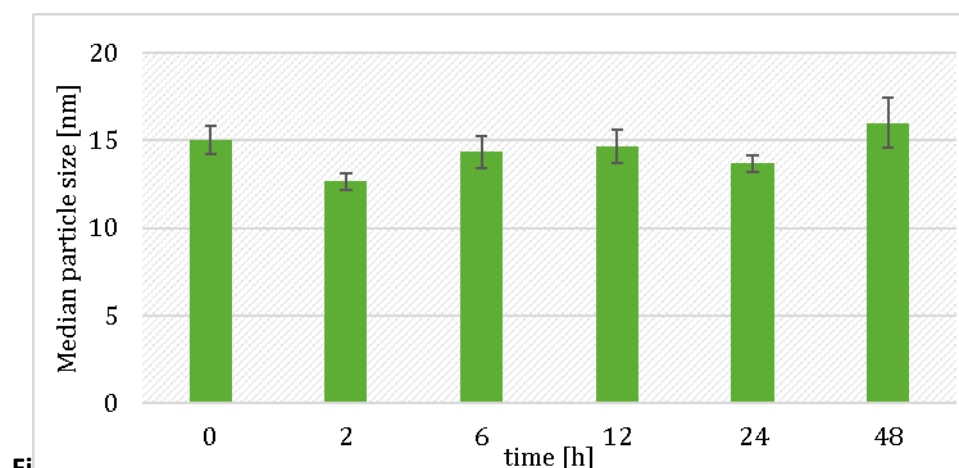


Source: own diagram, Fraunhofer IME

Figure 41: Calculated median particle size in the soft tissue – AgNO₃



Source: own diagram, Fraunhofer IME



Fi

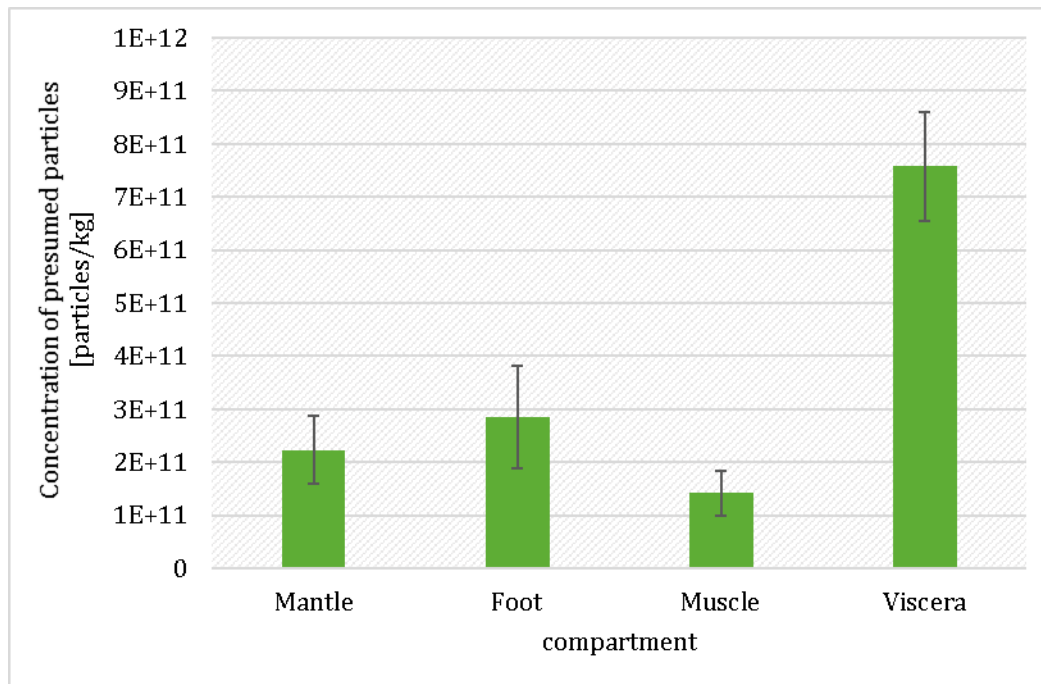
gure 42:

Calculated median particle size in media – AgNO₃

Source: own diagram, Fraunhofer IME

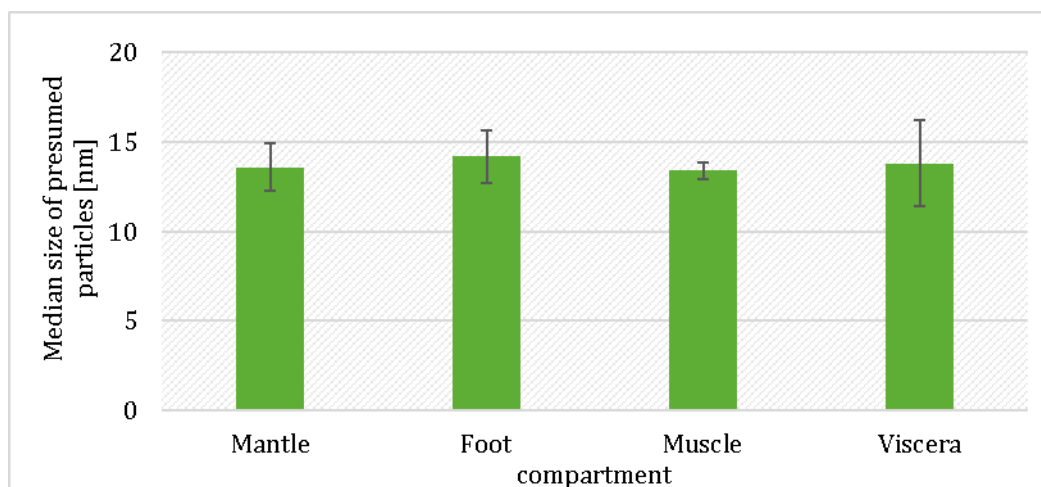
The comparison of the different compartments showed comparable results as described for NM 300K, even if differences between the viscera and the other compartments were smaller (Fig. 43 & 44). All particle concentrations were on a lower level than those measured under the NM 300K exposure scenario, indicating that observed presumed “particles” of AgNO₃ were likely background signals.

Figure 43: Concentrations of presumed particles in the different compartments at the end of the uptake phase – AgNO_3



Source: own diagram, Fraunhofer IME

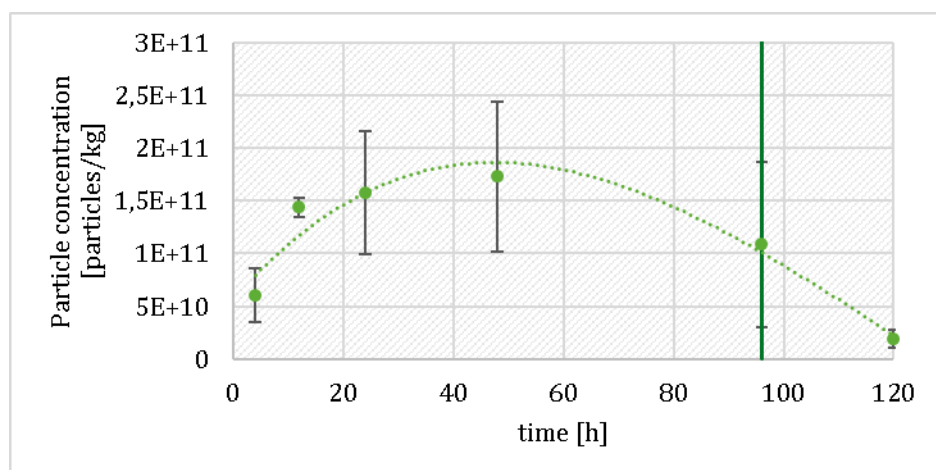
Figure 44: Calculated median size for the presumed particles in the different compartments at the end of the uptake phase – AgNO_3



Source: own diagram, Fraunhofer IME

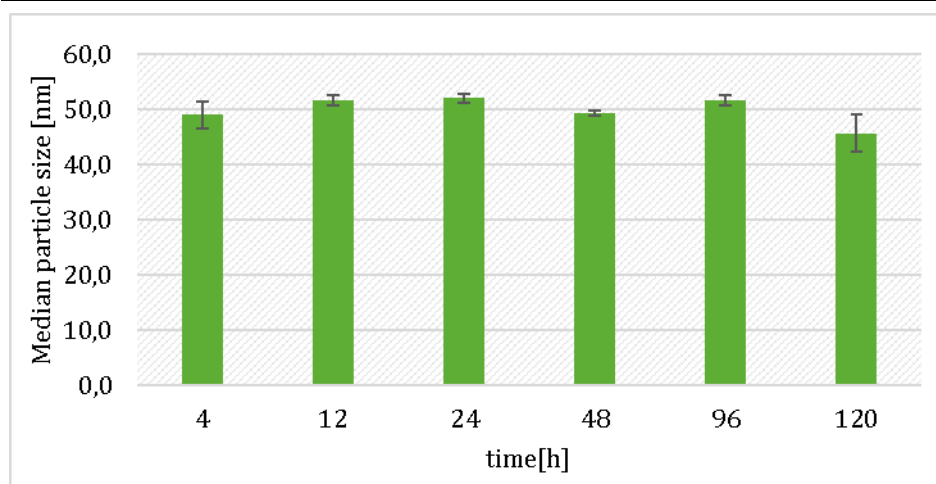
In the case of NM 105, an increase of the particle concentration in the whole soft tissue of the animals was observed (Fig. 45). The increase stopped at a lower level than in the case of the NM 300K exposure, but reached a stable level after 12 h and remained stable for the rest of the uptake phase. A higher standard deviation was observed in comparison to NM 300K. The measured particle concentration decreased during the depuration time. As shown in Fig. 46 the calculated median particle size in the tissues was around 50 nm during the whole uptake phase and on a similar level during the depuration phase (45.7 ± 3.3 nm). The calculated median particle size of NM 105 NPs in the test media was in a range of 65 and 83 nm during the uptake phase (Fig. 47).

Figure 45: Particle concentrations in the soft tissue during uptake and depuration phase of NM 105



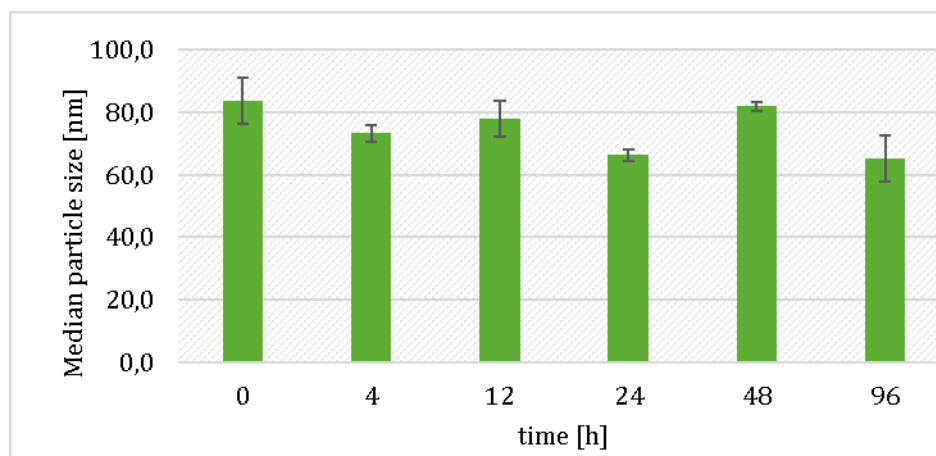
Source: own diagram, Fraunhofer IME

Figure 46: Calculated median particle size in the soft tissue – NM 105



Source: own diagram, Fraunhofer IME

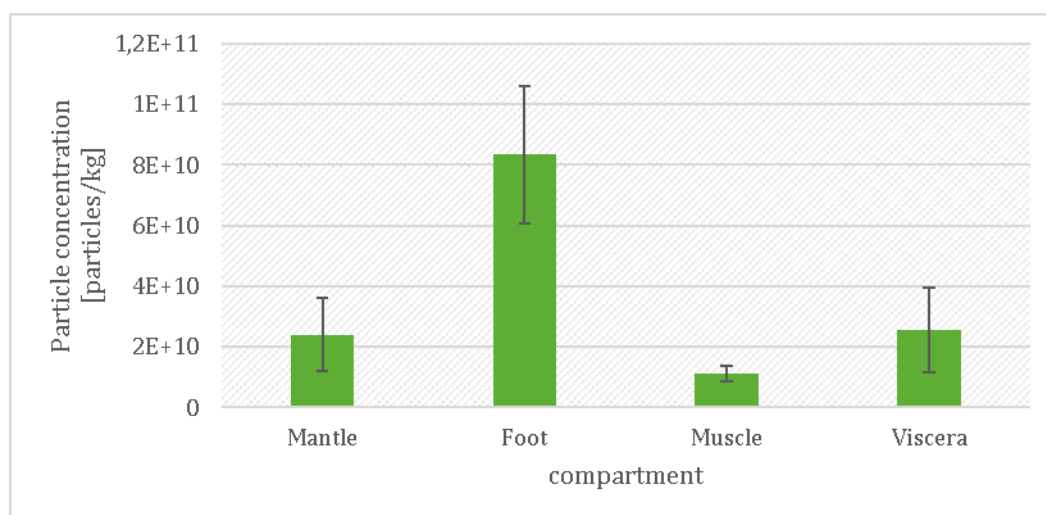
Figure 47: Calculated median particle size in media – NM 105



Source: own diagram, Fraunhofer IME

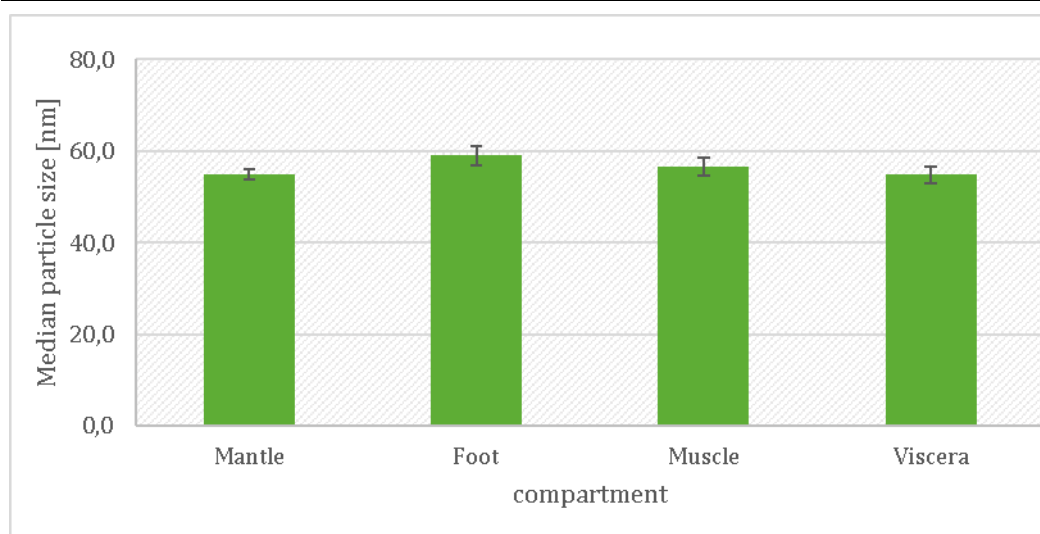
Fig. 48 shows particle concentrations measured in the different compartments of the mussels. The mean concentration of particles was four times higher in the foot than in the other compartments, which showed comparable levels. No differences in the particle sizes were observed in the different compartments (Fig. 49).

Figure 48: Particle concentrations in the different compartments at the end of the uptake phase – NM 105



Source: own diagram, Fraunhofer IME

Figure 49: Calculated median particle size in the different compartments at the end of the uptake phase – NM 105



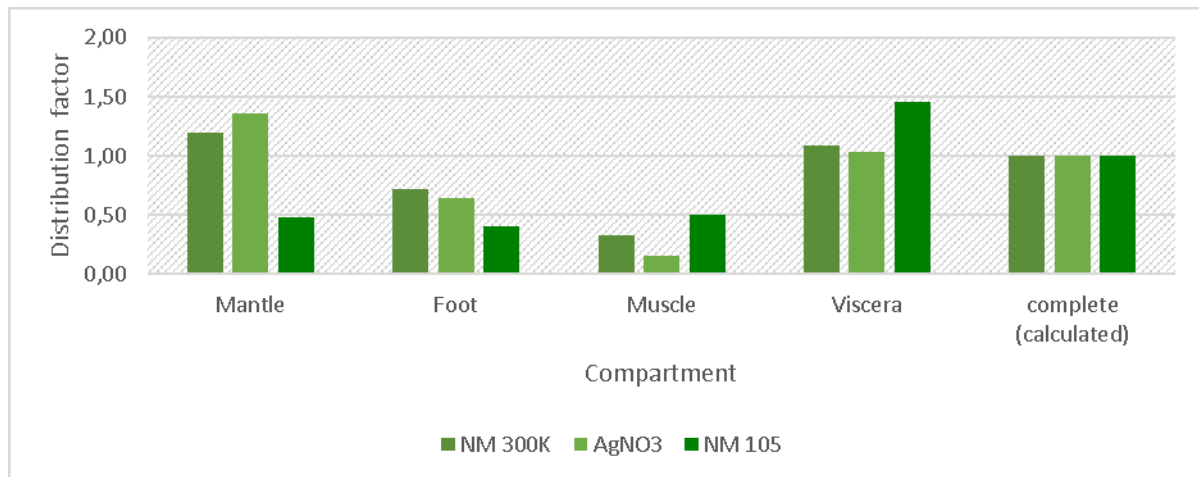
Source: own diagram, Fraunhofer IME

Results of the measurement of total concentrations

Fig. 50 shows the distribution factors for the total Ag and TiO₂ contents measured in the different compartments of the test animals exposed to NM 300K, AgNO₃ and NM 105 and sampled under steady state conditions at the end of the uptake phase. The contents of the different compartments were used to calculate the total content of Ag and TiO₂ in the complete animals. The mean total concentration (n = 5) of each compartment was divided by the mean value of the calculated for the complete samples (n = 5) to gain distribution factors for the different compartments.

Following the Ag exposure the mantle showed the highest distribution factor (1.20 and 1.36 for NM 300K and AgNO₃) followed by the viscera (1.09 and 1.04). The muscle tissue showed the lowest distribution factor for the total Ag content (0.33 and 0.15 for NM 300K and AgNO₃). However, the viscera tissue showed the highest distribution factor for the total TiO₂ content (1.45), whereas the other compartments were without any great differences with factors from 0.40 in the foot tissue to 0.50 in the muscle tissue (Fig. 50).

Figure 50: Distribution factors of total content of Ag/TiO₂ based on the total content of calculated complete soft tissue bodies



Source: own diagram, Fraunhofer IME

6.2.4.3 Evaluation

The results of the sp-ICP-MS measurements show that the uptake and accumulation of Ag from NM 300K was driven, at least partially, by the ingestion of AgNPs. Even the fact, that the viscera had the highest Ag particle concentration of the measured compartments (mantle) shows that ingested Ag was bioavailable also as AgNPs and not only as ions. However, the role of the ions must not be underestimated. A look at the calculated mean particle size of particles found in the muscle tissue of animals exposed to NM 300K highlights this fact when compared to the estimated comparable size of the measured particles in the AgNO₃ treatment. The adductor muscle has less contact to the exposure media, even by the flow of the filtered or ingested media. However, Ag might be transported to the muscle tissue as Ag⁺ by the haemolymph.

The slightly increased distribution factors of Ag calculated for the viscera for both, NM 300K and AgNO₃, may be explained on the one hand by the flow of the ingested water towards the viscera. The viscera contains the filtrating cilia and gills that extract the AgNPs from the water as well as the solved Ag⁺ ions, e.g. by Na⁺ and Cu⁺ uptake and transport mechanisms (e.g. Solioz and Odermatt, 1995; Bury and Wood, 1999; Fabrega *et al.*, 2011). Also sorption processes to organic matter in the digestion system or mucus and pseudo feces could lead to higher Ag body burden causing a higher distribution factor. On the other hand the high distribution factor for the viscera may be explained by the binding of Ag⁺ ions to Ag induced MTs (Marie *et al.*, 2006), that are strongly released in the tissue of the gills (belonging to the viscera) and the tissue of the mantle (Hardivillier *et al.*, 2006). This also may be a factor that explains the high distribution factor for Ag estimated for the mantle tissue.

The sp-ICP-MS measurements showed that NM 105 uptake and elimination was driven by the TiO₂ NPs. The high distribution factor for TiO₂ in the viscera may be explained by the fact, that the NM 105 particles were ingested and transported through the digestive system without transport across any tissue or cell barriers. The transport through the tissue by the haemolymph

can be rather excluded. The presence of very low particle concentrations in the different compartments may thus be simply explained by the particles adhesion to the tissue surface following contact to the exposure media. The higher particle concentration measured in the tissue of the foot may be explained by the uptake of NM 105 particles by pedal feeding and additional adhesion of particles to the relatively high surface of the foot that is exposed to the media outside the shells for a longer time than other compartments.

6.2.5 Bioaccumulation study nPS

6.2.5.1 Study design

The main study on the bioaccumulation of nPS was carried out using one test concentration in a semi-static design due to the limited availability of the test material. The test medium was replaced every 12 hours with fresh medium. The animals ($n = 40$) were exposed in a 10 L rectangular glass tank containing 2 L of the test medium. Because of this, only a limited amount of animals could be exposed during the test and thus no proof for a steady state to calculate a BAF_{ss} could be given by repeated samplings. Tissue concentrations measured can only provide a rough indication for the bioaccumulation potential of nPS due to the early development stage of the methods applied. Prior to the test start the animals were kept in a tank with uncontaminated water tank without feeding to ensure defecation to allow the collection of feces produced during the test. Feces were collected every 12 hours in combination with the water replacement and the material collected within 24 h was pooled in one sample. Aeration was ensured using an aquarium pump.

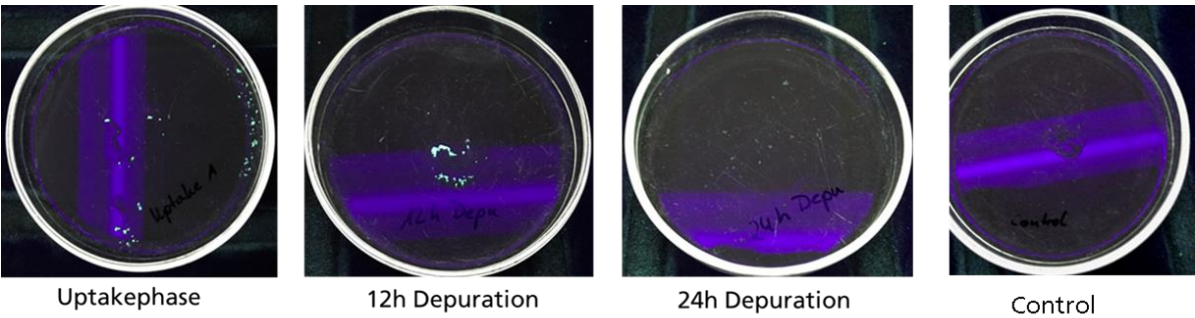
The duration of the uptake phase was 120 hours, followed by a 24 hours depuration phase. Triplicated samples, each consisting of 4 animals, were collected at the end of the uptake phase. The samples were digested using proteinase K as described in chapter 6.2.4.1 and measured using an AF4-FLD-MALLS. Additional samples (mussels & feces) were collected and mussels were dissected for further investigations using a HP-UVIS (DESEGA) at 254 nm and a fluorescence microscope (Leica CTR 6000).

6.2.5.2 Results

During the exposure period, a strong filtration activity was observed combined with a strong excretion of feces and pseudofeces. For a first overview a fluorescent lamp was used to make the nPS that were taken up by the animals optically visible. As shown in Fig. 51, the feces of *C.f.* collected during the exposure time showed fluorescence (yellow-green spots). The feces collected after 12 h of depuration showed less fluorescence and after 24 h of depuration showed nearly no fluorescence. Also the soft tissue of the animals showed fluorescence at the end of the uptake phase. The hot spots of the fluorescence in these animals were localized in the viscera and foot of the animals (Fig. 52, red arrows). After 24 h of depuration, no fluorescence was visible in the animals using the fluorescence lamp.

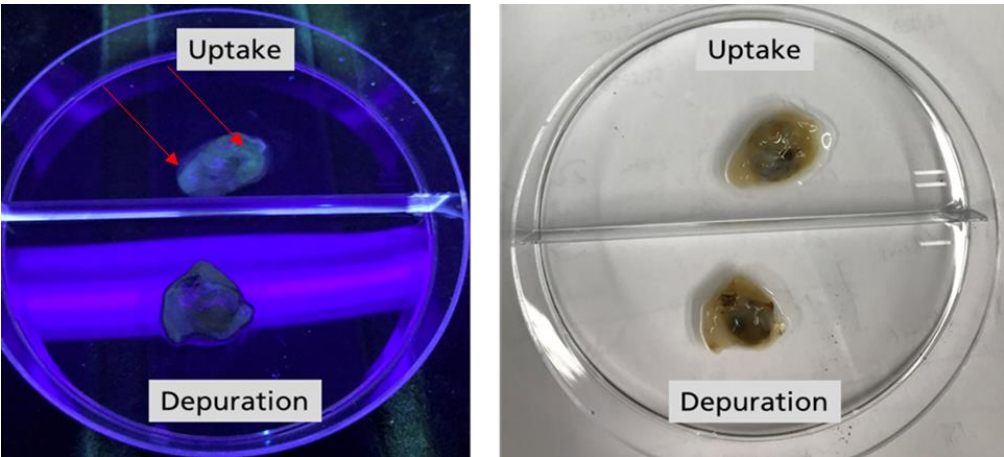
Additional samples of the soft tissue were observed using a fluorescence microscope. All samples showed fluorescence after the uptake phase, whereby the viscera showed the strongest intensity of fluorescence (Fig. 53). All compartments showed less fluorescence after 24 hours of depuration (Fig. 53). The strongest decrease in the fluorescence intensity was observed for the viscera. Only a weak decrease was observed for the mantle and foot tissue.

Figure 51: Feces of *C.f.* from the nPS bioaccumulation study under a fluorescence lamp, showing different intensities of fluorescence



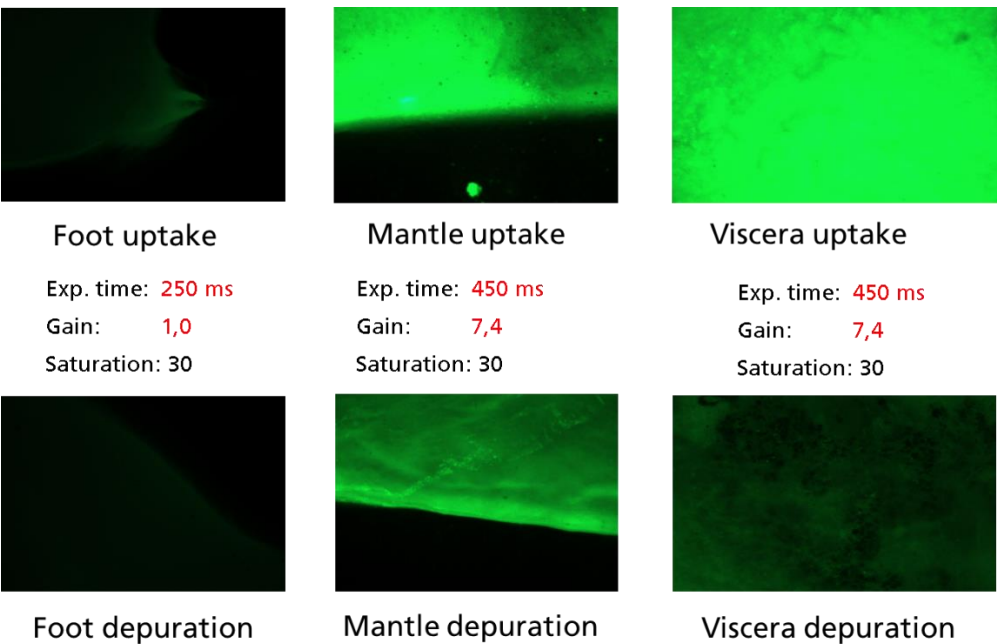
Source: Fraunhofer IME

Figure 52: Whole soft tissue of an animal sampled after the uptake phase (top) and an animal sampled after 24 h of depuration (bottom), left: fluorescence lamp, right: daylight



Source: Fraunhofer IME

Figure 53: Pictures (fluorescence microscope) of different compartments of *C.f.* sampled after the uptake phase (top) and after 24 h of depuration (bottom)



Source: Fraunhofer IME

7 General discussion

7.1 Dietary tests

Ground stinging nettle appeared to be the best food source of the tested diets leading to less pollution, build-up of biofilm and accumulation of organic matter, compared to the other food sources. Generally, the amount of food should be supplied on a level as low as possible to avoid sorption processes of the NPs to the food, but still high enough to allow sufficient nutrient uptake during the bioaccumulation studies and to trigger the filtration activity of the mussels.

7.2 Uptake, elimination and accumulation of Ag

Reviewing the bioaccumulation studies with AgNO₃ and NM 300K, the observed increases of the Ag body burden could be explained by the uptake of Ag from the exposure media. Reduced filtration activities were observed in all exposure periods containing Ag, although with variable intensity. Due to the fact that the degree of filtration inhibition depends on the concentration as well as on the presented form of Ag, reduced filtration may be explained as a kind of protective behavior. A slight decrease of the filtration rate was previously observed in response to increased metal exposure, e.g. for the green mussel *Perna viridis* (Vijayavel, Gopalakrishnan and Balasubramanian, 2007), the zebra mussel *Dreissena polymorpha* (Wildridge *et al.*, 1998) as well as for *C. fluminea* (Rodgers *et al.*, 1980; Doherty and Cherry, 1988). A complete bivalve closing behavior in response to higher heavy metal concentrations in the water was described as a strategy to protect bivalves from waterborne contaminants and to avoid toxic conditions (Doherty, Cherry and Cairns, 1987; Kádár *et al.*, 2001; Tran *et al.*, 2003; Fournier *et al.*, 2004; Liao, Jou and Chen, 2005; Tran, Fournier and Durrieu, 2007). Wildridge *et al.* (1998) described a concentration depending filtration decrease of *D. polymorpha* during potassium exposure which is in accordance to our observations of a higher reduction of the filtration rate at higher total Ag concentrations during AgNO₃ exposure. The lower inhibition of the filtration activity during exposure to NM 300K, compared to AgNO₃ similar total Ag concentration levels, indicates that this protection strategy was triggered only by the presence of metal ions released by NM 300K and not by the particles. The total Ag concentrations measured in our studies were mainly represented by the particulate fraction. The amount of dissolved Ag in the NM 300K test media was estimated in pretests to be between 1.6 and 21.5 % in test media aged for 24 h under static conditions. Considering the flow-through conditions in the exposure scenarios of this work, the percentage of dissolved Ag⁺ in the bioaccumulation studies was supposed to be on an even lower level.

Protective behavior may also explain differences in the time required to reach steady state conditions of Ag concentrations in the soft tissue of *C. fluminea*. The steady state condition was reached within 24 h at the higher AgNO₃ concentration, while it was reached after 72 h at the lower AgNO₃ concentration. The steady state body burden was two times lower in the higher concentrated AgNO₃ (0.24 mg Ag/kg) assay than in the lower one (0.5 mg Ag/kg), whereby the medium concentration of the higher concentrated treatment was around ten times higher compared to the lower concentrated treatment resulting in BAF_{ss} estimates of 710.7 and 30.5, respectively. This may be explained by the lower filtration rate in the higher concentrated treatment resulting in a lower uptake of Ag from the exposure medium. This process is very important to be considered in further investigations on the bioaccumulation potential of other ionic or ion-releasing substances or MNMs in bivalves as this mechanism may lead to totally different results regarding the calculated endpoints.

In the bioaccumulation studies with NM 300K the steady state conditions were reached within 24 h of the uptake phase. In this case the level of the steady state body burden in the soft tissue showed a positive correlation with the exposure concentration. The ten times higher concentrated exposure led to a four times higher body burden in the higher concentrated NM 300K assay. Aside from the fact, that the measured total Ag concentration in the media was represented by a smaller dissolved fraction (1-20 %) which can be accumulated by the animals, the investigations using sp-ICP-MS showed that also Ag NPs were definitely taken up by the mussels. However, it remains unknown how Ag NPs were incorporated into the different compartments, e.g. by phagocytosis across the gill epithelium and moved through the haemolymph. Hereafter we use the term “taken up” for particles that were ingested by the mussels and simply moved through the mussel’s body or digestive tract. This term should not be confounded with the term “uptake” that is typically used to describe the transfer of a compound into organic tissue. Nevertheless, the sp-ICP-MS investigations showed increasing particle concentrations with increasing tissue concentrations of total Ag during the NM 300K study. The major part of the particles could be found in the viscera, including the gills and the digestive tract. All other compartments just showed negligible particle concentrations. This clearly indicates that there was no significant transport of Ag NPs through the different compartments tissues or haemolymph and is thus pointing to the only negligible bioavailability of Ag NPs. In consideration of this and due to the fact, that we were able to observe a rapid and nearly complete elimination of Ag during the depuration phase, it can be assumed that only very low amounts of dissolved Ag⁺ released from the test material were really bioaccumulated by the test organisms. The ingested Ag NPs obviously simply moved through the digestive tract resulting in low BAF_{ss} values of 31 and 128.

During AgNO₃ exposure, the observed bioaccumulation of Ag resulted from the uptake of dissolved Ag⁺ from the exposure media. Thus the estimated endpoint was the BCF_{ss} and not BAF_{ss}. The BCF_{ss} value of 30.5 estimated for the high AgNO₃ treatment, may be explained by the strongly reduced filtration rate and thus the limited uptake of Ag⁺ from the test media. Due to less reduction of the filtration rate in the lower concentrated AgNO₃ treatment, the continuous uptake of small amounts of Ag⁺ may have led to the higher BCF_{ss} of 710.7. Similarly, a higher release of Ag⁺ in the higher concentrated NM 300K treatment (BAF_{ss} 31) compared to the lower concentrated treatment (BAF_{ss} 128), may have led to reduced filtration and thus the lower BAF_{ss}.

The high body burden observed in the study with the lower AgNO₃ concentration might be also explained by a second protective mechanism that may induce a reduced elimination of Ag during the depuration phase – the binding of Ag to metallothionein (MT). MT gene expression is upregulated by various metals like Cd, Au, Pt as well as by Ag, whereby the MT reaction correlates well with increasing metal body burden (Lansdown *et al.*, 1997; Lansdown, Sampson and Rowe, 1999; Lansdown, Sampson and Rowe, 2001). The MT expression in *C. fluminea* is well known and used for metal pollution assessment (Baudrimont *et al.*, 1999; Legeay *et al.*, 2005; Hardivillier *et al.*, 2006; Marie, Baudrimont and Boudou, 2006; Ringwood *et al.*, 2010). The ability of MT to bind up to 12 mol of Ag per mol MT may explain the accumulation and lack of elimination of Ag (sink) during the depuration phase (Nielson, Atkin and Winge, 1985; Liu, Kershaw and Klaassen, 1991; Lansdown *et al.*, 1997; Lansdown, 1999; Lansdown, 2002; Ikemoto *et al.*, 2004). The increase of MT in the tissue and thus the increase of the Ag binding capacity may explain the higher steady state concentration in the low concentration of AgNO₃ in comparison to that in the study with the higher concentration. At the lower exposure treatment the valve closing behavior is less pronounced due to lower media concentration and thus no filtration reduction is triggered. In this way incorporation and accumulation of Ag may occur until a body burden is reached that triggers the expression of MT. As long as the release of Ag⁺ from NM 300K is not effecting the valve closing behavior similar effects may occur. In this study,

in the low NM 300K treatment the release of Ag⁺ was leading to a limited body burden potentially having only a low effect on the expression of MTs and as reflected by the lower accumulation of Ag. At the higher exposure concentration, the higher release of Ag⁺ potentially led to reduced filtration behavior and reduced valve opening time. Therefore, tissue concentrations triggering the expression of MT could not be reached.

The distribution factors for accumulated Ag in the different compartments underpin the presumption, that only Ag⁺, even at a small level as measured in the NM 300K study, were really incorporated in the mussels' tissue. Both exposure scenarios, AgNO₃ and NM 300K, led to comparable distribution factors for total silver. The high distribution factors of Ag for both, NM 300K and AgNO₃ estimated for the viscera, may be explained on the one hand by the flow of the ingested water towards the viscera. The viscera contains the filtrating cilia and gills that extract the AgNPs from the water as well as the solved Ag⁺ ions, e.g. by Na⁺ and Cu⁺ uptake and transport mechanisms (Solioz and Odermatt, 1995; Bury and Wood, 1999; Fabrega *et al.*, 2011). Also sorption to natural organic matter and proteins in the digestion system or mucus and pseudo feces could lead to higher Ag concentrations causing a higher distribution factor (Ravindran *et al.*, 2010; Chinnapongse, MacCuspie and Hackley, 2011; Khan *et al.*, 2011; Gao *et al.*, 2012). On the other hand the high distribution factor of Ag estimated for the viscera may be explained by the binding of Ag to MTs (Marie, Baudrimont and Boudou, 2006), that are strongly released in the gill and mantle tissue (belonging to the viscera) in response to Ag exposure (Hardivillier *et al.*, 2006).

7.3 Uptake, elimination and accumulation of TiO₂

The increase in the total Ti tissue concentration during the bioaccumulation studies could be explained by the uptake and potential accumulation of NPs from the media. Single particle concentration measurements in the mussel tissue showed a progression along the uptake and depuration phase that mirrored the course of the measured total Ti concentrations. This indicates that TiO₂ NPs were taken up from the exposure media. However, the measured concentrations were probably mainly caused by particles localized in the digestive tract and in the viscera as shown by the distribution factors for TiO₂ with the viscera showing the highest distribution factor.

Therefore, the decrease in the soft tissue concentrations in the depuration phase might be simply explained by the elimination of the NPs. As described for NM 300K, it is debatable whether the particles were only ingested or really incorporated into the tissue. However, the very effective and fast elimination that was observed during the depuration phase of both tests with TiO₂ points to the assumption that the NPs were only ingested. Our observations are in accordance with the results of the work of Doyle, Ward and Mason (2015), where an elimination of more than 90 % within 12 h of previously ingested TiO₂ NPs was observed in *Mytilus edulis*.

The increased BAF_{ss} values (6,150 and 9,022) estimated for TiO₂ NPs may be explained by two factors: First by the higher filtration activity during the uptake phase, which can be explained by the increased filtration activity of the bivalves triggered by particulate matter. This effect should be stronger for NM 105 NPs that were measured to be in a range of 63 and 83 nm in the exposure media, while the Ag NPs of NM 300K were clearly smaller (15 to 17 nm). In addition, NM 105 NPs are known to show a high tendency to agglomerate which may again lead to a more effective uptake. Filter feeding mussels take up bigger and agglomerated NPs much more effectively than smaller und free particles (Hull *et al.*, 2011; García-Negrete *et al.*, 2013). Second, the higher BAF_{ss} values for the TiO₂ NPs may be explained by the lack of dissolved toxic ions in the test media that could trigger protective mechanism as observed for the Ag tests.

7.4 Uptake, elimination and accumulation of nPS

This study has shown that nPS are ingested by the animals as shown by high fluorescence observed under the fluorescence lamp. The strong fluorescence in the viscera may be explained by the gill uptake of nPS from the media and presence of fecal matter that bound the ingested nPS. The effective elimination of nPS from the viscera could be explained by the release of the feces and pseudo feces leading to the strong decrease in the intensity of fluorescence in the soft tissue samples collected during the depuration phase. The high filtration rate and excretion may have been induced by the nPS triggering the filtration activity of *C. fluminea* due to their particulate character. The higher intensity of fluorescence found in the foot tissue may have been caused by the uptake of nPS by pedal feeding processes. Accumulation of nPS in the feces or pseudo feces leading to a strong intensity of fluorescence shows that the nPS were ingested by mussels but quickly eliminated via the feces without incorporation in the tissue. The fast ingestion of the nPS and accumulation in fecal matter explains the strong observed decrease of nPS concentration in the test media during the preliminary test and the fast elimination of nPS in the viscera by defecation.

7.5 Suitability of the test system and the suggested endpoints

The bioaccumulation studies with the fresh water bivalve *C. fluminea* demonstrated the suitability of the new test system for the performance of bioaccumulation studies and the feasibility of such studies on MNMs with *C. fluminea* as filtering organism. During all studies a continuous exposure with stable MNM concentrations was achieved. The elucidation of bioavailability, uptake and elimination as well as accumulation of the test items was possible on the level of total and particle concentrations for the whole soft body as well as the single tissue compartments. By this, the fate of MNMs within the body or different tissues could be further elucidated. However, methods like correlative microscopy using transmission electron microscope are required for the absolute evidence that MNMs are really incorporated into the tissue or penetrated into cells. Nevertheless, the results obtained with this test system can be used to generate useful endpoints required for regulatory processes and could be included in a tiered bioaccumulation testing strategy for MNMs (Handy *et al.*, 2018). Even if some MNMs are only ingested but not really bioaccumulated, the estimated BAF_{ss} may still provide a valuable indication for the uptake of MNMs by bivalves if combined with information on the elimination rate estimated following the ingestion of MNMs. A fast elimination (time back to start concentration ≤ 24 h) points to the ingestion but no incorporation of MNMs in the animal tissues. A slow elimination (time back to start concentration > 24 h) provides clear indications for the bioaccumulation of the MNMs. However, it cannot be excluded that the bioaccumulation occurred by accumulation of dissolved / ionic fractions or particulate matter which would require further elucidations using advanced microscopy methods. For BAF estimates which are based on a real accumulation of the test item as indicated by low elimination rates, suitable criteria for the regulatory assessment of bioaccumulation should be defined and verified.

The steady state concentration represents the maximum loading capacity of MNMs taken up from the surrounding medium. Due to the high filtration rate of the bivalves the high loading capacity for MNMs, as shown in the studies on TiO₂, may lead to an increased risk of secondary poisoning for predatory species in the aquatic food chain even if no real bioaccumulation occurred.

Benthic invertebrates that feed on bivalve feces and / or pseudo feces may also cause the transfer of MNMs into the aquatic food chain. The high filtration rate of bivalves leads to the release of feces / pseudo feces with high concentrations of MNMs. Further investigations are

required to elucidate the uptake of highly contaminated feces or pseudo feces by benthic invertebrates that feed on fecal matter. Due to the fact that bivalves and other filtering benthic organisms represent the main part of the biomass in fresh water systems, the benthic food chain is supposed to play a central role regarding the ecological impact of MNMs (Karatayev, Burlakova and Padilla, 1997; Roditi, Strayer and Findlay, 1997; Gergs, Rinke and Rothhaupt, 2009; McMahon, 1983).

Mussel may also represent an important route of MNMs into the human diet (McMahon, 1983; Ferry *et al.*, 2009). The human intake of MNMs via freshwater or marine bivalves needs to be further investigated.

The suitability of the new test system for bioaccumulation studies with freshwater bivalves was shown in this study. The use of marine bivalves for bioaccumulation studies is described in two guidance documents (e.g. American Society for Testing and Materials, 2003). However, the systems described are supposed to be not suitable for a constant exposure of MNMs. The new test system may thus also represent a potential alternative for testing MNMs in marine bivalves. In addition to the bioaccumulation assessment of MNMs, the test system may be also suitable to investigate the uptake / bioaccumulation of microplastic in bivalves.

Generally, pretests should be carried out to describe the fate of the test item in the test system and to estimate a suitable exposure concentration to avoid protective behavior as described for Ag⁺. At least two test concentrations should be applied to investigate concentration related effects on the bioaccumulation of MNMs.

8 List of references

- Alves, L. C., Borgmann, U. and Dixon, D. G. (2009) 'Kinetics of uranium uptake in soft water and the effect of body size, bioaccumulation and toxicity to *Hyalella azteca*', *Environmental Pollution*, 157(8–9), pp. 2239–2247. doi: <http://dx.doi.org/10.1016/j.envpol.2009.04.006>.
- American Society for Testing and Materials (2003) 'ASTM E1022 – 94 (2013) standard guide for conducting bioconcentration tests with fishes and saltwater bivalve mollusks'. Available at: https://www.arpa.e.it/cms3/documenti/_cerca_doc/ecotossicologia/ASTM_E_1022_bioconcentrazione.
- Amler, M. R. W., Fischer, R. and Rogalla, N. S. (2000) *Muscheln*. Enke.
- Aschberger, K., Micheletti, C., Sokull-Klüttgen, B. and Christensen, F. M. (2011) 'Analysis of currently available data for characterising the risk of engineered nanomaterials to the environment and human health — Lessons learned from four case studies', *Environment International*. 37(6), pp. 1143–1156. doi: 10.1016/J.ENVINT.2011.02.005.
- Baker, T. J., Tyler, C. R. and Galloway, T. S. (2014) 'Impacts of metal and metal oxide nanoparticles on marine organisms', *Environmental Pollution*. 186, pp. 257–271. doi: 10.1016/J.ENVPOL.2013.11.014.
- Balbi, T., Smerilli, A., Fabbri, R., Ciacci, C., Montagna, M., Grasselli, E., Brunelli, A., Pojana, G., Marcomini, A., Gallo, G. and Canesi, L. (2014) 'Co-exposure to n-TiO₂ and Cd²⁺ results in interactive effects on biomarker responses but not in increased toxicity in the marine bivalve *M. galloprovincialis*', *Science of The Total Environment*. 493, pp. 355–364. doi: 10.1016/J.SCITOTENV.2014.05.146.
- Ball, A. L., Borgmann, U. and Dixon, D. G. (2006) 'Toxicity of a cadmium-contaminated diet to *Hyalella azteca*', *Environmental Toxicology and Chemistry*. 25(9), pp. 2526–2532. doi: 10.1897/05-650R.1.
- Basen, T., Gergs, R., Rothhaupt, K.-O. and Martin-Creuzburg, D. (2012) 'Phytoplankton food quality effects on gammarids: benthic–pelagic coupling mediated by an invasive freshwater clam', *Canadian Journal of Fisheries and Aquatic Sciences*, 70(2), pp. 198–207.
- Baudrimont, M., Andrès, S., Metivaud, J., Lapaquellerie, Y., Ribeyre, F., Maillet, N., Latouche, C. and Boudou, A. (1999) 'Field transplantation of the freshwater bivalve *Corbicula fluminea* along a polymetallic contamination gradient (river Lot, France): II. Metallothionein response to metal exposure', *Environmental Toxicology and Chemistry*. 18(11), pp. 2472–2477. doi: 10.1002/etc.5620181113.
- Baun, A., Hartmann, N. B., Grieger, K. and Kusk, K. O. (2008) 'Ecotoxicity of engineered nanoparticles to aquatic invertebrates: a brief review and recommendations for future toxicity testing', *Ecotoxicology*. 17(5), pp. 387–395. doi: 10.1007/s10646-008-0208-y.
- Benn, T. M. and Westerhoff, P. (2008) 'Nanoparticle silver released into water from commercially available sock fabrics', *Environmental Science & Technology*. 42(11), pp. 4133–4139. doi: 10.1021/es7032718.
- Bone, A. J., Colman, B. P., Gondikas, A. P., Newton, K. M., Harrold, K. H., Cory, R. M., Unrine, J. M., Klaine, S. J., Matson, C. W. and Di Giulio, R. T. (2012) 'Biotic and abiotic interactions in aquatic microcosms determine fate and toxicity of Ag nanoparticles: part 2—toxicity and ag speciation', *Environmental Science & Technology*. 46(13), pp. 6925–6933. doi: 10.1021/es204683m.
- Borgmann, U. (1998) 'A mechanistic model of copper accumulation in *Hyalella azteca*', *Science of The Total Environment*, 219(2–3), pp. 137–145. doi: [http://dx.doi.org/10.1016/S0048-9697\(98\)00229-0](http://dx.doi.org/10.1016/S0048-9697(98)00229-0).
- Bragg, P. D. and Rainnie, D. J. (1974) 'The effect of silver ions on the respiratory chain of *Escherichia coli*', *Canadian Journal of Microbiology*. 20(6), pp. 883–889. doi: 10.1139/m74-135.
- Bury, N. R. and Wood, C. M. (1999) 'Mechanism of branchial apical silver uptake by rainbow trout is via the proton-coupled Na⁺ channel', *American Journal of Physiology-Regulatory, Integrative and Comparative Physiology*. 277(5), pp. R1385–R1391. doi: 10.1152/ajpregu.1999.277.5.R1385.
- Chinnapongse, S. L., MacCuspie, R. I. and Hackley, V. A. (2011) 'Persistence of singly dispersed silver nanoparticles in natural freshwaters, synthetic seawater, and simulated estuarine waters', *Science of The Total Environment*. 409(12), pp. 2443–2450. doi: 10.1016/J.SCITOTENV.2011.03.020.
- Cleveland, D., Long, S. E., Pennington, P. L., Cooper, E., Fulton, M. H., Scott, G. I., Brewer, T., Davis, J., Petersen, E. J. and Wood, L. (2012) 'Pilot estuarine mesocosm study on the environmental fate of Silver nanomaterials

leached from consumer products', *Science of The Total Environment*. 421–422, pp. 267–272. doi: 10.1016/J.SCITOTENV.2012.01.025.

Conway, J. R., Hanna, S. K., Lenihan, H. S. and Keller, A. A. (2014) 'Effects and implications of trophic transfer and accumulation of CeO₂ nanoparticles in a marine mussel', *Environmental Science & Technology*. 48(3), pp. 1517–1524. doi: 10.1021/es404549u.

Cossu, C., Doyotte, A., Jacquin, M. C., Babut, M., Exinger, A. and Vasseur, P. (1997) 'Glutathione reductase, selenium-dependent glutathione peroxidase, glutathione levels, and lipid peroxidation in freshwater bivalves, *Unio tumidus*, as biomarkers of aquatic contamination in field studies', *Ecotoxicology and Environmental Safety*. 38(2), pp. 122–131. doi: 10.1006/EESA.1997.1582.

Custer, C. M. and Custer, T. W. (1996) 'Food habits of diving ducks in the great lakes after the zebra mussel invasion (hábitos alimenticios del patos zambullidores en los grandes lagos luego de la invasión de la almeja *Dreissena polymorpha*)', *Journal of Field Ornithology*. pp. 86–99. doi: 10.2307/4514086.

Darrigran, G. (2002) 'Potential impact of filter-feeding invaders on temperate inland freshwater environments', *Biological Invasions*. 4(1/2), pp. 145–156. doi: 10.1023/A:1020521811416.

Doherty, F. G. and Cherry, D. S. (1988) 'Tolerance of the Asiatic clam *Corbicula spp.* to lethal level of toxic stressors—A review', *Environmental Pollution*, 51(4), pp. 269–313. doi: [http://dx.doi.org/10.1016/0269-7491\(88\)90167-4](http://dx.doi.org/10.1016/0269-7491(88)90167-4).

Doherty, F. G., Cherry, D. S. and Cairns, J. (1987) 'Valve closure responses of the Asiatic clam *Corbicula fluminea* exposed to cadmium and zinc', *Hydrobiologia*, 153(2), pp. 159–167. doi: 10.1007/bf00006647.

Doyle, J. J., Ward, J. E. and Mason, R. (2015) 'An examination of the ingestion, bioaccumulation, and depuration of titanium dioxide nanoparticles by the blue mussel (*Mytilus edulis*) and the eastern oyster (*Crassostrea virginica*)', *Marine Environmental Research*. 110, pp. 45–52. doi: 10.1016/J.MARENRES.2015.07.020.

Doyotte, A., Cossu, C., Jacquin, M.-C., Babut, M. and Vasseur, P. (1997) 'Antioxidant enzymes, glutathione and lipid peroxidation as relevant biomarkers of experimental or field exposure in the gills and the digestive gland of the freshwater bivalve *Unio tumidus*', *Aquatic Toxicology*. 39(2), pp. 93–110. doi: 10.1016/S0166-445X(97)00024-6.

ECHA (2017) 'Guidance on Information Requirements and Chemical Safety Assessment Chapter R.11: PBT/vPvB assessment', *European Chemicals Agency*, (4), p. 494. doi: 10.2823/128621.

European Commission (2012) 'Communication from the Commission to the European Parliament, the Council and the European Economic and Social Committee - second regulatory review on nanomaterial's. <http://eur-lex.europa.eu/LexUriServ/LexUriServ.do?uri=COM:2012:0572:FIN:en:PDF>

European Parliament Council (2006) 'Regulation (EC) No 1907/2006 of the European Parliament and of the Council of 18 December 2006 concerning the Registration, Evaluation, Authorisation and Restriction of Chemicals (REACH), establishing a European Chemicals Agency, amending Directive 1999/45/EC and repealing Council Regulation (EEC) No 793/93 and Commission Regulation (EC) No 1488/94 as well as Council Directive 76/769/EEC and Commission Directives 91/155/EEC, 93/67/EEC, 93/105/EC and 2000/21/EC', *Official J Eu*. Available at: <http://eur-lex.europa.eu/legal-content/EN/TXT/PDF/?uri=CELEX:02006R1907-20170102&from=EN> (Accessed: 4 January 2018).

Fabrega, J., Luoma, S. N., Tyler, C. R., Galloway, T. S. and Lead, J. R. (2011) 'Silver nanoparticles: Behaviour and effects in the aquatic environment', *Environment International*, 37(2), pp. 517–531. doi: <http://dx.doi.org/10.1016/j.envint.2010.10.012>.

Fan, X., Wang, P., Wang, C., Hu, B. and Wang, X. (2017) 'Lead accumulation (adsorption and absorption) by the freshwater bivalve *Corbicula fluminea* in sediments contaminated by TiO₂ nanoparticles'. doi: 10.1016/j.envpol.2017.08.080.

Farkas, J., Bergum, S., Nilsen, E. W., Olsen, A. J., Salaberría, I., Ciesielski, T. M., Bączek, T., Konieczna, L., Salvenmoser, W. and Jenssen, B. M. (2015) 'The impact of TiO₂ nanoparticles on uptake and toxicity of benzo(a)pyrene in the blue mussel (*Mytilus edulis*)', *Science of The Total Environment*. 511, pp. 469–476. doi: 10.1016/J.SCITOTENV.2014.12.084.

Feng, Q. L., Wu, J., Chen, G. Q., Cui, F. Z., Kim, T. N. and Kim, J. O. (2000) 'A mechanistic study of the

antibacterial effect of silver ions on *Escherichia coli* and *Staphylococcus aureus*', *Journal of Biomedical Materials Research*. 52(4), pp. 662–668. doi: 10.1002/1097-4636(20001215)52:4<662::AID-JBM10>3.0.CO;2-3.

Ferry, J. L., Craig, P., Hexel, C., Sisco, P., Frey, R., Pennington, P. L., Fulton, M. H., Scott, I. G., Decho, A. W., Kashiwada, S., Murphy, C. J. and Shaw, T. J. (2009) 'Transfer of gold nanoparticles from the water column to the estuarine food web', *Nature Nanotechnology*. 4(7), pp. 441–444. doi: 10.1038/nnano.2009.157.

Fournier, E., Tran, D., Denison, F. and Massabuau, J.-C. (2004) 'Valve closure response to uranium exposure for a freshwater bivalve (*Corbicula fluminea*): quantification of the influence of pH', *Environmental Toxicology and Chemistry*, 23(5), pp. 1108–1114. Available at: <https://setac.onlinelibrary.wiley.com/doi/pdf/10.1897/02-604> (Accessed: 30 April 2018).

Gao, J., Powers, K., Wang, Y., Zhou, H., Roberts, S. M., Moudgil, B. M., Koopman, B. and Barber, D. S. (2012) 'Influence of Suwannee River humic acid on particle properties and toxicity of silver nanoparticles', *Chemosphere*. 89(1), pp. 96–101. doi: 10.1016/J.CHEMOSPHERE.2012.04.024.

García-Negrete, C. A., Blasco, J., Volland, M., Rojas, T. C., Hampel, M., Lapresta-Fernández, A., Jiménez de Haro, M. C., Soto, M. and Fernández, A. (2013) 'Behaviour of Au-citrate nanoparticles in seawater and accumulation in bivalves at environmentally relevant concentrations', *Environmental Pollution*. 174, pp. 134–141. doi: 10.1016/J.ENVPOL.2012.11.014.

Geret, F., Serafim, A. and Bebianno, M. J. (2003) 'Antioxidant Enzyme Activities, Metallothioneins and Lipid Peroxidation as Biomarkers in *Ruditapes decussatus*?'', *Ecotoxicology*. 12(5), pp. 417–426. doi: 10.1023/A:1026108306755.

Gergs, R., Rinke, K. and Rothhaupt, K.-O. (2009) 'Zebra mussels mediate benthic–pelagic coupling by biodeposition and changing detrital stoichiometry', *Freshwater Biology*. 54(7), pp. 1379–1391. doi: 10.1111/j.1365-2427.2009.02188.x.

Gottschalk, F. and Nowack, B. (2011) 'The release of engineered nanomaterials to the environment', *Journal of Environmental Monitoring*. 13(5), p. 1145. doi: 10.1039/c0em00547a.

Griffitt, R. J., Luo, J., Ao, J., Bonzongo, J. C. and Barber, D. S. (2008) 'Effects of particle composition and species on toxicity of metallic nanomaterials in aquatic organisms', *Environ Toxicol Chem*, 27. doi: 10.1897/08-002.1.

Handy, R. D., Ahtaiainen, J., Navas, J. M., Goss, G., Bleeker, E. A. J. and von der Kammer, F. (2018) 'Proposal for a tiered dietary bioaccumulation testing strategy for engineered nanomaterials using fish', *Environmental Science: Nano*. 5(9), pp. 2030–2046. doi: 10.1039/C7EN01139C.

Hankin, S. M., Peters, S. A. K., Poland, C. A., Foss Hansen, S., Holmqvist, J., Ross, B. L., Varet, J. and Aitken, R. J. (2011) *FINAL Specific Advice on Fulfilling Information Requirements for Nanomaterials under REACH (RIP-on 2) - Final Project Report*. Available at: http://orbit.dtu.dk/fedora/objects/orbit:88421/datastreams/file_6235005/content (Accessed: 4 January 2018).

Hardivillier, Y., Denis, F., Demattei, M.-V., Bustamante, P., Laulier, M. and Cosson, R. (2006) 'Metal influence on metallothionein synthesis in the hydrothermal vent mussel *Bathymodiolus thermophilus*', *Comparative Biochemistry and Physiology Part C: Toxicology & Pharmacology*. 143(3), pp. 321–332. doi: 10.1016/J.CBPC.2006.03.006.

Hull, M. S., Chaurand, P., Rose, J., Auffan, M., Bottero, J.-Y., Jones, J. C., Schultz, I. R. and Vikesland, P. J. (2011) 'Filter-feeding bivalves store and biodeposit colloiddally stable gold nanoparticles', *Environmental Science & Technology*. 45(15), pp. 6592–6599. doi: 10.1021/es200809c.

Ikemoto, T., Kunito, T., Anan, Y., Tanaka, H., Baba, N., Miyazaki, N. and Tanabe, S. (2004) 'Association of heavy metals with metallothionein and other proteins in hepatic cytosol of marine mammals and seabirds', *Environmental Toxicology and Chemistry*. 23(8), p. 2008. doi: 10.1897/03-456.

Kádár, E., Salánki, J., Jugdaohsingh, R., Powell, J. J., McCrohan, C. R. and White, K. N. (2001) 'Avoidance responses to aluminium in the freshwater bivalve *Anodonta cygnea*', *Aquatic Toxicology*. 55(3–4), pp. 137–148. doi: 10.1016/S0166-445X(01)00183-7.

Karatayev, A. Y., Howells, R. G., Burlakova, L. E. and Sewell, B. D. (2009) 'History of spread and current distribution of *Corbicula fluminea* (MÜLLER) in Texas', [http://dx.doi.org/10.2983/0730-8000\(2005\)24\[553:HOSACD\]2.0.CO;2](http://dx.doi.org/10.2983/0730-8000(2005)24[553:HOSACD]2.0.CO;2). doi: 10.2983/0730-8000(2005)24[553:HOSACD]2.0.CO;2.

- Karatayev, A. Y., Burlakova, L. E. and Padilla, D. K. (1997) 'The effects of *Dreissena polymorpha* (Pallas) invasion on aquatic communities in eastern Europe', *Journal of Shellfish Research*, 16, pp. 187–203.
- Khan, S. S., Srivatsan, P., Vaishnavi, N., Mukherjee, A. and Chandrasekaran, N. (2011) 'Interaction of silver nanoparticles (SNPs) with bacterial extracellular proteins (ECPs) and its adsorption isotherms and kinetics', *Journal of Hazardous Materials*. 192(1), pp. 299–306. doi: 10.1016/J.JHAZMAT.2011.05.024.
- Korea Ministry of Government Legislation (2008) *Korean Laws in English - Toxic Chemicals Control Act*. Available at: <http://www.moleg.go.kr/english/korLawEng?pstSeq=47535> (Accessed: 4 January 2018).
- Kühr, S., Schneider, S., Meisterjahn, B., Schlich, K., Hund-Rinke, K. and Schlechtriem, C. (2018) 'Silver nanoparticles in sewage treatment plant effluents: chronic effects and accumulation of silver in the freshwater amphipod *Hyalella azteca*', *Environmental Sciences Europe*. 30(1), p. 7. doi: 10.1186/s12302-018-0137-1.
- Lansdown, A. B. G. (2002) 'Metallothioneins: potential therapeutic aids for wound healing in the skin', *Wound Repair and Regeneration*. (10.1111), 10(3), pp. 130–132. doi: 10.1046/j.1524-475X.2002.20101.x.
- Lansdown, A. B. G., Sampson, B., Laupattarakasem, P. and Vuttivirojana, A. (1997) 'Silver aids healing in the sterile skin wound: experimental studies in the laboratory rat', *British Journal of Dermatology*. (10.1111), 137(5), pp. 728–735. doi: 10.1046/j.1365-2133.1997.19432058.x.
- Lansdown, A. B. G., Sampson, B. and Rowe, A. (2001) 'Experimental observations in the rat on the influence of cadmium on skin wound repair', *International Journal of Experimental Pathology*. (10.1111), 82(1), pp. 35–41. doi: 10.1046/j.1365-2613.2001.00180.x.
- Lansdown, A. B. G., Sampson, B. and Rowe, A. (1999) 'Sequential changes in trace metal, metallothionein and calmodulin concentrations in healing skin wounds', *Journal of Anatomy*. Wiley/Blackwell (10.1111), 195(3), pp. 375–386. doi: 10.1046/j.1469-7580.1999.19530375.x.
- Lansdown A.B.G. (1999) 'Metallothionein : implications in wound healing', *Wound Rep Reg*, 8, p. A306. Available at: <https://ci.nii.ac.jp/naid/10016983845/> (Accessed: 8 June 2018).
- Legeay, A., Achard-Joris, M., Baudrimont, M., Massabuau, J.-C. and Bourdineaud, J.-P. (2005) 'Impact of cadmium contamination and oxygenation levels on biochemical responses in the Asiatic clam *Corbicula fluminea*', *Aquatic Toxicology*, 74, pp. 242–253. doi: 10.1016/j.aquatox.2005.05.015.
- Levard, C., Hotze, E. M., Lowry, G. V. and Brown, G. E. (2012) 'Environmental transformations of silver nanoparticles: impact on stability and toxicity', *Environmental Science & Technology*. 46(13), pp. 6900–6914. doi: 10.1021/es2037405.
- Liao, C.-M., Jou, L.-J. and Chen, B.-C. (2005) 'Risk-based approach to appraise valve closure in the clam *Corbicula fluminea* in response to waterborne metals', *Environmental Pollution*, 135(1), pp. 41–52. doi: <http://dx.doi.org/10.1016/j.envpol.2004.10.015>.
- Liu, J., Kershaw, W. C. and Klaassen, C. D. (1991) 'The protective effect of metallothionein on the toxicity of various metals in rat primary hepatocyte culture', *Toxicology and Applied Pharmacology*. 107(1), pp. 27–34. doi: 10.1016/0041-008X(91)90327-B.
- Loeschner, K., Navratilova, J., Købler, C., Mølhave, K., Wagner, S., von der Kammer, F. and Larsen, E. H. (2013) 'Detection and characterization of silver nanoparticles in chicken meat by asymmetric flow field flow fractionation with detection by conventional or single particle ICP-MS', *Analytical and Bioanalytical Chemistry*, 405(25), pp. 8185–8195. doi: 10.1007/s00216-013-7228-z.
- Marie, V., Baudrimont, M. and Boudou, A. (2006) 'Cadmium and zinc bioaccumulation and metallothionein response in two freshwater bivalves (*Corbicula fluminea* and *Dreissena polymorpha*) transplanted along a polymetallic gradient', *Chemosphere*. 65(4), pp. 609–617.
- Marie, V., Gonzalez, P., Baudrimont, M., Bourdineaud, J.-P. and Boudou, A. (2006) 'Metallothionein response to cadmium and zinc exposures compared in two freshwater bivalves, *Dreissena polymorpha* and *Corbicula fluminea*', *BioMetals*, 19(4), pp. 399–407. doi: 10.1007/s10534-005-4064-4.
- McGillicuddy, E., Murray, I., Kavanagh, S., Morrison, L., Fogarty, A., Cormican, M., Dockery, P., Prendergast, M., Rowan, N. and Morris, D. (2017) 'Silver nanoparticles in the environment: Sources, detection and ecotoxicology', *Science of The Total Environment*. 575, pp. 231–246. doi: 10.1016/J.SCITOTENV.2016.10.041.

- McMahon, R. F. (1983) 'Ecology of an invasion pest bivalve, *Corbicula*', *The mollusca. Ecology*. 6, pp. 505–561.
- Ministry of Environment and Urbanization(MoEU) of Turkey (2017) 'Draft by-law on registration, evaluation, authorization and restriction of chemicals'. Available at: http://files.chemicalwatch.com/KKDİK_ingilizce.pdf (Accessed: 4 January 2018).
- Mitrano, D. M., Ranville, J. F., Bednar, A., Kazor, K., Hering, A. S. and Higgins, C. P. (2014) 'Tracking dissolution of silver nanoparticles at environmentally relevant concentrations in laboratory, natural, and processed waters using single particle ICP-MS (spICP-MS)', *Environ. Sci.: Nano*. 1(3), pp. 248–259. doi: 10.1039/C3EN00108C.
- Moore, M. N. (2006) 'Do nanoparticles present ecotoxicological risks for the health of the aquatic environment?', *Environment International*. 32(8), pp. 967–976. doi: 10.1016/J.ENVINT.2006.06.014.
- Mueller, N. C. and Nowack, B. (2008) 'Exposure Modeling of Engineered Nanoparticles in the Environment', *Environmental Science & Technology*. 42(12), pp. 4447–4453. doi: 10.1021/es7029637.
- Naiki, Y. (2010) 'Assessing Policy Reach: Japan's Chemical Policy Reform in Response to the EU's REACH Regulation', *Journal of Environmental Law*. 22(2), pp. 171–195. doi: 10.1093/jel/eqq002.
- Narbonne, J. F., Djomo, J. E., Ribera, D., Ferrier, V. and Garrigues, P. (1999) 'Accumulation kinetics of polycyclic aromatic hydrocarbons adsorbed to sediment by the mollusk *Corbicula fluminea*', *Ecotoxicology and Environmental Safety*, 42(1), pp. 1–8. doi: <http://dx.doi.org/10.1006/eesa.1998.1701>.
- van Nes, E. H., Noordhuis, R., Lammens, E. H. H. R., Portielje, R., Reeze, B. and Peeters, E. T. H. M. (2008) 'Modelling the effects of diving ducks on zebra mussels *Dreissena polymorpha* in lakes', *Ecological Modelling*. 211(3–4), pp. 481–490. doi: 10.1016/J.ECOLMODEL.2007.10.001.
- Nielson, K. B., Atkin, C. L. and Winge, D. R. (1985) 'Distinct metal-binding configurations in metallothionein*', *The Journal of biological chemistry*. American Society for Biochemistry and Molecular Biology, 260(9), pp. 5342–5350. Available at: <http://www.jbc.org/content/260/9/5342.short> (Accessed: 8 June 2018).
- Norwood, W. P., Borgmann, U. and Dixon, D. G. (2007) 'Chronic toxicity of arsenic, cobalt, chromium and manganese to *Hyalella azteca* in relation to exposure and bioaccumulation', *Environmental Pollution*, 147(1), pp. 262–272.
- Organisation for Economic Co-operation and Development (OECD) (2014) 'Expert Meeting Report : Joint meeting of the Chemicals Committee and the Working party on Chemicals, Pesticides and Biotechnology', . Publications in the Series on the Safety of Manufactured Nanomaterials. Paris. OECD Publishing.
- Organisation for Economic Co-operation and Development (OECD) (2012) 'Test No. 305: Bioaccumulation in fish: aqueous and dietary exposure', *OECD Guidelines for Testing of Chemicals*. Paris. OECD Publishing.
- Othman, M. S. and Pascoe, D. (2001) 'Growth, development and reproduction of *Hyalella azteca* (Saussure, 1858) in laboratory culture', *Crustaceana*, 74(2), pp. 171–181.
- Phelps, H. L. (1994) 'The Asiatic Clam (*Corbicula fluminea*) Invasion and System-Level Ecological Change in the Potomac River Estuary near Washington, D. C.', *Estuaries*. 17(3), p. 614. doi: 10.2307/1352409.
- Piccinno, F., Gottschalk, F., Seeger, S. and Nowack, B. (2012) 'Industrial production quantities and uses of ten engineered nanomaterials in Europe and the world', *Journal of Nanoparticle Research*. 14(9), p. 1109. doi: 10.1007/s11051-012-1109-9.
- Rajagopal, S., van der Gelde, G. and bij de Vaate, A. (2000) 'Reproductive biology of the Asiatic clams *Corbicula fluminalis* and *Corbicula fluminea* in the river Rhine', *Fundamental and Applied Limnology*. 149(3), pp. 403–420. doi: 10.1127/archiv-hydrobiol/149/2000/403.
- Ravindran, A., Singh, A., Raichur, A. M., Chandrasekaran, N. and Mukherjee, A. (2010) 'Studies on interaction of colloidal Ag nanoparticles with Bovine Serum Albumin (BSA)', *Colloids and Surfaces B: Biointerfaces*. 76(1), pp. 32–37. doi: 10.1016/J.COLSURFB.2009.10.005.
- Regoli, F. and Orlando, E. (1994) 'Accumulation and subcellular distribution of metals (Cu, Fe, Mn, Pb and Zn) in the Mediterranean mussel *Mytilus galloprovincialis* during a field transplant experiment', *Marine Pollution Bulletin*. 28(10), pp. 592–600. doi: 10.1016/0025-326X(94)90360-3.
- Ringwood, A. H., McCarthy, M., Bates, T. C. and Carroll, D. L. (2010) 'The effects of silver nanoparticles on oyster embryos', *Marine Environmental Research*. 69, pp. S49–S51. doi: 10.1016/J.MARENVRES.2009.10.011.

- Rodgers, J., Cherry, D., Graney, R., Dickson, K. and Cairns, J. (1980) 'Comparison of heavy metal interactions in acute and artificial stream bioassay techniques for the Asiatic Clam (*Corbicula fluminea*)', ASTM International. doi: 10.1520/STP27424S.
- Roditi, H. A., Strayer, D. L. and Findlay, S. E. G. (1997) 'Characteristics of zebra mussel (*Dreissena polymorpha*) biodeposits in a tidal freshwater estuary', *Archiv für Hydrobiologie*, 140(2), pp. 207–219.
- Sannac, S., Tadjiki, S. and Moldenhauer, E. (2013) 'Single particle analysis using the Agilent 7700x ICP-MS', *Agil. Technol.*
- Schmidt, B., Loeschner, K., Hadrup, N., Mortensen, A., Sloth, J. J., Bender Koch, C. and Larsen, E. H. (2011) 'Quantitative Characterization of Gold Nanoparticles by Field-Flow Fractionation Coupled Online with Light Scattering Detection and Inductively Coupled Plasma Mass Spectrometry', *Analytical Chemistry*, 83(7), pp. 2461–2468. doi: 10.1021/ac102545e.
- Schreurs, W. J. and Rosenberg, H. (1982) 'Effect of silver ions on transport and retention of phosphate by *Escherichia coli*.', *Journal of bacteriology*, 152(1), pp. 7–13. Available at: <http://www.ncbi.nlm.nih.gov/pubmed/6749823> (Accessed: 14 December 2018).
- Shuhaimi-Othman, M. and Pascoe, D. (2007) 'Bioconcentration and depuration of copper, cadmium, and zinc mixtures by the freshwater amphipod *Hyaella azteca*', *Ecotoxicology and Environmental Safety*, 66(1), pp. 29–35. doi: 10.1016/J.ECOENV.2006.03.003.
- Soliz, M. and Odermatt, A. (1995) 'Copper and silver transport by CopB-ATPase in membrane vesicles of *Enterococcus hirae*.', *The Journal of biological chemistry*, 270(16), pp. 9217–21. doi: 10.1074/JBC.270.16.9217.
- Sousa, R., Guilhermino, L. and Antunes, C. (2005) 'Molluscan fauna in the freshwater tidal area of the River Minho estuary, NW of Iberian Peninsula', *Annales de Limnologie - International Journal of Limnology*, 41(2), pp. 141–147. doi: 10.1051/limn/2005009.
- Tedesco, S., Doyle, H., Blasco, J., Redmond, G. and Sheehan, D. (2010) 'Exposure of the blue mussel, *Mytilus edulis*, to gold nanoparticles and the pro-oxidant menadione', *Comparative Biochemistry and Physiology Part C: Toxicology & Pharmacology*, 151(2), pp. 167–174. doi: 10.1016/J.CBPC.2009.10.002.
- Tran, D., Ciret, P., Durrieu, G. and Massabuau, J.-C. (2003) 'Estimation of potential and limits of bivalve closure response to detect contaminants: Application to cadmium', *Environmental Toxicology and Chemistry*, 22(4), pp. 914–920. Available at: <https://setac.onlinelibrary.wiley.com/doi/pdf/10.1002/etc.5620220432> (Accessed: 30 April 2018).
- Tran, D., Fournier, E. and Durrieu, G. (2007) 'Inorganic mercury detection by valve closure response in the freshwater clam *Corbicula fluminea*: Integration of time and water metal concentration changes', *Environmental Toxicology and Chemistry*, 26(7), pp. 1545–1551. Available at: <https://setac.onlinelibrary.wiley.com/doi/pdf/10.1897/06-390R1.1> (Accessed: 30 April 2018).
- US-EPA (2004) 'High Production Volume Challenge Program High Production Volume Challenge Program', C. Available at: www.epa.gov.
- Vale, G., Franco, C., Diniz, M. S., Santos, M. M. C. dos and Domingos, R. F. (2014) 'Bioavailability of cadmium and biochemical responses on the freshwater bivalve *Corbicula fluminea* – the role of TiO₂ nanoparticles', *Ecotoxicology and Environmental Safety*, 109, pp. 161–168. doi: <http://dx.doi.org/10.1016/j.ecoenv.2014.07.035>.
- Vale, G., Mehennaoui, K., Cambier, S., Libralato, G., Jomini, S. and Domingos, R. F. (2016) 'Manufactured nanoparticles in the aquatic environment-biochemical responses on freshwater organisms: A critical overview', *Aquatic Toxicology*, 170, pp. 162–174. doi: 10.1016/J.AQUATOX.2015.11.019.
- Vidal, M.-L., Bassères, A. and Narbonne, J.-F. (2001) 'Potential biomarkers of trichloroethylene and toluene exposure in *Corbicula fluminea*', *Environmental Toxicology and Pharmacology*, 9(3), pp. 87–97. doi: 10.1016/S1382-6689(00)00068-5.
- Vijayavel, K., Gopalakrishnan, S. and Balasubramanian, M. P. (2007) 'Sublethal effect of silver and chromium in the green mussel *Perna viridis* with reference to alterations in oxygen uptake, filtration rate and membrane bound ATPase system as biomarkers', *Chemosphere*, 69(6), pp. 979–986. doi: 10.1016/J.CHEMOSPHERE.2007.05.011.

- Voelker, D., Schlich, K., Hohndorf, L., Koch, W., Kuehnen, U., Polleichtner, C., Kussatz, C. and Hund-Rinke, K. (2015) 'Approach on environmental risk assessment of nanosilver released from textiles', *Environmental Research*, 140, pp. 661–672.
- Ward, J. E. and Kach, D. J. (2009) 'Marine aggregates facilitate ingestion of nanoparticles by suspension-feeding bivalves', *Marine Environmental Research*. doi: 10.1016/j.marenvres.2009.05.002.
- Wildridge, P. J., Werner, R. G., Doherty, F. G. and Neuhauser, E. F. (1998) 'Acute effects of potassium on filtration rates of adult Zebra Mussels, *Dreissena polymorpha*', *Journal of Great Lakes Research*. 24(3), pp. 629–636. doi: 10.1016/S0380-1330(98)70850-0.
- de Wolf, W., Comber, M., Douben, P., Gimeno, S., Holt, M., Léonard, M., Lillicrap, A., Sijm, D., van Egmond, R., Weisbrod, A. and Whale, G. (2007) 'Animal use replacement, reduction, and refinement: development of an integrated testing strategy for bioconcentration of chemicals in fish.', *Integrated environmental assessment and management*, 3(1), pp. 3–17. doi: 10.1897/1551-3793(2007)3[3:AURRAR]2.0.CO;2.
- Zhang, C., Hu, Z. and Deng, B. (2016) 'Silver nanoparticles in aquatic environments: Physiochemical behavior and antimicrobial mechanisms', *Water Research*. 88, pp. 403–427. doi: 10.1016/J.WATRES.2015.10.025.
- Zhang, X., Sun, H., Zhang, Z., Niu, Q., Chen, Y. and Crittenden, J. C. (2007) 'Enhanced bioaccumulation of cadmium in carp in the presence of titanium dioxide nanoparticles', *Chemosphere*. 67(1), pp. 160–166. doi: 10.1016/J.CHEMOSPHERE.2006.09.003.
- Zhu, X., Zhou, J. and Cai, Z. (2011) 'TiO₂ nanoparticles in the marine environment: Impact on the toxicity of tributyltin to Abalone (*Haliotis diversicolor supertexta*) Embryos', *Environmental Science & Technology*. 45(8), pp. 3753–3758. doi: 10.1021/es103779h.